

**Master of Science in
«Cultural Heritage Materials and Technologies»**

LIDA KYRIOPOULOU

(R.N. 1012202002004)

DIPLOMA THESIS:

**Theoretical and Non-destructive documentation approach
of the late 16th c. panel painting entitled "The Hospitality
of Abraham" Benaki museum collection**



SUPERVISING COMMITTEE:

- Dr. Eleni Kouloumpi
- Prof. Nikolaos Zacharias

EXAMINATION COMMITTEE:

- Dr. Eleni Kouloumpi
- Prof. Nikolaos Zacharias
- Ass. Prof. Maria Xanthopoulou

KALAMATA, OCTOBER 2023

Contents

Table of Figures	3
Table of Tables.....	14
Acknowledgments.....	15
Introduction	17
1. The art of portable icon painting.....	20
1.1. The history of portable icon painting.....	20
1.2 The Byzantine icons.....	20
1.3. The icons of the Cretan School	23
2. Techniques of portable icons painting	48
3. The Hospitality of Abraham	57
3.1. Historical Evolution	57
3.2. Description	61
3.3. The influence of Byzantine tradition and Western art on the artist's style.....	64
3.3.1. The Influence of Byzantine Tradition	64
3.3.2. The Influence of the Western Art.....	66
4. Review of non-destructive techniques	87
4.1. Imaging techniques	87
4.2. Spectroscopic techniques	90
5. Research Methodology.....	95
5.1. Goals of Research	95
5.2. Research Protocols	95
5.2.1. Portable Microscope.....	96

5.2.2. Multispectral Imaging	96
5.2.3. X-ray Fluorescence Spectrometry	98
5.2.4. Raman Spectroscopy	98
6. Results and discussion	103
6.1. Multispectral Imaging	103
6.1.1. False color Imaging.....	111
6.2. Portable Stereomicroscope.....	112
6.3. X-Ray Fluorescence Spectrometry	112
6.4. Raman Spectroscopy	135
7. Discussion/Conclusion.....	152
7.1. Future Research.....	153
Bibliography.....	155

Table of Figures

Figure 1: The Hospitality of Abraham, late 16th c., panel painting, Athens, Benaki Museum of Greek Culture (derived from: https://www.benaki.org/index.php?option=com_collectionitems&view=collectionitem&Itemid=162&id=108267&lang=el).	28
Figure 2: Mary & Child, the second half of 6 th c., encaustic icon, Mount Sinai, Monastery of Agia Aikatairini (derived from: https://en.m.wikipedia.org/wiki/File:Mary_%26_Child_Icon_Sinai_6th_century.jpg).	29
Figure 3: Ascension, 9th-10th c., panel painting, Mount Sinai, Monastery of Agia Aikaterini (derived from: https://www.pemptousia.gr/2011/06/stin-analipsi-tou-kiriou/).....	30
Figure 4: Archangel Michael and the monk Archippus at Chonae, the second half of 12 th c., panel painting, Mount Sinai, Monastery of Agia Aikaterini (derived from: https://en.m.wikipedia.org/wiki/File:Michael_Miracle_Icon_Sinai_12th_century.jpg).	31
Figure 5: Evangelist Matthew, end of 14 th -15 th c., panel painting, Ohrid, Panagia Perivleptos (derived from: http://www.krakow2000.pl/2000wydarzenia/11_kolebka.htm).....	32
Figure 6: Annunciation, early 14 th c., panel painting, Ohrid, Panagia Perivleptos, (derived from: https://el.m.wikipedia.org/wiki/%CE%91%CF%81%CF%87%CE%B5%CE%AF%CE%BF:Ohrid_annunciation_icon.jpg).	33
Figure 7: Agios Ioannis Theologos, end of 14 th .-early 15th c., panel painting, Mytilene, Byzantine and Christian Museum of Holy Cathedral of Mytilene (https://russianicons.wordpress.com/tag/greek-icons/page/4/).	34

Figure 8: Christos Pantokrator, 1363, panel painting, Saint Petersburg, Hermitage Museum (https://www.icon-art.info/book_contents.php?book_id=29&chap=10&ch_12=9#pic543) 35

Figure 9: Theophanes Strelitzas Bathas, St George and St Demetrios, c 1550, panel painting, Mount Athos, Monastery of Megisti Lavra (derived from: <http://www.diakonima.gr/2009/09/10/the-holy-monastery-of-the-great-lavra/>). 36

Figure 10: Theophanes Strelitzas Bathas, Nativity Scene, 1546, egg tempera on wood, Mount Athos, Stavronikita Monastery (derived from: <https://www.macedonian-heritage.gr/Athos/General/Art.html>)..... 37

Figure 11: Theophanes Strelitzas Bathas, Adam_naming_the_animals, 16th c., Meteora, St. Nicholas Anapavsa Monastery (derived from: https://el.wikipedia.org/wiki/%CE%91%CF%81%CF%87%CE%B5%CE%AF%CE%BF:Adam_naming_the_animals_-_St._Nicholas_Anapavsa_Monstery,_Meteora_-_Theophanes_of_Crete,_16th_c..jpg). 38

Figure 12: Michael Damaskinos, First Ecumenical Council, 1591, panel painting, Heraklion, Museum of Hagia Aikaterini of Sina (derived from: <http://iakm.gr/agia/Page?lang=gr&name=infotext&id=501&sub=504&sub2=555>). 39

Figure 13: Michael Damaskinos, Hagios Ioannis, second mid-16th c., panel painting, Zakynthos, Byzantine Museum (derived from: <https://paletaart.wordpress.com/2012/09/13/%CE%B4%CE%B1%CE%BC%CE%B1%CF%83%CE%BA%CE%B7%CE%BD%CF%8C%CF%82-%CE%BC%CE%B9%CF%87%CE%B1%CE%AE%CE%BB-michael-damaskinos-153035-159293/%CE%B4%CE%B1%CE%BC%CE%B1%CF%83%CE%BA%CE%B7%CE%BD%CF%8C%CF%82-%CE%BC%CE%B9%CF%87%CE%B1%CE%AE%CE%BB-%CE%B1%CE%B3->

%CE%B9%CF%89%CE%AC%CE%BD%CE%BD%CE%B7%CF%82-
 %CE%BF-%CF%80%CF%81%CF%8C%CE%B4%CF%81%CE%BF/). 40
 Figure 14: Michael Damaskinos, Saints Sergius, Justin and Bacchus,. 1584-
 1593, egg tempera on panel, Corfu, Antivouniotissa Museum (derived from:
<http://iakm.gr/agia/Page?name=enotita&lang=gr&id=501&sub=555>). 41
 Figure 15: Georgios Klontzas, Saint George the Dragonslayer, second mid of
 16th c., egg tempera on panel, Athens, Christian and Byzantine Museum
 (derived from:
https://www.byzantinemuseum.gr/el/permanentexhibition/from_Byzantium_to_Modern_Era/society_art_in_Venetian_Crete/). 41
 Figure 16: Georgios Klontzas, The Sacrifice of Abraham and the Adoration
 of the Magi, 16th c., private collection
 (https://en.wikipedia.org/wiki/Georgios_Klontzas). 42
 Figure 17: Domekikos Theotokopoulos, Dormition of the Virgin, 1565-1566,
 tempera on panel, Ermoupolis, Holy Cathedral of the Dormition of the Virgin
 (derived from:
[https://el.wikipedia.org/wiki/%CE%9A%CE%BF%CE%AF%CE%BC%CE%B7%CF%83%CE%B7_%CF%84%CE%B7%CF%82_%CE%98%CE%B5%CE%BF%CF%84%CF%8C%CE%BA%CE%BF%CF%85_\(%CE%98%CE%B5%CE%BF%CF%84%CE%BF%CE%BA%CF%8C%CF%80%CE%BF%CF%85%CE%BB%CE%BF%CF%82\)](https://el.wikipedia.org/wiki/%CE%9A%CE%BF%CE%AF%CE%BC%CE%B7%CF%83%CE%B7_%CF%84%CE%B7%CF%82_%CE%98%CE%B5%CE%BF%CF%84%CF%8C%CE%BA%CE%BF%CF%85_(%CE%98%CE%B5%CE%BF%CF%84%CE%BF%CE%BA%CF%8C%CF%80%CE%BF%CF%85%CE%BB%CE%BF%CF%82))). 43
 Figure 18: Domenikos Theotokopoulos, Evangelist. Luke Painting the Virgin,
 156-1567, tempera on panel, Athens, Benaki Museum of Greek Culture
 (derived from: https://en.wikipedia.org/wiki/File:El_Greco_-_St_Luke_Painting_the_Virgin_-_Google_Art_Project.jpg). 44
 Figure 19: Domenikos Theotokopoulos, The Adoration of the Magi, 1565-
 1567, tempera on panel, Athens, Benaki Museum of Greek Culture (derived
 from:
<https://el.m.wikipedia.org/wiki/%CE%91%CF%81%CF%87%CE%B5%CE>

%AF%CE%BF:El_Greco_-_The_Adoration_of_the_Magi_-_Google_Art_Project_(721007).jpg).	45
Figure 20: Domenikos Theotokopoulos, The Burial of the Count of Orgaz, 1586, oil on canvas, Toledo, Church of Santo Tome (derived from: https://el.wikipedia.org/wiki/%CE%97_%CF%84%CE%B1%CF%86%CE%AE_%CF%84%CE%BF%CF%85_%CE%BA%CF%8C%CE%BC%CE%B7_%CF%84%CE%BF%CF%85_%CE%9F%CF%81%CE%B3%CE%BA%CE%AC%CE%B8).	46
Figure 21: Domenikos Theotokopoulos, View of Toledo, 1541-1614, oil on canvas, New York, Metropolitan Museum (derived from: https://en.wikipedia.org/wiki/View_of_Toledo).	47
Figure 22: Panselinos Emanuel, Hagios Ioannis the Theologian dictates the Gospel to his discipline Prochorus, mural, Hagion Oros, cathedral church of Protato (derived from: Καπετανίδης: Τεχνικές Μέθοδοι Βυζαντινής και Μεταβυζαντινής Αγιογραφίας Μέρος Πρώτο: χρωστικές, pg. 10). .Σφάλμα! Δεν έχει οριστεί σελιδοδείκτης.	
Figure 23: Stratigraphy of a typical painting (derived from: Kouloumpi, E., Moutsatsou, A. M., & Terlixi, A.-V. (2012). Canvas and Panel Paintings: Techniques and Analyses. In Analytical Archaeometry: Selected topics. Royal Society of Chemistry, pg. 363).	56
Figure 24: The Hospitality of Abraham, end of 16 th c. panel painting, Athens, Benaki Museum of Greek Culture (derived from: https://www.benaki.org/index.php?option=com_collectionitems&view=collectionitem&id=108267&Itemid=383&lang=el).	67
Figure 25: The Hospitality of Abraham (detail: the right side of the painting), end of 16 th c. panel painting, Athens, Beanki Museum of Greek Culture (derived from: https://www.benaki.org/index.php?option=com_collectionitems&view=collectionitem&id=108267&Itemid=383&lang=el).	68

Figure 26: The Hospitality of Abraham (detail: the left part of the painting), end of 16th c. panel painting, Athens, Beanki Museum of Greek Culture, (derived from: https://www.benaki.org/index.php?option=com_collectionitems&view=collectionitem&id=108267&Itemid=383&lang=el).69:Figure 27: The Hospitality of Abraham (detail: Abraham), end of 16th c. panel painting, Athens, Beanki Museum of Greek Culture (derived from: https://www.benaki.org/index.php?option=com_collectionitems&view=collectionitem&id=108267&Itemid=383&lang=el). 70

Figure 28: The Hospitality of Abraham (detail: the angel on the left side of the painting), end of 16th c. panel painting, Athens, Beanki Museum of Greek Culture (derived from: https://www.benaki.org/index.php?option=com_collectionitems&view=collectionitem&id=108267&Itemid=383&lang=el). 70

Figure 29: The Hospitality of Abraham (detail: Sarah), end of 16th c. panel painting, Athens, Beanki Museum of Greek Culture (derived from: https://www.benaki.org/index.php?option=com_collectionitems&view=collectionitem&id=108267&Itemid=383&lang=el). 71

Figure 30: The Hospitality of Abraham (detail: the central angel), end of 16th c. panel painting, Athens, Beanki Museum of Greek Culture (derived from: https://www.benaki.org/index.php?option=com_collectionitems&view=collectionitem&id=108267&Itemid=383&lang=el). 72

Figure 31. The Hospitality of Abraham (the standing figure on the left), end of 16th c. panel painting, Athens, Beanki Museum of Greek Culture: (derived from: https://www.benaki.org/index.php?option=com_collectionitems&view=collectionitem&id=108267&Itemid=383&lang=el). 73

Figure 32: The Hospitality of Abraham (detail: the left angel), end of 16th c. panel painting, Athens, Beanki Museum of Greek Culture (derived from:

https://www.benaki.org/index.php?option=com_collectionitems&view=collectionitem&id=108267&Itemid=383&lang=el).	74
Figure 33: The Hospitality of Abraham (the table), end of 16 th c. panel painting, Athens, Beanki Museum of Greek Culture (derived from: https://www.benaki.org/index.php?option=com_collectionitems&view=collectionitem&id=108267&Itemid=383&lang=el).	74
Figure 34: The Hospitality of Abraham (detail: the vases in front of the left angel's feet), end of 16 th c. panel painting, Athens, Beanki Museum of Greek Culture (derived from: https://www.benaki.org/index.php?option=com_collectionitems&view=collectionitem&id=108267&Itemid=383&lang=el).	75
Figure 35: The Hospitality of Abraham, c. mid 14th century, panel painting, Benaki Museum, Athens (derived from: https://el.wikipedia.org/wiki/%CE%97_%CF%86%CE%B9%CE%BB%CE%BF%CE%BE%CE%B5%CE%BD%CE%AF%CE%B1_%CF%84%CE%BF%CF%85_%CE%91%CE%B2%CF%81%CE%B1%CE%AC%CE%BC_(%CE%9C%CE%BF%CF%85%CF%83%CE%B5%CE%AF%CE%BF_%CE%9C%CF%80%CE%B5%CE%BD%CE%AC%CE%BA%CE%B7)).	75
Figure 36: The Hospitality of Abraham, the beginning of 15th century, panel painting, Christian and Byzantine Museum, Athens (derived from: https://www.ebyzantinemuseum.gr/?i=bxm.el.exhibit&id=43).	76
Figure 37 Angelo Akotantos, The Hospitality of Abraham, second hand of the 14th century, panel painting, Palais-Musée des Archevêques, Narbonne (derived from: Χαραλάμπους-Μουρίκη, 1964, p. ΠΙΝΑΞ 35).	77
Figure 38: Enthroned Madonna and Child, 1250-1275, tempera on poplar panel, National Galley of Art, Wahington (derived from: https://el.m.wikipedia.org/wiki/%CE%91%CF%81%CF%87%CE%B5%CE%AF%CE%BF:Italo-Byzantinischer_Maler_des_13._Jahrhunderts_001.jpg).	78

Figure 39: Archangel Michael, 14th century, Byzantine and Christian Museum, Athens (derived from: https://www.byzantinemuseum.gr/el/permanentexhibition/byzantine_world/the_final_flowering/?bxm=1353). 79

Figure 40: Filippo Brunelleschi, Spedale degli Innocenti, 1419-1423, Florence (derived from: https://en.wikipedia.org/wiki/File:Spedale_innocenti,_veduta_02.JPG). 80

Figure 41: Filippo Brunelleschi & Luca Fancelli, Palazzo Pitti, 1458, Florence (derived from: 80

Figure 42: Cathedral Church of the Blessed Virgin Mary, 1258, Salisbury (derived from: https://el.wikipedia.org/wiki/%CE%9A%CE%B1%CE%B8%CE%B5%CE%B4%CF%81%CE%B9%CE%BA%CF%8C%CF%82_%CE%BD%CE%B1%CF%8C%CF%82_%CF%84%CE%BF%CF%85_%CE%A3%CF%8C%CE%BB%CF%83%CE%BC%CF%80%CE%B5%CF%81%CE%B9)... 81

Figure 43: Trefoil arches, Bayeux Cathedral, 11th century, Calvados (derived from: https://pl.wikipedia.org/wiki/%C5%81uk_tr%C3%B3jlistny). 82

Figure 44: Paolo Veronese, Mystic Marriage of Saint Catherine, 1571, oil on canvas, Gallerie dell'Accademia, Venice (derived from: https://el.wikipedia.org/wiki/%CE%91%CF%81%CF%87%CE%B5%CE%AF%CE%BF:Paolo_Veronese_014.jpg). 83

Figure 45: The Baptism of Christ. Fresco, 14th century, mural, Hagios Nikolaos Orfanos, Thessaloniki (<https://www.thessmemory.gr/%CE%B2%CF%85%CE%B6%CE%B1%CE%BD%CF%84%CE%B9%CE%BD%CE%B7-%CE%B8%CE%B5%CF%83%CF%83%CE%B1%CE%BB%CE%BF%CE%BD%CE%B9%CE%BA%CE%B7/%CF%84%CE%B1-%CE%BA%CE%B1%CE%BB%CE%BB%CE%B9%CF%84%CE%B5%CF%87%CE%BD%CE%B9%CE%BA%CE%AC-%CE%B4%CF%8E%CF%81%CE%B1-%CF%84%CF%89%CE%BD>-

%CE%BC%CE%AC%CE%B3%CF%89%CE%BD- %CF%83%CF%84%CE%BF%CE%BD/).	84
Figure 46: Head of a teenage man, 490-480 B.C., marble, Museum of Acropolis, Athens (https://www.theacropolismuseum.gr/kefali-agalmatos-o-xanthos-efibos).	85
Figure 47: Perino del Vaga, the Nativity, 1534, oil on panel, National Gallery of Art, New York (derived from: https://www.nga.gov/collection/art-object-page.46130.html).	86
Figure 48: Points of Portable Microscope, X-ray Spectrometer, and Raman Spectrometer analysis (digital processing Lida Kyriopoulou).	96
Figure 49: The process of Multispectral Imaging technique (derived from: personal archive Lida Kyriopoulou).	99
Figure 50: The process of Multispectral Imaging technique (derived from personal archive Lida Kyriopoulou).	100
Figure 51: Image acquisition with a portable stereomicroscope (derived from personal archive Lida Kyriopoulou).	101
Figure 52: Analysis procedure with X-ray Fluorescence Spectrometer (derived from: personal archive Lida Kyriopoulou).	101
Figure 53: Analysis procedure with Raman Spectrometer (derived from: personal archive Lida Kyriopoulou).	102
Figure 54: Points of physicochemical analyses (digital processing Lida Kyriopoulou).	103
Figure 55: Figure Coloured imaging of the reflection of the visible region (derived from: personal archive Lida Kyriopoulou).	104
Figure 56: Figure Imaging of the reflection of the spectral region 450-550nm (derived from: personal archive: Lida Kyriopoulou).	104
Figure 57: Imaging of the reflection of the spectral region 750-850nm (derived from: personal archive Lida Kyriopoulou).	104
Figure 58: Imaging of the reflection of the spectral region 850-950nm (derived from: personal archive Lida Kyriopoulou).	104

Figure 59: Imaging of the reflection of the spectral region with average 1000nm (derived from: personal archive Lida Kyriopoulou).....	105
Figure 60: False colour infrared image (derived from: personal archive Lida Kyriopoulou).....	105
Figure 61: Coloured imaging of the reflection of the visible region (derived from: personal archive Lida Kyriopoulou).	106
Figure 62: Imaging of the reflection of the spectral region 450-550nm (derived from: personal archive Lida Kyriopoulou).....	106
Figure 63: Imaging of the reflection of the spectral region 750-850nm (derived from: personal archive Lida Kyriopoulou).....	106
Figure 64: Imaging of the reflection of the spectral region 850-950nm (derived from: personal archive Lida Kyriopoulou).....	106
Figure 65: Imaging of the reflection of the spectral region with average 1000nm (derived from: personal archive Lida Kyriopoulou).....	107
Figure 66: False colour infrared image (derived from: personal archive Lida Kyriopoulou).....	107
Figure 67: Coloured imaging of the reflection of the visible region (derived from: personal archive Lida Kyriopoulou).	108
Figure 68: Imaging of the reflection of the spectral region 450-550nm (derived from personal archive Lida Kyriopoulou).	108
Figure 69: Imaging of the reflection of the spectral region 750-850nm (derived from: personal archive Lida Kyriopoulou).....	108
Figure 70: Imaging of the reflection of the spectral region 850-950nm (derived from: personal archive Lida Kyriopoulou).....	108
Figure 71: Imaging of the reflection of the spectral region with average 1000nm (derived from: personal archive Lida Kyriopoulou).....	109
Figure 72: False colour infrared image (derived from: personal archive Lida Kyriopoulou).....	109
Figure 73: Coloured imaging of the reflection of the visible region (derived from: personal archive Lida Kyriopoulou).	110

Figure 74: Imaging of the reflection of the spectral region 450-550nm (derived from: personal archive Lida Kyriopoulou).	110
Figure 75: Imaging of the reflection of the spectral region 900-1000nm (derived from: personal archive Lida Kyriopoulou).	110
Figure 76: Imaging of the reflection of the spectral region with average 1000nm (derived from: personal archive Lida Kyriopoulou).	110
Figure 77: False colour infrared image (derived from: personal archive Lida Kyriopoulou).	111
Figure 79: XRF analysis points (digital processing Lida Kyriopoulou). ...	112
Figure 79: XRF analysis results of paint 1 (derived from: personal archive Lida Kyriopoulou).	114
Figure 80: XRF analysis results of paint 2 (derived from: personal archive Lida Kyriopoulou).	115
Figure 81: XRF analysis of paint 3 (derived from: personal archive Lida Kyriopoulou).	116
Figure 82: XRF analysis results of paint 5 (derived from: personal archive Lida Kyriopoulou).	116
Figure 83: Portable stereomicroscope picture of paint 6 (derived from: personal archive Lida Kyriopoulou).	117
Figure 84: XRF analysis results of paint 6 (derived from: personal archive Lida Kyriopoulou).	117
Figure 85: XRF analysis results of paint 7 (derived from: personal archive Lida Kyriopoulou).	118
Figure 86: XRF analysis results of paint 8 (derived from: personal archive Lida Kyriopoulou).	119
Figure 87: XRF analysis results of paint 9a (derived from: personal archive Lida Kyriopoulou).	119
Figure 88: XRF analysis results of paint 9b (derived from: personal archive Lida Kyriopoulou).	120

Figure 89: XRF analysis results of paint 10 (derived from: personal archive Lida Kyriopoulou).....	120
Figure 90: XRF analysis results of paint 11 (derived from: personal archive Lida Kyriopoulou).....	122
Figure 91: Portable stereomicroscope picture of paint 11 (derived from: personal archive Lida Kyriopoulou).	122
Figure 92: Portable stereomicroscope picture of paint 12 (derived from: personal archive Lida Kyriopoulou).	124
Figure 93: XRF analysis results of paint 12 (derived from: personal archive Lida Kyriopoulou).....	124
Figure 94: XRF analysis results of paint 13 (derived from: personal archive Lida Kyriopoulou).....	125
Figure 95: XRF analysis results of paint 14 (derived from: personal archive Lida Kyriopoulou).....	126
Figure 96: XRF analysis results of paint 15 (derived from: personal archive Lida Kyriopoulou).....	126
Figure 97: XRF analysis results of paint 16 (derived from: personal archive Lida Kyriopoulou).....	127
Figure 98: Portable stereomicroscope picture of paint 16 (derived from: personal archive Lida Kyriopoulou).	128
Figure 99: Raman analysis points (digital processing Lida Kyriopoulou).	135
Figure 100: Raman analysis results of paint 1 (derived from: personal archive Lida Kyriopoulou).....	136
Figure 101: Raman analysis results of paint 2 points (derived from: personal archive Lida Kyriopoulou).....	137
Figure 102: Portable stereomicroscope picture of paint 2 (derived from: personal archive Lida Kyriopoulou).	138
Figure 103: Raman analysis results of paint 3 (derived from: personal archive Lida Kyriopoulou).....	139

Figure 104: Raman analysis results of paint 6 (derived from: personal archive Lida Kyriopoulou).....	140
Figure 105: Raman analysis results of paint 4 (derived from: personal archive Lida Kyriopoulou).....	141
Figure 106: Raman analysis results of paint 5 (derived from: personal archive Lida Kyriopoulou).....	142
Figure 107: Raman analysis results of paint 7 (derived from: personal archive Lida Kyriopoulou).....	143
Figure 108: Raman analysis results of paint 8 (derived from: personal archive Lida Kyriopoulou).....	144
Figure 109: Raman results of paint 10 (derived from: personal archive Lida Kyriopoulou).....	145
Figure 110: Raman results of paint 11 (derived from: personal archive Lida Kyriopoulou).....	146
Figure 111: Raman analysis results of paint 14 (derived from: personal archive Lida Kyriopoulou).....	147
Figure 112: Raman analysis results of paint 15 (derived from: personal archive Lida Kyriopoulou).....	148
Figure 113: Raman analysis results of paint 16 (derived from: personal archive Lida Kyriopoulou).....	149

Table of Tables

Table 1: Summary of the results obtained with the XRF analysis technique.	134
Table 2: Summary of the results obtained with the Raman analysis technique.	151

Acknowledgments

For the preparation of my study, many people helped without their valuable help I could not have completed it. I want to thank:

Dr. Eleni Kouloumpi, Conservation Scientist at the Laboratory of Physicochemical Research of the National Gallery – Alexandros Soutzos Museum, and Chief Supervisor of my dissertation for her help in choosing my thesis topic, organizing the diagram, and interpreting the results of the analytical methods.

Professor Dr. Nikolaos Zacharias, Director of the MSc CultTech Program and second supervisor of my dissertation, for his guidance throughout my dissertation.

Professor Dr. Maria Xanthopoulou, Associate Professor of Byzantine Archaeology at the University of the Peloponnese, Department of History, Archaeology and Cultural Heritage Management, and member of the examination committee, for her comments on the theoretical approach of the theme.

Stelios Kesidis, Conservator of Cultural Heritage Ph.D. candidate in the Laboratory of Archaeometry, Department of History, Archaeology and Cultural Resources Management, of the University of the Peloponnese, for his help on the conduction of the XRF analyses and the interpretation of the Raman Spectroscopy results.

Dr. Anna P. Moutsatsou, Conservation Scientist at the National Gallery - Alexandros Soutzos Museum for the conduction of the multispectral imaging technique on painting, and her help in the interpretation of the data.

Professor Peter Vandenabeele, Professor at the Department of Archaeology and Department of Chemistry of Ghent University, for the conduction of the Raman Spectroscopy technique.

Georgios Magginis, Scientific Director of the Benaki Museum, for his permission to study the painting.

Vasilis Paschalis, Head of the Conservation Department of Benaki Museum, for his help in conducting the analyses on the museum premises.

Mara Verykokou, Curator of the Byzantine and Post-Byzantine collection of the Benaki Museum for providing the archival material relating to the panel painting.

Dr. Eleni Palamara, Post-Doctoral fellow in the Laboratory of Archaeometry, Department of History, Archaeology, and Cultural Resources Management, of the University of the Peloponnese for her involvement in the providing of the Raman and XRF equipment.

Celia Valadu, Ph.D. candidate in the Laboratory of Archaeometry, Department of, History, Archaeology, and Cultural Resources Management, of the University of the Peloponnese Staff Member of the University of Peloponnese, for her help and support throughout the duration of my studies on the MSc Program.

Introduction

During the last decades, the physicochemical documentation of paintings has been gaining ground in Greece. Teams of scientists have conducted many studies, resulting in a rich bibliography. Ostensive, I would like to mention the laboratory of physicochemical research of the National Gallery of Greece, headed by Eleni Kouloumpi, Anna Moutsatsou, and Agni Terlixis, in which many imaging and chromatographic techniques are carried out, Georgios Mastrotheodoros, research associate of National Center for Scientific Research “Demokritos”, Institute of Nuclear & Particle Physics¹, Thomas Mafredas, Ph.D. researcher at the University of West Attica, Department of Conservation of Antiquities and Works of Art², and Ioannis (Yiannis) Karapanagiotis, Professor at the workshop of Chemical and Environmental Technology, Aristotle University of Thessaloniki, Faculty of Science³. The rigorous work of the scientific community demonstrates that the use of physicochemical methods to support archaeological and historical documentation of paintings is becoming increasingly imperative.

So, I decided that the interpretation of an artwork both from the archaeological and physicochemical perspective would give a multifaceted approach to the subject.

The subject of this thesis is the theoretical and non-destructive documentation approach of the late 16th-century icon painting entitled *The Hospitality of Abraham*, now in the Benaki Museum (Figure 1). The reason I chose this painting is that it is a characteristic example of the Cretan School of painting,

¹ Mastrotheodoros, Beltsios, & Bassiakos, 2021; Mastrotheodoros, Theodosis, & Filippaki, 2020.

² Mafredas, 2018; Mafredas, Kouloumpi, & Boyatzis, 2021.

³ Kouloumpi, Moutsatsou, & Terlixis, 2012; Kouloumpi E., Moutsatsou, Trompeta, & Olafsdottir, 2007; Κουλουμπή, Μουτσάτσου, Τερλιξή, Κατσιμπίρη, & Δουλγερίδης, 2006.

that Byzantine tradition and Italian art, especially Venetian Mannerism were mixed. The research aims to investigate the influence of Byzantine tradition and Western art on the artist's style, as well as the construction techniques and color palette that he chose. For the questions to be answered, the painting will be studied typologically and iconographically and then imaging and spectroscopic analyses will be conducted on it.

In the first chapter, the history of portable icon painting will be presented, then the evolution of the Byzantine Art of the portable icons will be expounded and, in the end, the Cretan School of portable paintings will be detailed

The second chapter presents the construction techniques that artists adopted from the first byzantine portable icons made with the encaustic technique until the 16th century when the use of oil as a medium became popular. Also, the pigments chosen during the Byzantine and Post-Byzantine period will be expounded in detail. The reason why these particular periods of art are presented is because the professor Manolis Chatzidakis thought that the studied painting is a work of the post-byzantine School of Cretan Art, in the end of the 16th century.

The third chapter is dedicated to the iconographical and stylistic analysis of the painting. It discusses the biblical story of the Hospitality of Abraham, its history and development as an iconographical theme, and its use in the painting studied here. Afterwards, the painting will be described pictorially and, in the end, the influences of Byzantine tradition and Western art in the picture will be studied.

The fourth chapter contains an extensive report of the physicochemical analyses used for the documentation of painted artifacts. More specifically, the principles of operation of each method and their applications in paintings will be mentioned, along with their advantages and disadvantages.

In the fifth chapter, the goals of the research and the research protocol that was followed during the application of the physicochemical techniques will be presented.

In the sixth chapter, the results obtained from the analytical methods will be presented and the conclusions by studying the results of each method separately and in combination will be presented.

In the final chapter, the conclusions drawn after the completion of the theoretical and physicochemical study of the work will be presented and proposals for future research will be made.

1. The art of portable icon painting

1.1. The history of portable icon painting

The origins of the portable icons must be traced back to Roman Period. Portraits of deified emperors and their families were displayed in temples and public places, and they had ritualistic and idealized character. Also, wooden paintings depicting gods of the popular pagan religions of the time, such as Isis, served as prototypes. In addition, the sepulchral portraits of Fayum, which were placed on mummies are considered as source of inspire⁴.

1.2 The Byzantine icons

Byzantine art is chronologically subdivided into three periods. The first period is Proto-byzantine and covers the era of Constantine I and his successors, the 4th and 5th centuries. According to literary sources, the use of the image can be documented from the 4th century but the oldest surviving samples date back to the 6th century in the Sinai and are today in Kiev and Rome. The earliest images were placed in tombs - like the Fayum portraits of saints and martyrs - to remind their attributes to later generations. Since the 6th century, they have appeared in churches, homes, and workplaces⁵. Unfortunately, there are not many surviving monuments decorated with icons, and therefore science cannot have a complete idea of the painting trends and themes of the first two centuries⁶.

The second period, the so-called Meso-byzantine, started in the 6th century when the emperor of the Byzantine Empire was Justinian I (482-565). When it comes to portable icons, they were usually constructed with waxing (warm wax with pigment) or the encaustic technique (the act of burning in colors)⁷. The oldest surviving icons were found in the Sinai, some of which ended up

⁴ Βοκοτόπουλος, 1995, p. 12.

⁵ Πανσελήνου, 2000, p. 100.

⁶ Ζαμβακέλλης, 1985, p. 19.

⁷ Ζαμβακέλλης, 1985, pp. 19-20.

in Rome and Kiev in the 19th century. Sinai's paintings, attributed to Constantinople workshops, are characterized by a classicizing style with very loose brushstrokes and idealistic expressions in the faces (Figure 2). The volume in the faces and architectures is successfully rendered. The images found in Rome are most likely the work of local workshops. The line plays an important role, the shapes are heavier, although the volume is rendered less successfully⁸.

The period of flourishing followed the centuries of *Iconomachy* when a general cultural decline was observed⁹. *Iconomachy* is the religious movement which lasted two centuries (726-842). Painting during this time is aniconic and gives the impression of decadence¹⁰. However, it seems to have continued in areas outside the Byzantine state. The edicts of Iconomachy did not apply in the Palestinian territories, as they were under Arab rule. From that point of view, Sinai was the only center where the production of icons and their evolution was not interrupted, as icons dating back to the 7th and 8th centuries survived. The classical tradition of the preceding period was succeeded by a more unsophisticated style. The shapes are two-dimensional, with thick outlines, the color palette is limited to the shades of red and chestnut (Figure 3)¹¹.

The rebellion to the images gradually subsided, and the icons began to be used more and more in rituals¹². During the 11th century, the marble temple was replaced by the wooden altarpiece, which was gradually decorated with icons¹³. Artists turned to Hellenistic prototypes during the Macedonian Dynasty (867-1056). This interest in the ancient Greek style is concentrated

⁸ Βοκοτόπουλος, 1998, p. 23.

⁹ Ζαμβακέλλης, 1985, p. 19.

¹⁰ Ζαμβακέλλης, 1985, p. 20.

¹¹ Βοκοτόπουλος, 1995, p. 23.

¹² Βοκοτόπουλος, 1995, p. 13.

¹³ Πανσελήνου, 2000, p. 175.

in the so-called *Macedonian School*. Movement and posture are less austere, and the figures are more beautiful with pleasing colors (Figure 4), the drawing is perfect, the chromatic scale is widened, and the background is made lighter by sun light¹⁴.

The Late Byzantine period started after the fall of Constantinople by the Latins in 1204. The characteristics icons of the Macedonian School of Art were preserved in the Komnenian Dynasty (1081-1185/ 1204-1261)¹⁵. Towards the end of the 13th century, the figures became quite bulky. The facial features were often coarse, and the depiction of emotions was emphasized, with the rendering of intense gazes and gestures (Figure 4). After 1300, the characteristics of the bulky style were abandoned. The movements became calmer, the facial expressions softer, and the figures were lither and unstable, exuding a sophisticated grace. In general, there was a tendency towards refinement and a return to classical standards (Figure 6). In the second half of the 14th century, two trends coexisted in metropolitan art (art of Constantinople). The one is an expressionistic style, with intensely moving figures, that were painted with quick strokes, their naked parts were depicted with vivid, free lights. and the dress folds were intensely rendered (Figure 7). The other one is more classical, with rhythm and symmetry in the compositions, restricted movements, calm expression, and soft dress folds (Figure 8)¹⁶.

After the fall of Constantinople and the abolishment of the Byzantine Empire, Greeks did not live under the same cultural context because, on the one hand, Crete and the islands were ruled by Venetians, and on the other hand,

¹⁴ Ζαμβακέλλης, 1985, 21.

¹⁵ Ζαμβακέλλης, 1985, p. 21.

¹⁶ Βοκοτόπουλος, 1995, p. 25-26.

continental Greece was under Ottoman rule. The former were more privileged because Venetian rulers allowed their subjects to develop artistic activities¹⁷.

1.3. The icons of the Cretan School

Crete, a Venetian possession since 1210, took this role as the economic and political conditions were favorable¹⁸. During the first two centuries of Venetian rule, many ecclesiastical monuments of the island were decorated with murals. From the mid-15th century, the works of Cretan Painters stood out for their quality. They were affected by the metropolitan art of the 14th century, which is more characteristic at the church of Perivleptos in Mystra. The scenes are characterized by rhythm and harmony, the figures are elegant, and their movements are restricted. Also, the role of the line is limited. The adoption of Palaeologan art was possibly due to the artistic contacts between Constantinople and Crete, as attested by written sources¹⁹.

Contrary to what was believed in the previous decades, most Cretan artists did not migrate to Venice. Archival sources have been found and attest that almost all Cretan artists lived and worked on the island²⁰. They familiarized themselves with western art through the work of Venetian painters existing in Crete. For example, some paintings that are attributed to the Vivarini family's workshop, Palma il Vecchio and Titian decorated the monastery of Hagios Frangkiskos in Heraklion. Also, there were works of Italian artists at the houses of urbanites and noble Venetians and Cretans of Heraklion²¹.

The coexistence of the orthodox tradition with the catholic element led to the so-called Cretan Renaissance, in the 16th century. Its most important representatives were Theophanes Strelitzas Bathas, Michael Damaskinos

¹⁷ Χατζηδάκης, 1987, p. 73.

¹⁸ Βοκοτόπουλος, 1998, p. 11.

¹⁹ Βοκοτόπουλος, 1998, pp. 11-12.

²⁰ Βοκοτόπουλος, 1998, pp. 12-13.

²¹ Κωνσταντουδάκη-Κιτρομηλίδου, 1999, p. 90.

(1530/1535--), Georgios Klontzas (c.1535-1608) and Domenikos Theotokopoulos (1541-1614).

Theophanes Strelitzas Bathas, also known as Theophanes the Cretan, was born in Heraklion, but he went to Mount Athos and became a monk. He is considered one of the greatest painters of the Cretan School. His art is Byzantine, but it is affected slightly by western art. His works are characterized by naturalism, the drawing is complicated but not especially decorative, and the *chiaroscuro* is sharp. Also, human figures are simple and slender but not rigid, and their limbs are intensely lined. Theophanes was mainly a muralist, and his most characteristic work is the murals that decorate the monastery of Megisti Lavra at Mount Athos²² but is also thought to be a painter of icons. Although those icons that are attributed to him are not signed, they show all the characteristics of his style, when compared to his known mural work²³. Generally speaking, Theophanes depicts the saints as *Akritai* soldiers (a term used in the Byzantine Empire in the 9th–11th centuries to denote the frontier soldiers guarding the Empire's eastern border, facing the Muslim states of the Middle East). They are tall, wild figures, weather-beaten with an intense, sad gaze. The young saints wear full battle dresses, are armed with various weapons (Figure 9), and the holy men are presented like Mount Athos' hermits of that period in full Byzantine style (Figure 10)²⁴. Although his style is mainly Byzantine, some of his works have vivid Renaissance elements. At the monastery of Hagios Nikolaos Anapafsa in Meteora, his painting *Adam naming the animals* (Figure 11) renders zoomorphic creatures, birds, and torches, typical decorations of renaissance *grottesche* (general adjective for the strange, mysterious, magnificent, fantastic, hideous, ugly, incongruous, unpleasant, or disgusting, and thus is often used to describe

²² Κριτσωτάκης, 1934, pp. 116-118.

²³ Speake, 2000, p. 1630.

²⁴ Κριτσωτάκης, 1934, pp. 116-118.

weird shapes and distorted forms).²⁵. After Theophanes death, his art influenced many later painters, especially those who worked in Mount Athos²⁶.

Michael Damaskinos is the primary representative of the Post-byzantine hagiography and the Cretan School. He mainly worked on portable pictures²⁷. It is unknown when he was born, but it is speculated that the year of his birth was between 1530 and 1535²⁸. At some point, he went to Mount Athos. There he met Theophanes the Cretan, and his art was profoundly influenced by him²⁹. We do not know when he moved to Venice, but certainly, he was there in 1569. He stayed for many years, and he painted many pictures in the church of Hagios Georgios of the Greeks. He also worked on the copy of Italian paintings of the 16th century. One of his most important paintings was the depiction of the first Ecumenical Council, in 1591 (Figure 12). He developed two styles, one inspired by the Palaeologan tradition and the other influenced by the western style. In the works using the former style, he rendered rose sarkoma (lighter flesh tones) on brown proplasma (dark basic color of the shaded areas of each particular part of the icon). He outlined the subjects with vivid brown and formed the naked human limbs with intense white lines. The shape is softer than Palaeologan art, but the ampler folds of the garments are drier and more inflexible (Figure 13). In his western-style works, the shadows are limited, and the human figures have wet eyes and half-open mouths. A characteristic westernized painting is *Saint Sergius, Saint Bacchus, and Saint Justina treading on a decapitated three-headed dragon* (Figure 14). The western elements are the rich blonde hair of Saint Justina, her elaborate

²⁵ Κωσταντουδάκη-Κιτρομηλίδου, 1999, p. 92.

²⁶ Harris, 2000, p. 1630.

²⁷ Κριτσωτάκης, 1934, p. 131.

²⁸ Βοκοτόπουλος, 1998, p. 24.

²⁹ Κριτσωτάκης, 1934, pp. 132-133.

hairstyle, and her pale face. Also, her crown, with the two cupids that hold a ruby, is inspired by the Venetian paintings of the period³⁰.

Georgios Klontzas was another top artist at the end of the 16th century³¹. He specialized in the painting of portable pictures and triptychs. He mainly made multifaceted compositions of micrographic size enriched with secondary scenes³². He removed himself from Byzantine art and followed Venetian Mannerism to a great extent. He had Italian copper engravings as a prototype but formed his personal style, as he created characteristic countenances and added to traditional themes many buildings of the Italian Renaissance's architecture (Figure 15). His figures were mainly tall and slim, and they often wore Frankish and Oriental costumes of that time (Figure 16). His influence on the artists of the 17th century is not as profound as Michael Damaskinos', but many of them imitated the iconographical types he inserted³³.

One of the most important artists in the West is Dominikos Theotokopoulos, better known as El Greco, the Greek. He was born in Heraklion, Crete, in 1541³⁴. He excelled early as an artist, for as early as 22 he was called maestro³⁵. He lived in Crete until the age of 26-27 (probably until 1567). The Cretan period of Domenikos Theotokopoulos includes so far at least four works: 1) the Dormition of the Theotokos (1565-1566) (Figure 33), 2) the Evangelist Luke paints the image of the Virgin Mary (1560-1567) (Figure 34), 3) the Adoration of the Magi (1565-1567) (Figure 35), 4) the Extreme Humiliation (painted according to an archival document, before the end of 1566 and today destroyed and unconsecrated). The number is too limited for a production that must have covered a period of eight or ten years. The important discovery of

³⁰ Βοκοτόπουλος, 1998, pp. 27-32.

³¹ Βοκοτόπουλος, 1998, p. 34.

³² Χατζηδάκης, 1987, p. 91.

³³ Βοκοτόπουλος, 1998, pp. 35-40.

³⁴ Κριτσωτάκης, 1934, p. 122. Χατζηδάκης, 1987, p. 309.

³⁵ Χατζηδάκης, 1987, p. 309.

the painter's signature on the picture of the Dormition of the Theotokos located in Syros allowed for a more substantial review of other works by the painter, which lacked his signature. The three surviving works have some essential features in common: high quality, free preliminary drawing under the painting surface, harmony in color and light reflections, adoption of Italian influences, speed of execution, pictorial quality³⁶.

The ambitious young artist emigrated to tour the great artistic centers of the West in 1567³⁷. Most likely he stayed in Venice until 1570. What is certain is that he was a pupil of Titian. The art of Titian has been associated with the mature period of Theotokopoulos, however, a closer association of Theotokopoulos with the art of Tintoretto is observed³⁸.

Theotokopoulos then emigrated to Spain and, after a short sojourn in Madrid, ended up in Toledo where he stayed for the rest of his life. In his early years in Spain, his works maintained a slight influence on the Venetian style. The new period of Theotokopoulos' art began with his famous work *the Burial of the Count of Orgaz* (Figure 36). As Theotokopoulos got older, his artistic activity increased rather than decreased. His last works are, *St. Martin on horseback* (1597-1599), *the Outpouring of the Holy Spirit* (1597-1600), *Christ on the Mount of Olives* (1605-1607), and *View of Toledo* (1604-1614) (Figure 37). The figures in the last phase of his art are elongated as if they have lost the weight of the body, the colors create sharp contrasts, and the light haunting creates a mysterious atmosphere³⁹. Theotokopoulos died in 1614 in Toledo. For centuries his art was rejected until the early 20th century, when his work was appreciated by expressionist painters⁴⁰.

³⁶ Κωσταντουδάκη-Κιτρομηλίδου, 1999, p. 93.

³⁷ Βοκοτόπουλος, 1998, p. 23.

³⁸ Χατζηδάκης, 1950, pp. 398-399.

³⁹ Κριτσωτάκης, 1934, pp. 126-127.

⁴⁰ Χατζηδάκης, 1950, p. 373.

Most of the next-generation painters who acted in the first decades of the 17th century rejected the innovations of Damaskinos and Klontzas and returned to the 15th and early 16th-century prototypes. After the catastrophic war of 1645-1669, which ended with the surrender of Heraklion to Ottomans, many artists fled to the Ionian Islands, Venice, and Cyclades. The role of Crete as the artistic center had come to an end⁴¹.



Figure 1: *The Hospitality of Abraham*, late 16th c., panel painting, Athens, Benaki Museum of Greek Culture (derived from: https://www.benaki.org/index.php?option=com_collectionitems&view=collectionitem&Itemid=162&id=108267&lang=el).

⁴¹ Βοκοτόπουλος, 1998, pp. 42-43.



Figure 2: Mary & Child,, second half of 6th c., encaustic icon, Mount Sinai, Monastery of Agia Aikatairini
(derived from: [https://en.m.wikipedia.org/wiki/File:Mary %26 Child Icon Sinai 6th century.jpg](https://en.m.wikipedia.org/wiki/File:Mary_%26_Child_Icon_Sinai_6th_century.jpg)).



Figure 3: Ascension, 9th-10th c., panel painting, Mount Sinai, Monastery of Agia Aikaterini (derived from: <https://www.pemptousia.gr/2011/06/stin-analipsi-tou-kiriou/>).

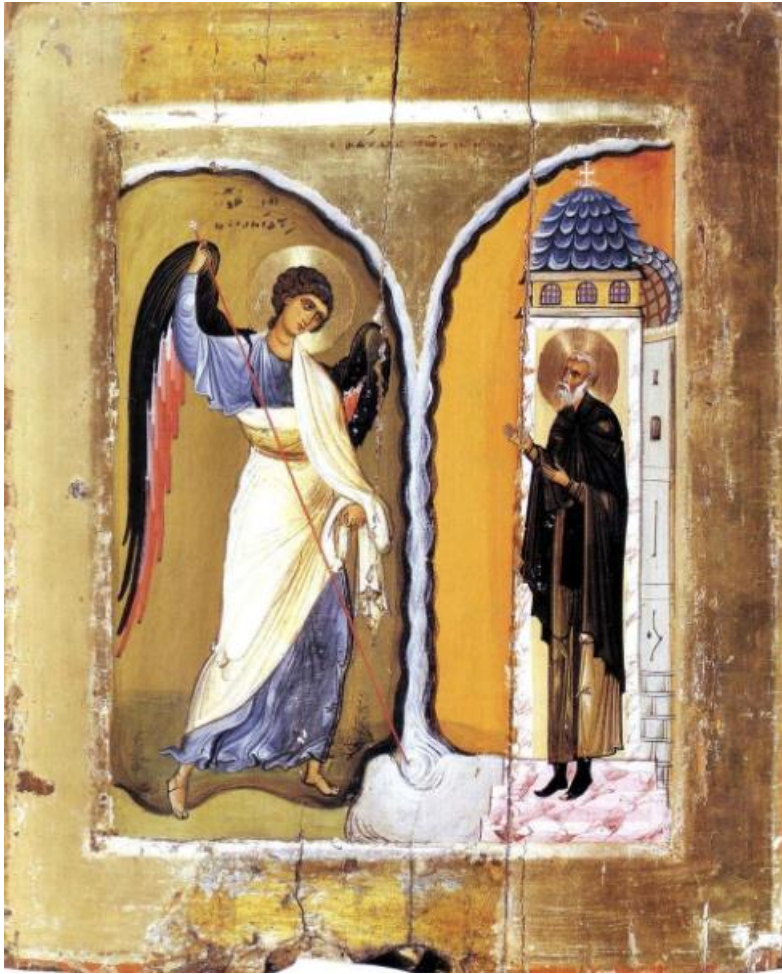


Figure 4: Archangel Michael and the monk Archippus at Chonae, the second half of 12th c., panel painting, Mount Sinai, Monastery of Agia Aikaterini (derived from: https://en.m.wikipedia.org/wiki/File:Michael_Miracle_Icon_Sinai_12th_century.jpg).



Figure 5: Evangelist Matthew, end of 14th-15th c., panel painting, Ohrid, Panagia Perivleptos (derived from: http://www.krakow2000.pl/2000wydarzenia/11_kolebka.htm).



Figure 6: Annunciation, early 14th c., panel painting, Ohrid, Panagia Perivleptos, (derived from: https://el.m.wikipedia.org/wiki/%CE%91%CF%81%CF%87%CE%B5%CE%AF%CE%BF:Ohrid_annunciation_icon.jpg).

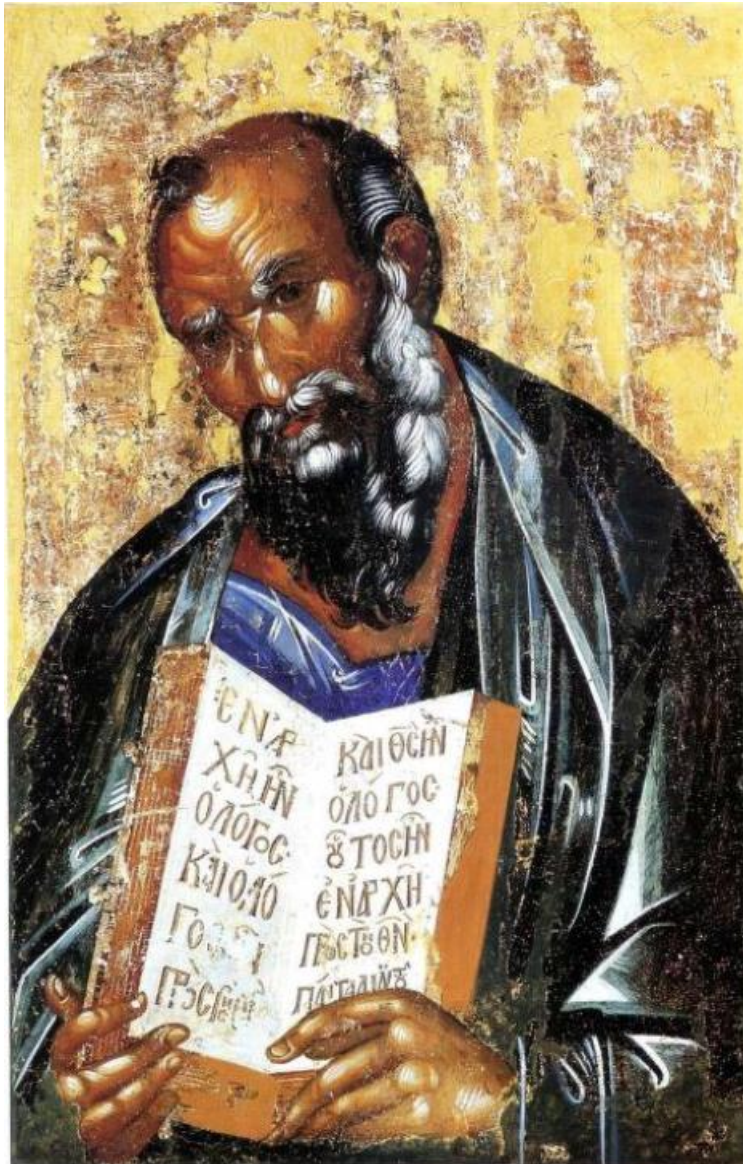


Figure 7: Agios Ioannis Theologos,, end of 14th.-early 15th c., panel painting, Mytilene, Byzantine and Christian Museum of Holy Cathedral of Mytilene (<https://russianicons.wordpress.com/tag/greek-icons/page/4/>).

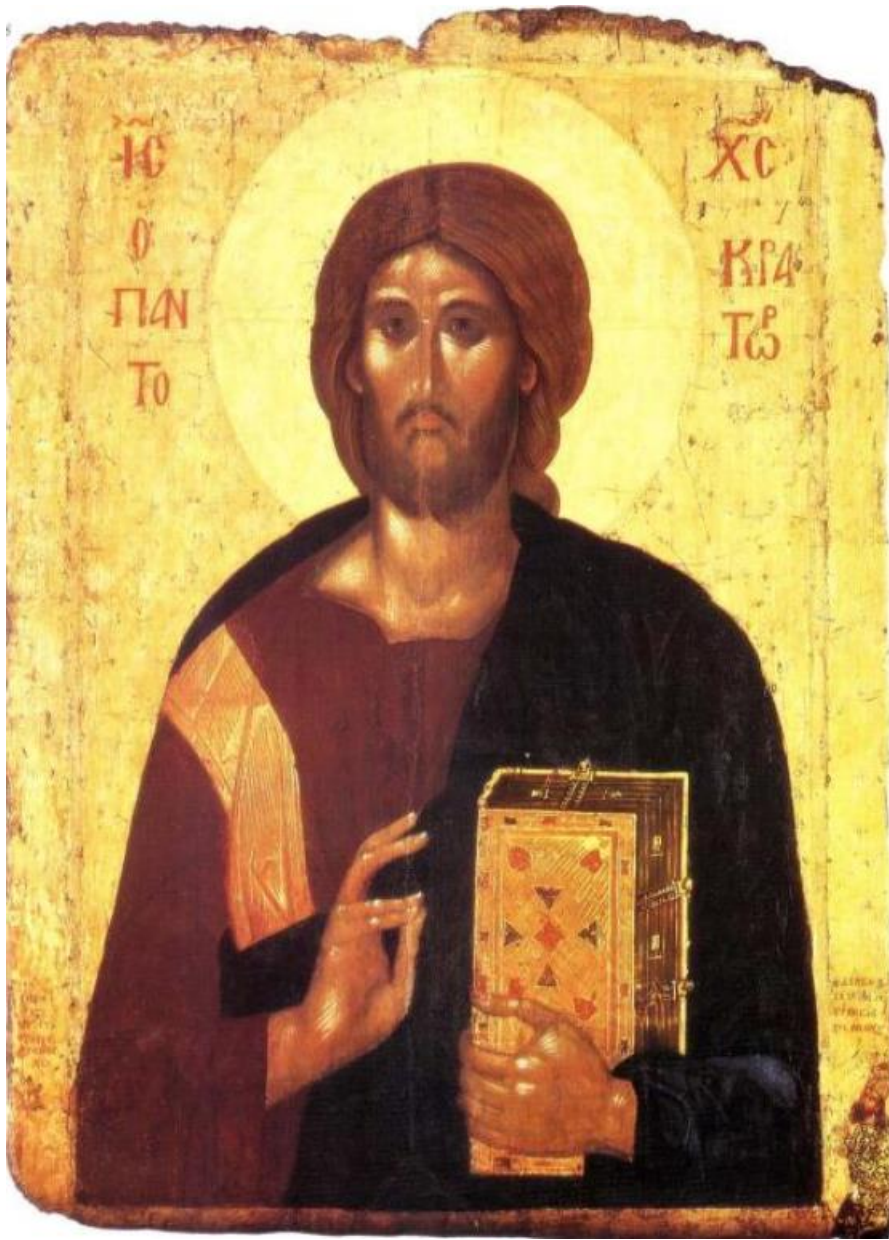


Figure 8: *Christos Pantokrator*, 1363, panel painting, Saint Petersburg, Hermitage Museum (https://www.icon-art.info/book_contents.php?book_id=29&chap=10&ch_12=9#pic543)



Figure 9: Theophanes Strelitzas Bathas, *St George and St Demetrios*, c 1550, panel painting, Mount Athos, Monastery of Megisti Lavra (derived from: <http://www.diakonima.gr/2009/09/10/the-holy-monastery-of-the-great-lavra/>).



Figure 10: Theophanes Strelitzas Bathas, Nativity Scene, 1546, egg tempera on wood, Mount Athos, Stavronikita Monastery (derived from: <https://www.macedonian-heritage.gr/Athos/General/Art.html>).



Figure 11: Theophanes Strerlitzas Bathas, *Adam_naming_the_animals*, 16th c., Meteora, St. Nicholas Anapavsa Monastery (derived from: https://el.wikipedia.org/wiki/%CE%91%CF%81%CF%87%CE%B5%CE%AF%CE%BF:Adam_naming_the_animals_-_St._Nicholas_Anapavsa_Monstery,_Meteora_-_Theophanes_of_Crete,_16th_c..jpg).



Figure 12: Michael Damaskinos, First Ecumenical Council, 1591, panel painting, Heraklion, Museum of Hagia Aikaterini of Sina (derived from: <http://iakm.gr/agia/Page?lang=gr&name=infotext&id=501&sub=504&sub2=555>).



Figure 13: Michael Damaskinos, *Hagios Ioannis*, second mid-16th c., panel painting, Zakynthos, Byzantine Museum (derived from: <https://paletteart.wordpress.com/2012/09/13/%CE%B4%CE%B1%CE%BC%CE%B1%CF%83%CE%BA%CE%B7%CE%BD%CF%8C%CF%82-%CE%BC%CE%B9%CF%87%CE%B1%CE%AE%CE%BB-michael-damaskinos-153035-159293/%CE%B4%CE%B1%CE%BC%CE%B1%CF%83%CE%BA%CE%B7%CE%BD%CF%8C%CF%82-%CE%BC%CE%B9%CF%87%CE%B1%CE%AE%CE%BB-%CE%B1%CE%B3-%CE%B9%CF%89%CE%AC%CE%BD%CE%BD%CE%B7%CF%82-%CE%BF-%CF%80%CF%81%CF%8C%CE%B4%CF%81%CE%BF/>).



Figure 14: Michael Damaskinos, *Saints Sergius, Justin and Bacchus*, 1584-1593, egg tempera on panel, Corfu, Antivouniotissa Museum (derived from: <http://iakm.gr/agia/Page?name=enotita&lang=gr&id=501&sub=555>).



Figure 15: Georgios Klontzas, *Saint George the Dragonslayer*, second mid of 16th c., egg tempera on panel, Athens, Christian and Byzantine Museum (derived from:

https://www.byzantinemuseum.gr/el/permanentexhibition/from_Byzantium_to_Modern_Era/society_art_in_Venetian_Crete/.



Figure 16: Georgios Klontzas, *The Sacrifice of Abraham and the Adoration of the Magi*, 16th c., private collection (https://en.wikipedia.org/wiki/Georgios_Klontzas).



Figure 17: Domekikos Theotokopoulos, *Dormition of the Virgin*, 1565-1566, tempera on panel, Ermoupolis, Holy Cathedral of the Dormition of the Virgin (derived from: [https://el.wikipedia.org/wiki/%CE%9A%CE%BF%CE%AF%CE%BC%CE%B7%CF%83%CE%B7_%CF%84%CE%B7%CF%82_%CE%98%CE%B5%CE%BF%CF%84%CF%8C%CE%BA%CE%BF%CF%85_\(%CE%98%CE%B5%CE%BF%CF%84%CE%BF%CE%BA%CF%8C%CF%80%CE%BF%CF%85%CE%BB%CE%BF%CF%82\)](https://el.wikipedia.org/wiki/%CE%9A%CE%BF%CE%AF%CE%BC%CE%B7%CF%83%CE%B7_%CF%84%CE%B7%CF%82_%CE%98%CE%B5%CE%BF%CF%84%CF%8C%CE%BA%CE%BF%CF%85_(%CE%98%CE%B5%CE%BF%CF%84%CE%BF%CE%BA%CF%8C%CF%80%CE%BF%CF%85%CE%BB%CE%BF%CF%82))).

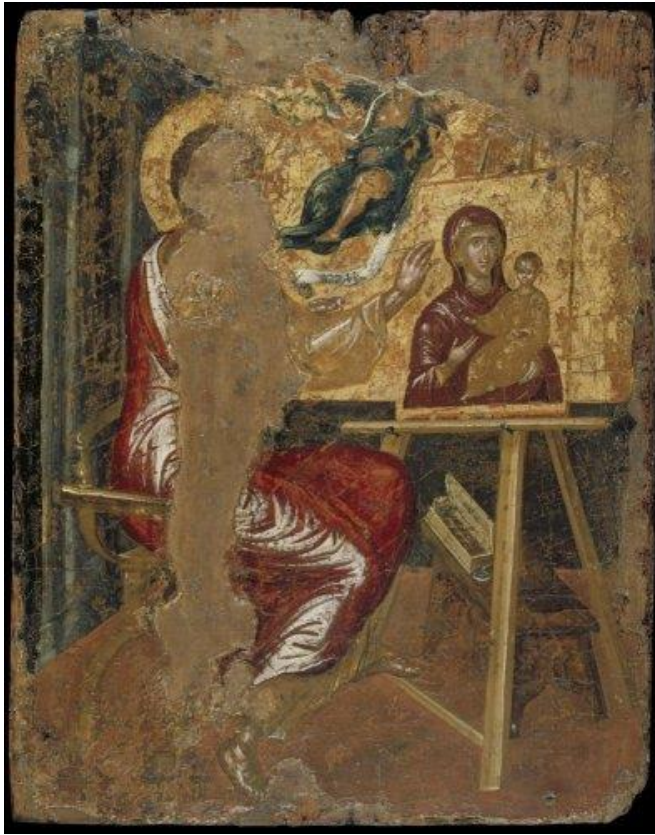


Figure 18: Domenikos Theotokopoulos, Evangelist. Luke Painting the Virgin, 156-1567, tempera on panel, Athens, Benaki Museum of Greek Culture (derived from: https://en.wikipedia.org/wiki/File:El_Greco_-_St_Luke_Painting_the_Virgin_-_Google_Art_Project.jpg).



Figure 19: Domenikos Theotokopoulos, *The Adoration of the Magi*, 1565-1567, tempera on panel, Athens, Benaki Museum of Greek Culture (derived from: [https://el.m.wikipedia.org/wiki/%CE%91%CF%81%CF%87%CE%B5%CE%AF%CE%BF:El_Grec_o_-_The_Adoration_of_the_Magi_-_Google_Art_Project_\(721007\).jpg](https://el.m.wikipedia.org/wiki/%CE%91%CF%81%CF%87%CE%B5%CE%AF%CE%BF:El_Grec_o_-_The_Adoration_of_the_Magi_-_Google_Art_Project_(721007).jpg)).



Figure 20: Domenikos Theotokopoulos, *The Burial of the Count of Orgaz*, 1586, oil on canvas, Toledo, Church of Santo Tome (derived from: https://el.wikipedia.org/wiki/%CE%97_%CF%84%CE%B1%CF%86%CE%AE_%CF%84%CE%BF%CF%85_%CE%BA%CF%8C%CE%BC%CE%B7_%CF%84%CE%BF%CF%85_%CE%9F%CF%81%CE%B3%CE%BA%CE%AC%CE%B8).



Figure 21: Domenikos Theotokopoulos, *View of Toledo*, 1541-1614, oil on canvas, New York, Metropolitan Museum (derived from: https://en.wikipedia.org/wiki/View_of_Toledo).

2. Techniques of portable icons painting

Portable icons are multilayered compositions between the support and the top layer, the varnish. The process differs, but there are fixed fundamental components⁴²:

- 1) The support, which is mainly canvas, wood, paper, and parchment⁴³.
- 2) The ground layer, or priming, which is usually a mixture of animal glue and gypsum⁴⁴ or chalk.
- 1) Pigments that are mainly powders from organic or inorganic materials, like animal, vegetable, or mineral sources⁴⁵.
- 2) Media/Binders that are fluid and used to make the pigments applicable and dispersible with a brush⁴⁶. In Europe, they are proteinaceous binders, polysaccharidic gums, siccative oils⁴⁷, natural waxes, or a mixture of two or more materials⁴⁸.
- 3) The completed icon is covered with a layer of varnish⁴⁹ coming mainly from natural resins.

Until the 6th century byzantine icons were constructed with the encaustic technique⁵⁰. Artists used a quadrangular wood, usually cedar, linden, or cypress, and made it rectangular. They preferred hard woods to soft ones because the primer and pigments were not absorbed. The primer was a layer of *gesso*, a mix of gypsum and glue. After this step, the artist started the painting. The pigments were mixed with warm wax to be more spreadable in that technique. The tools used were brushes of squirrel or camel hairs, and a

⁴² Mafredas, 2018, p. 66.

⁴³ Colombini & Modugno, 2004, p. 147.

⁴⁴ Colombini, Andreotti, Bonaduce, Modugno, & Ribechini, 2010, p. 716.

⁴⁵ Kenna, 1985, p. 347.

⁴⁶ Colombini, Andreotti, Bonaduce, Modugno, & Ribechini, 2010, p. 716.

⁴⁷ Colombini & Modugno, 2004, p. 147.

⁴⁸ Colombini, Andreotti, Bonaduce, Modugno, & Ribechini, 2010, p. 716.

⁴⁹ Kenna, 1985, p. 347.

⁵⁰ Ζαμβακέλλης, 1985, p. 33.

metal instrument, the *cestrum*, which may have had the same use as a modern knife⁵¹.

The first byzantine portable paintings were composed of various materials, like stone (marble or steatite), ivory, and metals. During the Byzantine Period, the use of well-prepared wood was systematized and prevailed⁵².

There has not been a saved handbook that presents Byzantine artists' materials and techniques. Maybe that happened because masters of workshops used to transmit their knowledge orally to the students, and the latter promised to reveal the secrets of their art only to their most qualified apprentices.

Tempera prevailed from the 7th century onwards, and most mobile pictures were composed with that technique. Artists chose a smooth piece of wood without gnarls, usually of walnut, cedar, linden tree, or pine tree. They reinforced the back part of the panel with crosspieces of wood. Then they cover it with a layer of gypsum mixed with boiled glue. Before that preparation, they sometimes glued a piece of linen or other thin fabric to the support⁵³. After that, the master transferred the drawing from the paper to the panel. Although some artisans painted freehand, in most cases, they used paper worksheets. With a sharp tool, successive holes were drilled in the design lines of the paper worksheets, and then the punched design was placed on the preparation. With the use of charcoal powder, the design was impressed on it⁵⁴. The Post-Byzantine monk and hagiographer Dionysius of Fourni (1670-1746) described another procedure of making copies from the prototype in his treatise *Interpretation of the Art of Painting (Hermeneia tes Zographikes Technes)* (1728-1733). More specifically, he wrote that the panel painter should mix black color and garlic juice and apply the mixture to the

⁵¹ Thompson, 1982, pp. 2-7.

⁵² Ζαμβακέλλης, 1985, pp. 32-35.

⁵³ Ζαμβακέλλης, 1985, pp. 32-35.

⁵⁴ Μαστροθεόδωρος, 2016, p. 23.

saints' figures. Then, he should mix a red color with garlic juice and paint the white and red parts of the face and the clothes with this mix. Consequently, he must moisturize a paper sheet of the prototype's size and carefully place and press it on the *gesso* ground preparation of the panel. Afterwards, he should lift the corner of the sheet to see if an impression has been left. If not, he must press a second time more heavily⁵⁵. Thus, an artist can make a copy identical to the prototype.

During the post-Byzantine Period, the techniques and materials for portable paintings generally did not change. However, under the impact of the Renaissance, oil colors started to be used more and more⁵⁶.

It is worth mentioning the primary pigments used in Byzantine and Post-Byzantine Art:

Red Pigments: 1) Hematite (iron oxide). The three kinds of hematite used are the caput mortuum, the red ochre, and the warm ochre. 2) Vermilion. Dionysius of Fournia described the composition of synthetic vermilion, which is composed of mercury and sulfur. He recommended its use on the cheeks and lips. 3) Red lake. It is in the form of dust and usually originated from useless pieces of red clothes. It was used for tempera and oil colors. 4) Minium. It tends to blacken on frescoes and fade on portable paintings.

Yellow pigments: 1) Ochre. It was the main yellow pigment for centuries, and depending on the mineral it originates from (goethite, limonite, etc.), it has different shades. 2) Orpiment. Dionysius of Fournia informed us that it was unsuitable for wall painting, so it is assumed that it was used for tempera and oil colors. It is opaque, and usually, it is combined with indigo for the composition of green color. 3) Yellow lakes. Dionysius of Fournia called all the plant-based yellow pigments used in the Middle Ages yellow lakes.

⁵⁵ Vassilaki, 2009, p. 320.

⁵⁶ Μαστροθεόδωρος, 2016, p. 22.

Green pigment: 1) Malachite. It has a low reflective index (1.5), so it cannot be used for oil colors. In addition, it blackens on wall painting. Therefore, it is suitable only for tempera and must be coarse-grain to render the dark green. 2) Green earth. It comes from the minerals celadonite and glauconite. The main region of origin of the former is Verona, and the latter is Czechoslovakia. It has a low reflective index (1.5-1.6), and thus, it is suitable for fresco and tempera. It is especially durable and thus was very popular during the Medieval and Renaissance Periods. 3) Verdigris. It is not opaque. It is sensitive to acids, alkalis, and sulfur fumes. When exposed to the sun, it turns grey or brown (Figure 22). It also dissolves in water. However, it was used widely during the Middle Ages and Renaissance because of its nice shade and low cost. Dionysius of Fourna described the way was composed. He said that pieces of copper with vinegar should be placed inside a copper vase and let dry under the sun until the vinegar is curdled. Then, the pieces of copper must be removed, and the resulting liquid be placed in another vase until dry.

Blue pigments: Blue pigments have the same rate of deterioration as green ones. Nevertheless, the reasons for this are different. The problem is the oils and the varnishes used because they tend to turn yellow over time. 1) Azurite. After the 9th century, azurite became especially popular because the Egyptian blue pigment disappeared, and indigo and ultramarine were expensive. In 1450 enamel appeared, so the use of azurite decreased. In the fresco, azurite changes because the alkalinity dissolves over time. In oil paint, it changes when free acids are formed, from the breakdown of the polymerized linseed oil during aging. Thus, it was observed that azurite is resistant only to egg tempera. 2) Blue ashes. Bluestone, which is copper sulfate, creates a blue solution in water. With the addition of ammonia, the solution becomes dark blue, and with the addition of lime, copper hydroxide is precipitated. When the dust dries, it becomes lighter blue because ammonia

evaporates. This pigment is the so-called Bremen blue. 3) Ultramarine. After the 9th century, it was used more and more often because of the disappearance of Egyptian blue. It comes from the mines of Batakshah's valley in Northeastern Afghanistan. Ultramarine has a low dispersion index (1.5), so it is not particularly opaque. In oil paintings, it must be combined with a white pigment. Its best rendering is with tempera. It resists alkalis but not acids because it decolorizes. In any case, it presents degradation in open spaces when mixed with binders because acids are produced by the depolymerization of the binders from solar radiation. 4) Indigo. In Europe, it derives from a plant called *Isatis Tictoria*, which grows in temperate areas. The leaf juice is colorless, but when it dries, it becomes blue. Its rendition in fresco and tempera is particularly good, but with oils, it turns yellow.

Brown pigments: Artists quite often made brown pigments by mixing yellow ochre, red hematite, and black pigment. Different shades were created depending on the differentiation in the ratio of the three elements. Also, painters used natural brown pigments independently or by adding them to the previous mixture. Two natural brown pigments are two variations of ochre. One was the so-called sienna, and the other was the brown ochre, an ordinary ochre of brown color instead of yellow. The most qualified brown ochre of the Byzantine and Post-Byzantine period was the one from the mines of Cyprus. In Byzantine Art, sienna was not found in any pieces of Art, and in the Post-Byzantine Period, it was found in few. The brown ochre cannot be traced because it does not differentiate chemically from the yellow ochre. The most important brown pigment, especially in Eastern hagiography, was ombre. It has a brown-green shade, and when it is baked, it becomes clear brown. Dionysius of Fournas recommended its use for the beards and faces of the figures.

White pigments: When there was a need for a white surface, the background of lime remained unpainted. This technique was usually used in the

parchments of saints or the angels' wings. White pigments were needed for the mixes and the white strokes. The chemical substance for those pigments was always calcite, i.e., calcium carbonate. 1) Cerussite. Dionysius ek Foura wrote that cerussite derives from lead. He also said it should be used with oils and egg yolk on wood paintings. It acts as a desiccant with oil and forms lead soaps with free fatty acids. Thus, a film is formed that is hard, homogenous, and without pores. In closed spaces, it does not deteriorate. In clean open spaces, it can be yellowish due to the oil, but that happens only in paler shades. Nevertheless, in closed spaces with smoke, thus sulfurous pectic compounds, the white lead is converted into a black sulfurous lead. However, if the pigment is lacquered, the blackening process is delayed and sometimes invisible. 2) In Europe, there is plenty of cheap natural mineral calcite, which formed during geological periods and originated from calcium microorganisms. The mineral is grounded, and the grain sizes are separated by the water sedimentation method. It has a refractive index of 1.5 and is therefore unsuitable for oil, while it is very satisfactory in watercolors and tempera. 3) Instead of calcite, other calcareous natural materials were often used, such as grated eggshells or sea shells, which gave a nicer white color. These materials were mainly used to lighten the shade of pigments that do not mix with cerussite, such as orpiment, cinnabar, and others.

Black pigments: They are usually charcoal of plant origin. Dionysius mentions three kinds of black. There is no more information about the two, which he calls mavroxy and black teggi. The third is easily distinguished because it is carbon black, and he mentions it as the best quality for complex cases. Charcoal was used as a black pigment. The existing variety is only due to the different origins and the way of production. Better quality is given by

willow, beech, and maple. After carbonization, the coal is ground to powder, washed with water to remove potash, then dried and ground again⁵⁷.

The golden leaves were usually used to decorate the halos of the holy figures and the background⁵⁸. The artist cast the gold into ingots and then rolled them until they became continued ribbons. The beating was succeeded by putting square sheets of gold between bigger sheets of parchments. The parchments had been previously rubbed with calcite gypsum. The resulting pile was hammered until parts of gold spread out of the edges of parchments. The process was repeated. After hammering, the golden sheets are cut into squares on a leather cushion with a cane blade knife. The golden pieces were then placed on the primer with the help of a tweezer⁵⁹. After the gilding, the gold leaves were polished with agate or wolf cuspid⁶⁰. Occasionally, alloying took place to achieve additional hardness, durability, and different shades. In water gilding, the golden leaves were placed upon a specially prepared ground of bole and grain. Bole is a soft, smooth, greasy, red-brown clay that, together with the gesso, acts as a cushion against which the gold can be burnished. Furthermore, its color affects the final shade. The grain is blended until it becomes foam and is left to be liquified again. The bole in the form of lumps is ground with water and then mixed with the grain. The mixture is applied upon the gesso in several layers. After it is left to dry, the ground is ready for gilding⁶¹.

During the Renaissance, when the ideas of human liberation and rebirth spread, artists started experimenting with different media. Flemish painters popularized the use of oil as a medium⁶². From the 15th century, most great

⁵⁷ Καπετανίδης, pp. 3-23.

⁵⁸ Ζαμβακέλλης, 1985, p. 35.

⁵⁹ Katsibiri, 2003, p. 38.

⁶⁰ Ζαμβακέλλης, 1985, p. 35

⁶¹ Katsibiri, 2003, pp. 41, 44-45.

⁶² Kouloumpi, Moutsatsou, & Terlix, 2012, pp. 361-362.

Low Countries and Italy painters used the oil painting technique⁶³. Also, Venetian artists of the 15th-16th century introduced the so-called *tempera-grassa* technique, in which oily media were combined with the tempera technique⁶⁴. Oil paints were made from powdered pigments that were mixed with a drying oil. Linseed oil was used most often, but walnut oil and poppy oil were also preferable. Artists sometimes warmed oil to avoid the cracking and shrinking of the colors. Once an oil painting was finished, a thin layer of varnish was spread for protection (Figure 23)⁶⁵.



Figure 22: Panselinos Emanuel, Hagios Ioannis the Theologian dictates the Gospel to his discipline Prochorus, mural, Hagion Oros, cathedral church of Protato (derived from: Καπετανίδης, Ν.. Τεχνικές Μέθοδοι Βυζαντινής και Μεταβυζαντινής Αγιογραφίας Μέρος Πρώτο: χρωστικές, pg. 10).

⁶³ Cartwright, 2020, pp. 5-6

⁶⁴ Kouloumpi, Moutsatsou, & Terlixi, 2012, p. 362.

⁶⁵ Cartwright, 2020, pp. 5-6.

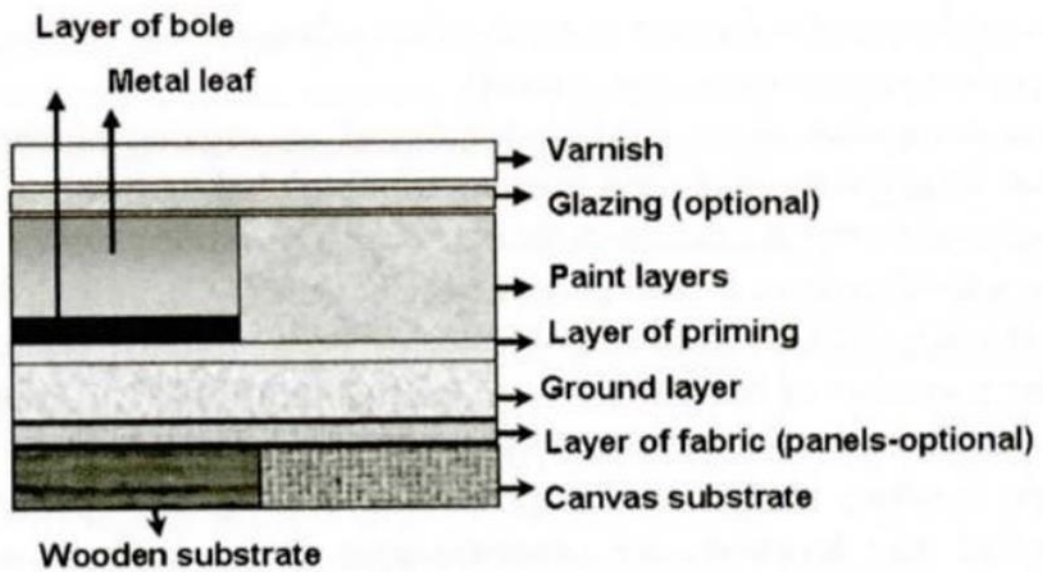


Figure 23: Stratigraphy of a typical painting (derived from: Kouloumpi, E., Moutsatsou, A. M., & Terlixi, A.-V. (2012). *Canvas and Panel Paintings: Techniques and Analyses*. In *Analytical Archaeometry: Selected topics*. Royal Society of Chemistry, pg. 363) .

3. The Hospitality of Abraham

3.1. Historical Evolution

The story of the Hospitality of Abraham was described in the book of Genesis of Bible in chapter 18 from line 18:1-15:

[18:1] The LORD appeared to Abraham by the oaks of Mamre, as he sat at the entrance of his tent in the heat of the day.

[18:2] He looked up and saw three men standing near him. When he saw them, he ran from the tent entrance to meet them, and bowed down to the ground.

[18:3] He said, "My lord, if I find favor with you, do not pass by your servant.

[18:4] Let a little water be brought, and wash your feet, and rest yourselves under the tree.

[18:5] Let me bring a little bread, that you may refresh yourselves, and after that you may pass on - since you have come to your servant." So they said, "Do as you have said."

[18:6] And Abraham hastened into the tent to Sarah, and said, "Make ready quickly three measures of choice flour, knead it, and make cakes. "

[18:7] Abraham ran to the herd, and took a calf, tender and good, and gave it to the servant, who hastened to prepare it.

[18:8] Then he took curds and milk and the calf that he had prepared, and set it before them; and he stood by them under the tree while they ate.

[18:9] They said to him, "Where is your wife Sarah?" And he said, "There, in the tent."

[18:10] Then one said, "I will surely return to you in due season, and your wife Sarah shall have a son." And Sarah was listening at the tent entrance behind him.

[18:11] Now Abraham and Sarah were old, advanced in age; it had ceased to be with Sarah after the manner of women.

[18:12] So Sarah laughed to herself, saying, "After I have grown old, and my husband is old, shall I have pleasure?"

[18:13] The LORD said to Abraham, "Why did Sarah laugh, and say, 'Shall I indeed bear a child, now that I am old?'

[18:14] Is anything too wonderful for the LORD? At the set time I will return to you, in due season, and Sarah shall have a son."

[18:15] But Sarah denied, saying, "I did not laugh"; for she was afraid. He said, "Oh yes, you did laugh."

[18:16] Then the men set out from there, and they looked toward Sodom; and Abraham went with them to set them on their way.

[18:17] The LORD said, "Shall I hide from Abraham what I am about to do,

[18:18] seeing that Abraham shall become a great and mighty nation, and all the nations of the earth shall be blessed in him?

[18:19] No, for I have chosen him, that he may charge his children and his household after him to keep the way of the LORD by doing righteousness and justice; so that the LORD may bring about for Abraham what he has promised him."

[18:20] Then the LORD said, "How great is the outcry against Sodom and Gomorrah and how very grave their sin!

[18:21] I must go down and see whether they have done altogether according to the outcry that has come to me; and if not, I will know."

[18:22] So the men turned from there, and went toward Sodom, while Abraham remained standing before the LORD.

[18:23] Then Abraham came near and said, "Will you indeed sweep away the righteous with the wicked?"

[18:24] Suppose there are fifty righteous within the city; will you then sweep away the place and not forgive it for the fifty righteous who are in it?

[18:25] Far be it from you to do such a thing, to slay the righteous with the wicked, so that the righteous fare as the wicked! Far be that from you! Shall not the Judge of all the earth do what is just?"

[18:26] And the LORD said, "If I find at Sodom fifty righteous in the city, I will forgive the whole place for their sake."

[18:27] Abraham answered, "Let me take it upon myself to speak to the Lord, I who am but dust and ashes.

[18:28] Suppose five of the fifty righteous are lacking? Will you destroy the whole city for lack of five?" And he said, "I will not destroy it if I find forty-five there."

[18:29] Again he spoke to him, "Suppose forty are found there." He answered, "For the sake of forty I will not do it."

[18:30] Then he said, "Oh do not let the Lord be angry if I speak. Suppose thirty are found there." He answered, "I will not do it, if I find thirty there."

[18:31] He said, "Let me take it upon myself to speak to the Lord. Suppose twenty are found there." He answered, "For the sake of twenty I will not destroy it."

[18:32] Then he said, "Oh do not let the Lord be angry if I speak just once more. Suppose ten are found there." He answered, "For the sake of ten I will not destroy it."

[18:33] And the LORD went his way, when he had finished speaking to Abraham; and Abraham returned to his place⁶⁶.

The Hospitality of Abraham is one of the few themes in the Old Testament that, due to its special symbolism, took a special place in iconography from the Early Christian Period and was used throughout the Byzantine Period until the Late Post-Byzantine Times⁶⁷.

Because God could not be pictured, the theme of Abraham's Hospitality is used symbolically to indicate His presence. In this theme, the middle angel is depicted instead of Christ, to His right side, the second angel symbolizes the Father and to the left, the third angel replaces the Holy Spirit⁶⁸.

The angels in Byzantine Hagiography should not have special gender characteristics, neither male nor female. While carrying out a peaceful mission, they wear an ancient garment in white, which symbolizes joy and innocence. On the sleeves, at shoulder height, they have a golden strip, the *clavus*. In a similar mission, they may wear the uniform of deacons with an *orarion* (long, narrow stole decorated with crosses worn by deacons and subdeacons of the Eastern Orthodox church). More formally dressed they wear imperial uniforms with *pallium* (a long strip on the left shoulder, falling straight in front, below the waist, and with the back part drawn round forward and hanging over the left arm) and gold ornaments with precious stones. This outfit can also be accompanied by a padded buckle that closes at the neck. When they have a mission of protection, escort, or punishment they are

⁶⁶ Genesis, 18:1-15.

⁶⁷ Χαραλάμπους-Μουρίκη, 1964, p. 87.

⁶⁸ Ζαμβακέλλης, 1985, p. 53.

usually in their military uniform. All angelic figures carry out divine commands, convey heavenly messages, accompany humans, protect them, or become their punishers. An indication of divine command or authority is the *scepter* held in the right hand. Angels when they are above the earth appear in clouds because the cloud symbolizes the power of God. When they step on the earth, sometimes they wear sandals or are barefoot, which is considered a sign of their holiness ⁶⁹.

3.2. Description

The Hospitality of Abraham is a panel painting that belongs to the Benaki Museum of Greek Culture. Its dimensions are 0.54X0.806X0,17 m. (Figure 24)⁷⁰. Until 1965, it was in the church of Konstantinos Benaki's grounds on Kato Souli, Attiki. It was given as a bequest by Konstantinos Benakis to the Benaki Museum and was maintained by the Byzantine and Christian Museum conservator Mrs. F. Kalamara in 1965. Studying the pictorial elements of the painting, Professor Manolis Chatzidakis concluded that the painting was executed by a workshop influenced by Georgios Klontzas and placed chronologically at the end of the 16th century⁷¹.

The image's background is gold, and the ground is vivid red ochre. Buildings surround the central scene. In the center, a banquet scene consists of six figures. Three of them are angels that sit at a circular table. It is indicative that this is the execution of a divine command because heavenly forms coexist with human ones.

On the right side of the painting is a classicist building with an arched window on the façade and three triangular niches, one under the window and the other two at both upper corners of the side. A series of four arched windows are on

⁶⁹ Ζαμβακέλλης, 1985, pp. 55-56.

⁷⁰ Μουσείο Μπενάκη, Αρ. Ευρ, 20547.

⁷¹ Δρακοπούλου & Χατζηδάκης, 1997, p. 89· Χατζηδάκη & Κατερίνη, 2005, p. 244, n. 10. Δελτίο Μουσείο Μπενάκη, Αρ. Ευρ, 20547.

the left side of the building. Its roof is pitched, and at the back of it is a chimney from which smoke comes out. At the right of the central background buildings is a tower with a doomed colonnade on the top (Figure 25). At the center of the background buildings is a horizontal classicist building with a series of arched windows and an elaborate entablature above them. The left side of the building has a bell-shaped roof with three semicircular windows on its base and a spherical finial on the top. To the left of the painting is depicted a loggia with a pitched roof. On the facade, the rectangular doorway is crowned by a semicircular niche. Two triangular niches are on both upper corners of the facade. At the left side of the loggia is a series of three arched doorways (Figure 26).

On the lower right side, Abraham is represented on his knees, addressing the angel on the right. He has long gray hair and a grey beard that betrays his age. His hair is tied at the back of his head, covering the nape and part of his back. He wears a dark green footed tunic and is covered with an olive mantle. He also wears a pair of brown sandals (Figure 27).

The angel on the right sits at the right side of the table, facing Abraham. It is young and has brown curly hair that is pulled back. A golden halo surrounds its head, and two wings sprout from the back of its body, black in the center and dark golden-yellow at the edge. It is clothed in a crimson, footed tunic and, over this, a green cloak that covers most of the body except the right forearm, the ankles, and the feet. On its feet, it wears brown sandals, a common element, when an angel steps on the Earth. It also holds a scepter, a characteristic symbol of divine command or authority as mentioned above (Figure 28).

To the left of this figure, Sarah is depicted standing and approaching the table. On her face are visible deep wrinkles. Her head, except her face, is covered

with a white headdress. Over this, she wears a red veil covering her head and the back of her torso. On her body, she wears a light purple tunic (Figure 29).

At the center of the table, the central angel sits on a domed throne. The dome of the throne ends in three lobes, and on both sides are two-pointed spires. Above the dome in the center is depicted a smaller dome with arched windows and spires left and right. This angel is larger than the other figures. It is young, with long, brown, curly hair pulled back. It has a golden halo around its head. On the back of its body, it has a pair of wings that are black in the center and dark yellow-golden at the edge. It wears a red tunic with a gold band encircling the upper part of its right sleeve. Over the tunic, it wears a dark green mantle (Figure 30).

To the left of the central angel stands a figure whose facial features have been lost by later preservation. He is probably a servant or a beggar. He has brown hair. He is clothed in a green tunic below an olive mantle (Figure 32).

At the left side of the table, the third angel sits. It is also young, with long brown curly hair pulled back and a golden halo around its head. At the back of its torso, it has a pair of wings same as the other two angels. It wears a dark green tunic with a light mauve mantle over it. It has decorated the mantle at the point of its chest with an amber brooch. As referred before, this ornament was a common element when an angel is dressed in an imperial uniform and has a peaceful mission (Figure 33). It holds a scepter and wears a pair of brown sandals. At its feet are two painted vessels, a helical oenochoe, and a kylix (Figure 34).

The central table is circular. Its base is triangular, and on both sides is a helical palmette. The table is covered by a white tablecloth with colorful fringes at the edge. Plenty of food is on the table, such as bread, lemons, oranges, and pomegranates. Also, there are many tablewares, such as knives, candlesticks, oenochoes, kraters, and a painted kylix (Figure 33).

3.3. The influence of Byzantine tradition and Western art on the artist's style.

The Hospitality of Abraham is quite a popular theme in Byzantine Art and its depiction continued during the Post-Byzantine Period. As mentioned in a previous chapter, Cretan Art has been strongly influenced by the Metropolitan Art of Palaiologan Times and by Western Art, mainly Venetian Mannerism as it was developed in the 15th and 16th centuries. The influences of the painting from Byzantine and Western Art, will be examined in the following subchapter.

3.3.1. The Influence of Byzantine Tradition

By observing icons with this theme, mainly from the 14th century (Figure 35), (Figure 36), (Figure 37), it becomes clear that in the Byzantine Tradition, the figures sit at a rectangular or square table. The middle angel is, on the central axis and the two other angels sit on the two narrow sides of the table, almost opposite to each other. In the same way, the scene is developed in the painting studied. Also, in Byzantine Art, the three angels symbolizing the Holy Trinity are depicted sitting at the table in such a way that they form an equilateral triangle, the geometric shape of absolute equality. This rule is applied in this picture. It is worth noting that before the 14th century, the table had a circular or semicircular shape, while in the 14th century, the square shape was established. Therefore, here the artist follows the earlier pattern. Abraham and Sarah, in works from the Byzantine Period that were found, stand on either side of the central angel. Here it is observed that the painter diverges from the norm and places Abraham kneeling next to the angel on the right, while the central angel is surrounded by Sarah and another figure. Another notable difference is that while in the localized images, all three angels have their left hand resting on the table, in the Benaki Museum

painting they do not touch the table at all. However, in all cases, the angel in the middle has its head slightly turned to the left⁷².

Next, we will examine the general stylistic characteristics of Byzantine Art adopted by the painter of the Benaki Museum work. A characteristic feature of Byzantine Painting that is also observed in work of art being examined is that the figures look as if they have lost their gravity to the point that the feet are depicted above the ground. Also, the size of all figures, except the central angel, is the same. In Byzantine Hagiography, all the persons in the scene are similar in height and size, and only the most important figures are a little larger than the others. In this case, the central angel symbolizes Christ, and his significance is noted in that way. In addition, another element of the Byzantine Tradition adopted in the painting are the calm and restrained movements and the complete absence of lyrism. In addition, the proportions of buildings, mountains, trees, rivers, and generally of the materials that are used symbolically and subsidiarily in the main theme are diminished in relation to humans in Byzantine Art. In this case, the entire set of buildings, walls, doors, windows, and roofs do not correspond to their natural proportions. The sky also never has its natural color. As in this case, the sky or background is often painted in gold or ocher.

With respect to the figures, the legs and arms are smaller in proportion to the rest body, a typical trait in Byzantine Hagiography. The wings have the Paleologan Style (Figure 39). The dark brown color of the skin is characteristic of Byzantine Art (Figure 38). In Byzantine Hagiography, each garment flutters in its direction and intensity, regardless of its surroundings. In this way, the impression of a single wind direction is eliminated⁷³. This

⁷² Χαράλάμπος-Μουρίκη Ν. , 1964, pp. 92-96.

⁷³ Ζαμβακέλλης, 1985, pp. 27-29.

phenomenon is intensely observed in the ruffles of the right angel's mantle (Figure 25).

3.3.2. The Influence of the Western Art

This subchapter will examine the elements from Western Art adopted in the Benaki Museum painting. First, the artist attempted to convey *linear perspective*, a technique developed by the Florentine artist Filippo Brunelleschi (1377-1446) during the *Early Renaissance* (1400-1495)⁷⁴. The buildings that frame the scene are rendered with more details than those of Byzantine Art and show similarities to the Florentine and Venetian buildings in the 15th and 16th centuries. More specifically, they are developed in width, and, an arcade is built along their façade in many of them, the so-called *loggia*⁷⁵ (Figure 40). They also have two or three series of arched windows (Figure 41)⁷⁶. The throne of the central angel has Gothic elements such as the three-lobed dome and stripes, features found in Gothic architecture (Figure 42) (Figure 43). the color palette, it seems that the painter adopts the manneristic style of vivid colors (rose, red, orange, and crimson) (Figure 47)⁷⁷.

In respect to the human figures, while in Byzantine Hagiography, the ratio of head to body is one to eight or nine, in the case of the Benaki Museum painting, the figures are rendered in the average natural ratio⁷⁸. The eyebrows are fainter compared to those of the Byzantine style. Hair curls are closer to the Renaissance Venetian Mannerism version (Figure 45) because they are not very strongly defined by *psimithies* and *grapsimata* as in Palaiologan Art (Figure 44). The eyes are softer compared to Byzantine Art, in which they had a keen deep look. The faces of the angels are rounder than the ones of the

⁷⁴ Vasari & du C. De Vere, 1912-1914, p. 198.

⁷⁵ Χαραλαμπίδης, 2014, p. 27.

⁷⁶ Χαραλαμπίδης, 2014, p.36

⁷⁷ Horton, 2015.

⁷⁸ Ζαμβακέλλης, 1985, p. 27.

Palaiologan Style, their cheeks are round, and their chin is heavy, reminiscent of the faces of the sculptures of Classical Art (Figure 46), which had emerged after the Medieval Era and was imitated by the Renaissance artists ⁷⁹.



Figure 24. *The Hospitality of Abraham*, end of 16th c. panel painting, Athens, Benaki Museum of Greek Culture (derived from: https://www.benaki.org/index.php?option=com_collectionitems&view=collectionitem&id=108267&Itemid=383&lang=el).

⁷⁹ Πλάντζος, 2013, p.134.



Figure 25: The Hospitality of Abraham (detail: the right side of the painting), end of 16th c. panel painting, Athens, Benaki Museum of Greek Culture (derived from: https://www.benaki.org/index.php?option=com_collectionitems&view=collectionitem&id=108267&Itemid=383&lang=el).



Figure 26: The Hospitality of Abraham (detail: the left part of the painting), end of 16th c. panel painting, Athens, Benaki Museum of Greek Culture, (derived from: https://www.benaki.org/index.php?option=com_collectionitems&view=collectionitem&id=108267&Itemid=383&lang=el).



Figure 27. *The Hospitality of Abraham* (detail: Abraham), end of 16th c. panel painting, Athens, Beanki Museum of Greek Culture (derived from: https://www.benaki.org/index.php?option=com_collectionitems&view=collectionitem&id=108267&Itemid=383&lang=el).



Figure 28: *The Hospitality of Abraham* (detail: the angel on the left side of the painting), end of 16th c. panel painting, Athens, Beanki Museum of Greek Culture (derived from:

https://www.benaki.org/index.php?option=com_collectionitems&view=collectionitem&id=108267&Itemid=383&lang=el).



Figure 29: *The Hospitality of Abraham* (detail: Sarah), end of 16th c. panel painting, Athens, Beanki Museum of Greek Culture (derived from: https://www.benaki.org/index.php?option=com_collectionitems&view=collectionitem&id=108267&Itemid=383&lang=el).



Figure 30: The Hospitality of Abraham (detail: the central angel), end of 16th c. panel painting, Athens, Beanki Museum of Greek Culture (derived from: https://www.benaki.org/index.php?option=com_collectionitems&view=collectionitem&id=108267&Itemid=383&lang=el).



Figure 31. The Hospitality of Abraham (the standing figure on the left), end of 16th c. panel painting, Athens, Benaki Museum of Greek Culture: (derived from: https://www.benaki.org/index.php?option=com_collectionitems&view=collectionitem&id=108267&Itemid=383&lang=el).



Figure 32: *The Hospitality of Abraham* (detail: the left angel), end of 16th c. panel painting, Athens, Beanki Museum of Greek Culture (derived from: https://www.benaki.org/index.php?option=com_collectionitems&view=collectionitem&id=108267&Itemid=383&lang=el).



Figure 33: *The Hospitality of Abraham* (the table), end of 16th c. panel painting, Athens, Beanki Museum of Greek Culture (derived from: https://www.benaki.org/index.php?option=com_collectionitems&view=collectionitem&id=108267&Itemid=383&lang=el).



Figure 34: *The Hospitality of Abraham* (detail: the vases in front of the left angel's feet), end of 16th c. panel painting, Athens, Benaki Museum of Greek Culture (derived from: https://www.benaki.org/index.php?option=com_collectionitems&view=collectionitem&id=108267&Itemid=383&lang=el).



Figure 35: *The Hospitality of Abraham*, c. mid 14th century, panel painting, Benaki Museum, Athens (derived from: [https://el.wikipedia.org/wiki/%CE%97_%CF%86%CE%B9%CE%BB%CE%BF%CE%BE%CE%B5%CE%BD%CE%AF%CE%B1_%CF%84%CE%BF%CF%85_%CE%91%CE%B2%CF%81%CE%B1%CE%AC%CE%BC_\(%CE%9C%CE%BF%CF%85%CF%83%CE%B5%CE%AF%CE%BF_%CE%9C%CF%80%CE%B5%CE%BD%CE%AC%CE%BA%CE%B7\)](https://el.wikipedia.org/wiki/%CE%97_%CF%86%CE%B9%CE%BB%CE%BF%CE%BE%CE%B5%CE%BD%CE%AF%CE%B1_%CF%84%CE%BF%CF%85_%CE%91%CE%B2%CF%81%CE%B1%CE%AC%CE%BC_(%CE%9C%CE%BF%CF%85%CF%83%CE%B5%CE%AF%CE%BF_%CE%9C%CF%80%CE%B5%CE%BD%CE%AC%CE%BA%CE%B7))).



Figure 36: *The Hospitality of Abraham*, the beginning of 15th century, panel painting, Christian and Byzantine Museum, Athens (derived from: <https://www.ebyzantinemuseum.gr/?i=bxm.el.exhibit&id=43>).



Figure 37 Angelo Akotantos, *The Hospitality of Abraham*, second hand of the 14th century, panel painting, Palais-Musée des Archevêques, Narbonne (derived from: Χαρολάμπους-Μουρίκη, 1964, p. ΠΙΝΑΞ 35).



Figure 38: Enthroned Madonna and Child, 1250-1275, tempera on poplar panel, National Gallery of Art, Washington (derived from: https://el.m.wikipedia.org/wiki/%CE%91%CF%81%CF%87%CE%B5%CE%AF%CE%BF:Italo-Byzantinischer_Maler_des_13._Jahrhunderts_001.jpg).



Figure 39: Archangel Michael, 14th century, Byzantine and Christian Museum, Athens (derived from: https://www.byzantinemuseum.gr/el/permanentexhibition/byzantine_world/the_final_flowering/?bxml=1353).



Figure 40: Filippo Brunelleschi, Spedale degli Innocenti, 1419-1423, Florence (derived from: https://en.wikipedia.org/wiki/File:Spedale_innocenti,_veduta_02.JPG).



Figure 41: Filippo Brunelleschi & Luca Fancelli, Palazzo Pitti, 1458, Florence (derived from: .



Figure 42: Cathedral Church of the Blessed Virgin Mary, 1258, Salisbury (derived from: https://el.wikipedia.org/wiki/%CE%9A%CE%B1%CE%B8%CE%B5%CE%B4%CF%81%CE%B9%CE%BA%CF%8C%CF%82_%CE%BD%CE%B1%CF%8C%CF%82_%CF%84%CE%BF%CF%85_%CE%A3%CF%8C%CE%BB%CF%83%CE%BC%CF%80%CE%B5%CF%81%CE%B9).



Figure 43: Trefoil arches, Bayeux Cathedral, 11th century, Calvados (derived from: https://pl.wikipedia.org/wiki/%C5%81uk_tr%C3%B3jlistny).



Figure 44: Paolo Veronese, *Mystic Marriage of Saint Catherine*, 1571, oil on canvas, Gallerie dell'Accademia, Venice (derived from:

https://el.wikipedia.org/wiki/%CE%91%CF%81%CF%87%CE%B5%CE%AF%CE%BF:Paolo_Vernese_014.jpg.



Figure 45: The Baptism of Christ. Fresco, 14th century, mural, Hagios Nikolaos Orfanos, Thessaloniki (<https://www.thessmemory.gr/%CE%B2%CF%85%CE%B6%CE%B1%CE%BD%CF%84%CE%B9%CE%BD%CE%B7-%CE%B8%CE%B5%CF%83%CF%83%CE%B1%CE%BB%CE%BF%CE%BD%CE%B9%CE%BA%CE%B7/%CF%84%CE%B1-%CE%BA%CE%B1%CE%BB%CE%BB%CE%B9%CF%84%CE%B5%CF%87%CE%BD%CE%B9%CE%BA%CE%AC-%CE%B4%CF%8E%CF%81%CE%B1-%CF%84%CF%89%CE%BD-%CE%BC%CE%AC%CE%B3%CF%89%CE%BD-%CF%83%CF%84%CE%BF%CE%BD/>).



Figure 46: Head of a teenage man, 490-480 B.C., marble, Museum of Acropolis, Athens (<https://www.theacropolismuseum.gr/kefali-agalmatos-o-xanthos-efibos>).



Figure 47: Perino del Vaga, *the Nativity*, 1534, oil on panel, National Gallery of Art, New York (derived from: <https://www.nga.gov/collection/art-object-page.46130.html>).

4. Review of non-destructive techniques

At the beginning of the 20th century, science and technology began to be used in cultural heritage. However, it is worth mentioning that from 1990 onwards, they were systematically used to study painting techniques and construction materials, with the simultaneous development of new exploratory methods.

In addition, the necessity of preserving the works' integrity and protection has led to the gradual development of non-destructive analysis methods. These techniques are based on the principle that materials can reflect, absorb and emit radiation in a way characteristic of their molecular composition, structure, and shape, as well as the non-destructive nature of these radiations in the materials of paintings.

Non-destructive analysis methods are divided into non-invasive and invasive (part of the work is removed, but the sample is not destroyed). We will focus on the first method, which is subdivided into imaging and spectroscopic techniques. The first ones enable the depiction of the painting, the identification of overpaintings and other subtle elements, and generally give an overview of the painting's techniques, construction materials, and structural condition. The second ones are used to identify materials and define the organic and inorganic compounds/elements based on the energy state of the bonds of the atoms of these compounds.

4.1. Imaging techniques

Imaging techniques use different types of radiation, which interact with matter. These interactions are then recorded, creating a visual picture of the distribution of components⁸⁰. These interactions are diffusion, reflection,

⁸⁰ Kozaris, 2013, p. 38.

scattering, and absorption⁸¹. Imaging techniques require a radiation source, the painting which will interact with the radiation and a detector.

Radiation is divided into particulate and electromagnetic. The particles used in particulate radiation are electrons, positrons, protons, neutrons, and electrons. In electromagnetic radiation, photons are used.

The way photons interact with matter is extremely important for understanding the capabilities of imaging methods. Depending on the energy of the photon and the material properties of the medium, the photon interacts differently with the material. More specifically, the photon can penetrate the material without interacting at all, be absorbed by the material and lose all its energy, and scatter or deflect losing some of its energy⁸².

Imaging techniques are divided into the following categories:

1. Visible imaging techniques, at which the visible light source can record information about the surface of the artwork. Depending on the angle and position of incidence (45° or 10, in front or behind the work) the type of information received also changes.
2. The techniques use ultraviolet reflection. In these techniques only the type of radiation reflected by ultraviolet radiation is used. These techniques are used to study the varnish layer and to illustrate faint inscriptions or figures.
3. Infrared reflection, which is based on the ability of near-infrared to penetrate the painting layers. It can give information about features that lie beneath the painting layers, such as any deviations from the final drawing, overpaintings, underlying signatures.
4. The technique of false colors. Painted areas that look the same in visible light but are made of different materials may have a different

⁸¹Kouloumpi, Moutsatou & Terlix, 2012, p. 368.

⁸² Kozaris, 2013, p. 40.

color in the infrared or reflected UV spectral range, depending on the light sources and detector selected.

In addition, there are imaging techniques that use X-radiation with a range of wavelength from 10^{-8} - 10^{11} m, which has penetrating ability. The most widespread technique is X-ray radiography (XRR). This technique is non-invasive and non-destructive and gives information about the substrate of a work of art and the painting layers. Based on the above, it is understandable that radiography can give information about the artist's *pentimenti*, the hidden changes under the upper color layer, and the synthetic mapping of heavy pigments. However, the XRR technique, apart from the possibilities it gives, has some limitations. First of all, it can detect mainly pigments with heavy elements. Light elements cannot be detected when heavy elements are present in large concentrations. When a panel has a substrate that has heavy elements such as Pb over its entire surface then a background of total absorption is given⁸³.

That's why cutting-edge techniques have been developed that overstep these limitations. These are tomographic techniques. In essence, multiple X-rays are taken, as the artwork rotates perpendicular to the axis of the source/detector. Then, through mathematical reconstruction, a three-dimensional image of the artwork is created as well as the internal stratigraphy⁸⁴. Computational laminography (CL) is used to analyze paintings on canvas⁸⁵. Synchrotron radiation can also be used because its high intensities and thin spectrum create images of high contrast and detail.⁸⁶

Finally, multispectral imaging (MSI) is particularly useful, by using well-defined bands of the electromagnetic spectrum from ultraviolet (UV) to infrared (IR). The reason why the use of multispectral imaging systems has

⁸³ Janssens, Dik, Cotte, & Susini, 2010, p. 815-816.

⁸⁴ Janssens, Dik, Cotte, & Susini, 2010, p. 816

⁸⁵ Alfeld & Broekaert, 2013, p. 227.

⁸⁶ Janssens, Dik, Cotte, & Susini, 2010, p. 816.

been considered routine for the study of paintings since the 1990s, is its fast and in situ application, the absence of expensive consumable supplies, and the recording of the entire surface of the works⁸⁷. The multispectral imaging systems available for use vary and can offer different kinds of information depending on their functions. Such functions are visible imaging, ultraviolet imaging in reflection and fluorescence mode, and infrared imaging in reflection, transmittance, and false Color modes⁸⁸. The development of these systems serves the use of all the above-mentioned modes of operation with the same equipment.

Although imaging techniques offer a range of capabilities and their use is quick and immediate, the extraction of diagnosis is not simple. Further post-processing methods are required to extract the maximum of the information provided.

4.2. Spectroscopic techniques

As mentioned above, spectroscopic techniques are extremely useful because they can recognize organic and inorganic chemical elements and compounds based on the energy state of atoms and their bonds.

Raman spectroscopy is an established analytical molecular technique for investigating the molecular environment of cultural heritage objects⁸⁹. Chemical bonds connect the atoms in a molecule or an elemental lattice. Depending on its complexity (number of atoms composing it), every molecule has a number of vibrational degrees of freedom, called normal vibrations. Each normal vibration corresponds to a frequency, which depends on the atomic mass, the binding forces, the molecular species, and the lattice structure. Consequently, each molecule type has a unique number of bonds

⁸⁷Alexopoulou, Kaminari, & Moutsatsou, 2018, p. 444.

⁸⁸Kouloumpi, Moutsatsou, & Terlix, 2012, p. 369.

⁸⁹Vandenabeele, et al., 2007, p. 678; Fotakis, et al., 2007, p. 95; Anglos, et al., 2009, p. 49.

and, therefore, a specific number of vibrational degrees of freedom. All these properties act as a fingerprint of the molecule and are used for its identification⁹⁰. The working principle of Raman spectroscopy is the measurement of vibrational transitions within materials caused by the inelastic scattering of electromagnetic radiation from molecules⁹¹. Scattering can be elastic or inelastic. When an incident monochromatic radiation of a given frequency illuminates a sample a portion of incoming photons will interact with the molecule through their oscillating electric field, setting the molecule to a non-stationary (virtual) excited state. As a result of the instability of the virtual state, molecules decay instantaneously to the ground state by one of three different processes⁹².

The majority of the scattered molecules will do so elastically, a phenomenon referred to as Rayleigh scattering. In Rayleigh scattering, the excited molecule emits a photon equal to the energy it received by the incident radiation and returns to its ground state. Hence, Rayleigh scattering provides no information about the vibrational energy levels of the molecule⁹³. For inelastic, or else referred to as Raman scattering to occur, the emitted photon must have lower Stokes or increased (anti-Stokes) energy than the Rayleigh photons, thereby generating a set of frequency-shifted Raman photons. However, Raman scattering is far less likely to occur compared to Rayleigh scattering⁹⁴. The Raman spectrum is produced by the spectral resolving of the scattered light. The Raman spectrum is a plot of the intensity of the scattered light as a function of the frequency difference between the incident and scattered radiation; the frequency difference is called the Raman shift and is expressed in units of wavenumbers

⁹⁰ Salzer, 2013, p. 66; Larkin, 2011, pp. 8-9; Fotakis, et al., 2007, p. 95.

⁹¹ Fotakis, et al., 2007, p. 95.

⁹² Smith & Clark, 2004, p. 1138; Rai & Dubey, 2018; Fotakis, et al., 2007, p. 99.

⁹³ Smith & Clark, 2004, p. 1138; Fotakis, et al., 2007, p. 99.

⁹⁴ Larkin, 2011, p. 17; Smith & Clark, 2004, p. 1138.

(cm-1)⁹⁵. Not all the vibrational modes of a molecule can be observed through Raman spectroscopy. The modes that change the polarizability of the molecule are Raman active⁹⁶.

Moreover, due to the weakness of the Raman scattering signal, several interferences and side effects can influence it. One such interference is the absorption of the laser light by the sample, reducing thus the number of photons reaching the analyte. This problem can be avoided by the use of a laser source with a different excitation wavelength⁹⁷. The analysis of samples employing Raman spectroscopy includes the irradiation of the sample by an excitation source, the collection of the scattered light into a spectrograph, and the recording of its intensity as a function of the wavelength⁹⁸.

On the other hand, infrared radiation (IR) can provide information about the type of organic compounds (resins, oils, pigments, etc.) and inorganic compounds (metals, minerals, etc.). This radiation is located near the range 4000-400 cm-1 of the electromagnetic spectrum. The energy of this radiation can excite the vibrations of the molecular bonds. Depending on the chemical bonds of each material, different amounts of radiation in different wavelengths are absorbed by the material; In this way, the material can be identified. However, recognition can be problematic for organic compounds because the absorption area can be exceeded. Infrared Spectroscopy can work with different configurations: Transmission Fourier Transform (FTIR), Attenuated Total Reflectance (ATR), Total Reflectance (TR), Fiber Optic Reflectance Spectroscopy (FORS), and Diffuse Fourier Infrared Reflection (DRIFT).

⁹⁵ Edwards & Vandenabeele, 2012, p. 52.

⁹⁶ Fotakis, et al., 2007, pp. 99-100; Smith & Clark, 2004, p. 1138; Larkin, 2011, pp. 15-18.

⁹⁷ Vandenabeele, 2013, pp. 39-40.

⁹⁸ Fotakis, et al., 2007, p. 102.

X-ray fluorescence (XRF) is a spectroscopic method for quantitative and qualitative analysis of chemical elements. A high energy photon from an X-ray source impacts the atom's electrons. If the energy of the impacting photons is greater than the binding energy of the electron with the atom, the photon gets absorbed by an electron of the atom, resulting in its excitation and ejection from the electron shell⁹⁹. When an electron gets ejected from the inner electronic shell (K shell) of the atom (ionization), it creates a vacancy "hole". To restore stability in the atom, an electron from another shell (L or M shell) fills that vacancy. Because electrons are quantized, during this process, they have to release excess energy. The release occurs in photon (fluorescence) with characteristic X-ray energy declarative of the element's identity¹⁰⁰. The probability of occurring depends on the initial vacancy's energy level and the atom's atomic weight¹⁰¹. Considering the aforementioned effect, some elements do not produce detectable XRF signals either because they have only one shell of electrons or because the Auger yield in low atomic number elements is greater than the fluorescence yield¹⁰². The energy of the emitted X-ray photon is equal to the difference in the energy levels participating in the procedure to fill the vacancy¹⁰³. Each element produces a number of characteristic lines. Thus, according to the shell from which the second electron will come to fill the vacancy and the shell of the vacancy, the emissions are named. K emissions occur when electrons of the L or M shell fill a K shell vacancy; they are named $K\alpha$ and $K\beta$ respectively, L emissions occur when electrons of the M or N shell fill an L shell vacancy; they are named $L\alpha$ and $L\beta$ respectively, and so on¹⁰⁴. The emission of the X-

⁹⁹ Janssens, 2013, p. 82; Donais & George, 2018, p. 2.

¹⁰⁰ Schlotz & Uhlig, 2000, p. 3; Donais & George, 2018, pp. 2-3; Polland & Heron, 2008, p. 34 Karydas, 2007, pp. 419-420.

¹⁰¹ Schlotz & Uhlig, 2000, p. 3; Polland & Heron, 2008, pp. 34-37.

¹⁰² Donais & George, 2018, pp. 2-3; Janssens, 2013, p. 82.

¹⁰³ Polland & Heron, 2008, p. 34; Schlotz & Uhlig, 2000, p. 3.

¹⁰⁴ Calvo Del Castillo & Strivay, 2012, pp. 63-65; Schlotz & Uhlig, 2000, p. 4; Janssens, 2013, p. 89.

ray photons occurs in different depths in the sample. On their way out, the X-ray photons have to travel through the sample, resulting in their reduction according to Beer's Law. The parameters on which the amount of reduction depends are the absorbance of the medium (sample), and the angle at which the photon travels towards the detector. Thus, X-ray photons generated at or greater than a specific depth (escape depth) cannot reach the detector. The escape depth depends on the absorbance of the sample and the energy of the emitted X-ray photons (greater in high Z elements). The detected characteristic lines of each element in the sample under analysis and their intensities are depicted in an XRF spectrum. The XRF spectrum is a bivariate plot of energy in KeV on the x-axis versus signal intensity on the y-axis¹⁰⁵. Apart from the analyzed materials' characteristic lines, there are some unwanted or interfering peaks. Such peaks are the Rayleigh and Compton peaks resulting from the material of the cathode of the X-ray source. Also, sum peaks can be observed for high-concentration elements.

The majority of crystal XRF analyses in paintings concern the identification of chemical elements of pigments. In this way, it is possible 1) to identify the artist's techniques and palette, 2) to trace the origin of pigments through the recognition of their trace elements, 3) to contribute to the authenticity of a painting by distinguishing pigments that have a safe dating, such as titanium white from zinc white and 4) to identify any areas in which changes have been made.

Finally, X-ray diffraction is a technique that measures the shape and size of the crystal of an inorganic compound, and this leads to the identification of the inorganic pigment. It is mainly used for the characterization of pigments and preparation. X-ray diffraction systems are experimental¹⁰⁶.

¹⁰⁵ Donais & George, 2018, p. 4.

¹⁰⁶ Herrera et al, 2009.

5. Research Methodology

5.1. Goals of Research

The aim of this study is the theoretical and scientific study of the Benaki Museum's panel painting *The Hospitality of Abraham* (ΓΕ 20547) to examine the influence of Byzantine tradition and Western Art on the artist's style and, finally, to find the artist's techniques and color palette and observe how he used the basic pigments that were chosen.

For the research question of Byzantine and Western Art's influence to be answered, the painting will be examined iconographically and stylistically to find the similarities with paintings mainly of Paleologan Tradition on the one hand and Italian Renaissance and Venetian Mannerism on the other. In addition, the artwork will be studied for the observation of the varnish layer surface as well as the visualization of faded inscriptions or forms and features underlying the pictorial layers, such as underdrawings, pentimenti (alterations made by the artist in the course of the painting).

Regarding the techniques and color palette, imaging, and physicochemical analyses will be used.

5.2. Research Protocols

The next step is the building of the research protocol. The main axis of this effort is based on the use of non-invasive and non-destructive methods that will be set in situ. The main goal is to skip the pretreatment stage, maintain the integrity of the work, and extract as much information as possible about the whole object.

Once the research protocols have been set, the next step is to select the analytical techniques that correspond to the research protocols. It was decided from the outset to use imaging, elemental and molecular techniques. With the use of imaging techniques, the visible and invisible elements of the painting will be observed, with elemental techniques, the inorganic pigments of the

painting layers will be identified, and with the molecular ones, the inorganic and organic compounds of pigments and varnish will be searched. For this reason, the portable stereomicroscope, multispectral imaging (MSI), X-ray fluorescence (XRF) spectroscopy, and Raman spectroscopy are chosen.

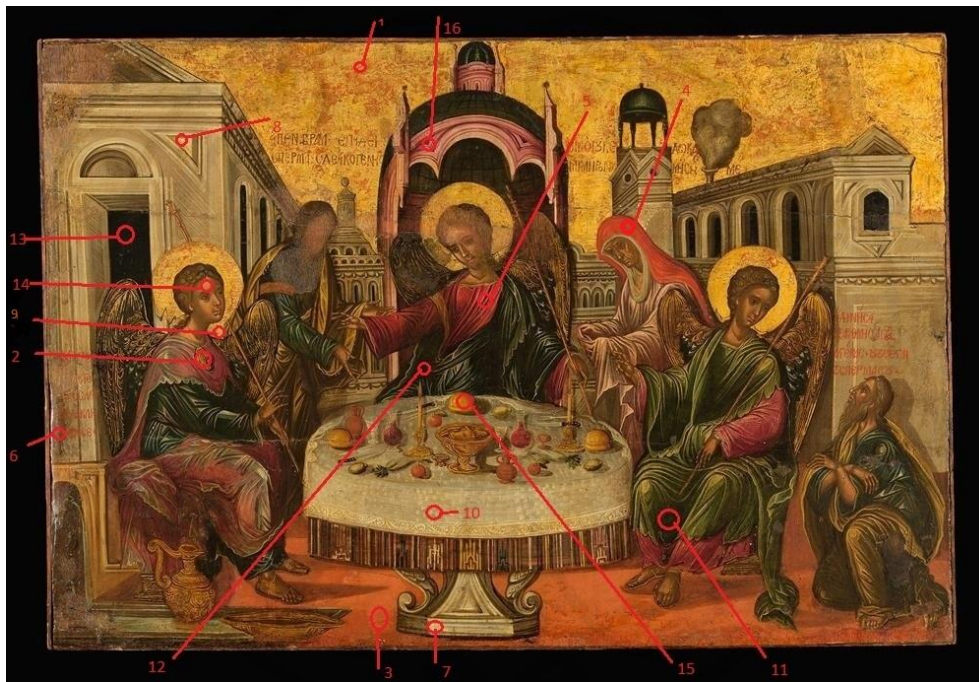


Figure 48: Points of Portable Microscope, X-ray Spectrometer, and Raman Spectrometer analysis (digital processing Lida Kyriopoulou).

5.2.1. Portable Microscope

A portable fibre optic microscope was used to detect the details of the painting surface, such as the way the artist does the brush strokes, and the mixing of different pigments to make the final color. The model of the portable stereomicroscope used was a fibre optics system (FOM/i-scope, Moritex).

5.2.2. Multispectral Imaging

Multispectral Imaging (MSI) was conducted for the detection of hidden elements of the painting, like overpaintings, underdrawings, pentimenti, etc.,

the discovery of construction techniques, the assessment of the materials' composition, and the chemical distribution mapping of materials. The technique was carried out in the Benaki Museum of Greek Culture by Dr. Anna P. Moutsatsou, Conservation Scientist of the National Gallery-Alexandros Soutzos Museum (Figure 49), (Figure 50). The camera used is MuSIS™ MS by the Forth Photonics (now DySIS medical) Company. For the process of observation/analysis using the multispectral camera, the research protocol of the laboratory of physicochemical analyses of the National Gallery was followed. The protocol includes observation of the object in reflection, transmission mode, and combination of reflection and transmission. The MuSIS™ MS system has spectral responsivity in the range 360 nm (UV) – 1000 nm (NIR) using a CCD optical detector with seven selectable spectral bands in black & white and colored mode. In particular, the seven spectral bands correspond to the spectra of 390 nm, 500 nm, 600 nm, 700 nm, 800 nm, 900 nm and 1000 nm. Additionally, it provides Infrared Imaging (FCIR) in two imaging modes for the technique of False Color. An FCIR image is a composite image synthesized by combining a color image with an infrared spectral image. In the first mode of FCIR, the IR imaging band is 650 - 750 nm, while in the second mode is 750 - 850 nm. The spectral bands are achieved by the use of an imaging monochromator and optical filtering. The camera is equipped with a 25 mm lens, capturing images at 1024x960 pixel resolution. Since in the context of digital photography, an ultraviolet observation was performed, the spectral bands from 500 nm to 1000 nm and the two false-color modes were used. The illumination sources used were two OSRAM Halogen Display/Optic Lamps 650 W with 3400 K color temperature. The camera was controlled by specially developed software through a laptop. The images obtained were later processed through Adobe Photoshop and ImageJ.

5.2.3. X-ray Fluorescence Spectrometry

As was mentioned in chapter 4, X-ray Fluorescence Spectrometry is a spectroscopic technique that uses X-ray radiation for the physicochemical analysis of materials. X-ray rays from a source strike the material resulting in the return of X-rays that can give information for the identification of the inorganic chemical elements of the material. X-ray fluorescence Spectroscopy was applied to the painting to track the inorganic pigments of the painting layers. It was conducted in the Benaki Museum of Greek Culture by Dr. Eleni Kouloumpi, Conservation Scientist at the National Gallery-Alexandros Soutzos Museum, and Stelios Kesidis, a Ph.D. candidate in the Laboratory of Archaeometry, Department of History, Archaeology, and Cultural Resources Management, University of the Peloponnese (Figure 52). A portable XRF spectrometer of type Bruker Titan S1 was used. The point analyses were performed in the following operational conditions: High voltage set at 20 kV, current at 40 u.a., and the collection time of each measurement was 20 seconds. The spectra show the energy range from 1-20 KeV, and the spectrometer mode is qualitative.

5.2.4. Raman Spectroscopy

Raman Spectroscopy is a spectroscopic technique that gives information for the identification of both organic and inorganic chemical compounds of materials. This technique can track the vibrational modes of molecules and, therefore identify the molecular composition of materials. Raman Spectroscopy was chosen to identify the inorganic and organic pigments of the painting layers and the inorganic and organic chemical compounds of the varnish. It was performed in the Benaki Museum of Greek Culture by Dr. Eleni Kouloumpi, Conservation Scientist at the National Gallery- Alexandros Soutzos Museum, Peter Vandenabeele, Professor at the Department of Archaeology and Department of Chemistry of the Ghent University, and

Stelios Kesidis, Conservator of Cultural Heritage Ph.D. candidate in the Laboratory of Archaeometry, Department of History, Archaeology, and Cultural Resources Management, of the University of the Peloponnese (Figure 53). Raman spectroscopy was performed using a BRAVO™ handheld Raman spectrometer (by Bruker Optics GmbH & Co.). The spectrometer is equipped with two near-infrared excitation lasers (DUO LASER™, wavelengths at 785 nm and 853 nm) and a CCD detector, allowing for a spectral range of 300-3200 cm^{-1} and a spectral resolution of 10-12 cm^{-1} . The two lasers operate in a patented sequentially shifted mode (SSE™, Sequentially Shifted Excitation), allowing for mitigation of fluorescence from samples. The duration of each measurement was typically 2 minutes, according to the type of the sample. Data acquisition and processing was carried out by using the OPUS 8.7.31 software, also provided by Bruker. Finally, the processing was concluded using the software Origin 2022 by OriginLab®.



Figure 49: The process of Multispectral Imaging technique (derived from: personal archive Lida Kyriopoulou).



Figure 50: The process of Multispectral Imaging technique (derived from personal archive Lida Kyriopoulou).



Figure 51: Image acquisition with a portable stereomicroscope (derived from personal archive Lida Kyriopoulou).



Figure 52: Analysis procedure with X-ray Fluorescence Spectrometer (derived from: personal archive Lida Kyriopoulou).



Figure 53: Analysis procedure with Raman Spectrometer (derived from: personal archive Lida Kyriopoulou).

6. Results and discussion

A series of analyses have been conducted on the painting. First of all, it was studied with the Multispectral Imaging technique. Then, physicochemical analyses were performed first with XRF and then Raman Spectrometer at 16 points of the painting (Figure 54). For the additional validation of the physicochemical analysis results, pictures were taken with a portable stereomicroscope.



Figure 54: Points of physicochemical analyses (digital processing Lida Kyriopoulou).

6.1. Multispectral Imaging

The panel painting was examined with the MuSISTM-MS multispectral imaging device, which belongs to the Laboratory of Physicochemical Research of the National Gallery- Alexandros Soutsos Museum.

B1	
----	--



Figure 55: Figure Coloured imaging of the reflection of the visible region (derived from: personal archive Lida Kyriopoulou).



Figure 56: Figure Imaging of the reflection of the spectral region 450-550nm (derived from: personal archive: Lida Kyriopoulou).



Figure 57: Imaging of the reflection of the spectral region 750-850nm (derived from: personal archive Lida Kyriopoulou).



Figure 58: Imaging of the reflection of the spectral region 850-950nm (derived from: personal archive Lida Kyriopoulou).

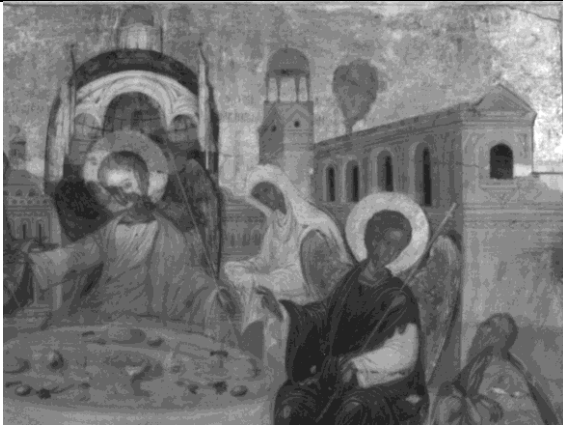


Figure 59: Imaging of the reflection of the spectral region with average 1000nm (derived from: personal archive Lida Kyriopoulou).



Figure 60: False colour infrared image (derived from: personal archive Lida Kyriopoulou).

The observations resulting from imaging the different spectral regions are no different from color-visible imaging. No obvious dry or wet underdrawing is recorded.

B2	
----	--



Figure 61: Coloured imaging of the reflection of the visible region (derived from: personal archive Lida Kyriopoulou).



Figure 62: Imaging of the reflection of the spectral region 450-550nm (derived from: personal archive Lida Kyriopoulou).

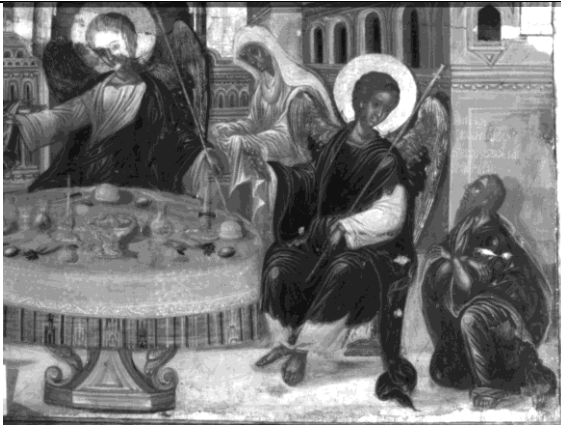


Figure 63: Imaging of the reflection of the spectral region 750-850nm (derived from: personal archive Lida Kyriopoulou).



Figure 64: Imaging of the reflection of the spectral region 850-950nm (derived from: personal archive Lida Kyriopoulou).

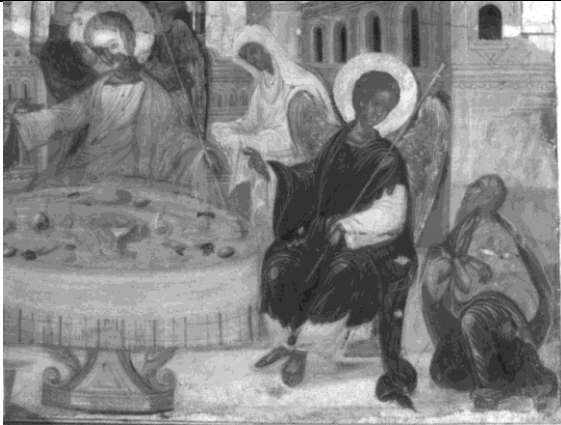


Figure 65: Imaging of the reflection of the spectral region with average 1000nm (derived from: personal archive Lida Kyriopoulou).



Figure 66: False colour infrared image (derived from: personal archive Lida Kyriopoulou).

B3



Figure 67: Coloured imaging of the reflection of the visible region (derived from: personal archive Lida Kyriopoulou).



Figure 68: Imaging of the reflection of the spectral region 450-550nm (derived from personal archive Lida Kyriopoulou).



Figure 69: Imaging of the reflection of the spectral region 750-850nm (derived from: personal archive Lida Kyriopoulou).



Figure 70: Imaging of the reflection of the spectral region 850-950nm (derived from: personal archive Lida Kyriopoulou).



Figure 71: Imaging of the reflection of the spectral region with average 1000nm (derived from: personal archive Lida Kyriopoulou).



Figure 72: False colour infrared image (derived from: personal archive Lida Kyriopoulou).

Drawing with dry medium showing that the table was originally designed larger is recorded in the spectral region average 1000 nm. The lines recorded in the same spectral region, on the legs of the table, have been created with a liquid medium and are also perceptible in the visible region. Also, in the 450-550 nm spectral range, a horizontal line is recorded approximately in the middle of the image attributed to surface wear. Areas of retouching, perceptible in the visible area, are also recorded.

B4	
----	--



Figure 73: Coloured imaging of the reflection of the visible region (derived from: personal archive Lida Kyriopoulou).



Figure 74: Imaging of the reflection of the spectral region 450-550nm (derived from: personal archive Lida Kyriopoulou).

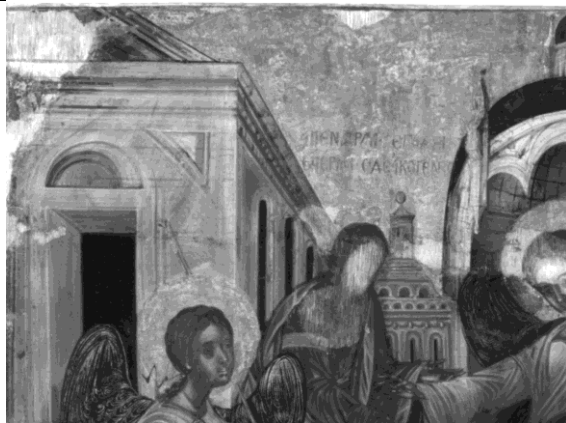


Figure 75: Imaging of the reflection of the spectral region 900-1000nm (derived from: personal archive Lida Kyriopoulou).



Figure 76: Imaging of the reflection of the spectral region with average 1000nm (derived from: personal archive Lida Kyriopoulou).



Figure 77: False colour infrared image (derived from: personal archive Lida Kyriopoulou).

In the imaging of the infrared regions, lines of under-drawing with dry means are recorded on the architectural element. This reveals that both the entrance and the lintel (hyperthyron) were initially drawn differently.

6.1.1. False color Imaging

In general, the false colors were not clear. Some indications of the use of mixtures are presented below.

Red lead is probably used for the red tunic of the central angel and the handkerchief of Sarah (very orange).

The brown-red pigment of outstretched hand of the central angel is in the same shade and is perhaps mixed with red lead.

Azurite was probably used for the rendering of the green-blue robe of the central angel.

The green robe of Abraham on the right has green earth or copper pigment (malachite, copper green?)

It is not obvious what color prevails in false color for the light pink-orange tunic of Abraham. If it's yellow, maybe there is a thin red lacquer (on white). If olive green prevails, perhaps it is an earthy pigment (ochre, umber) on white.

Facial sarcomas, apart from the central angel, have been painted with earthy pigments. The central angel might also have some non-earthy red pigments.

For the blue-green robes, azurite and/ or green earth were likely chosen with ultramarine highlights or indigo.

6.2. Portable Stereomicroscope

For the pictures with a portable stereomicroscope, a fiber optics system (FOM/i-scope, Moritex) was used. Stereomicroscope images are shown where necessary to justify the XRF and Raman results.

6.3. X-Ray Fluorescence Spectrometry

The application of X-Ray Fluorescence (XRF) Spectrometry on the painting

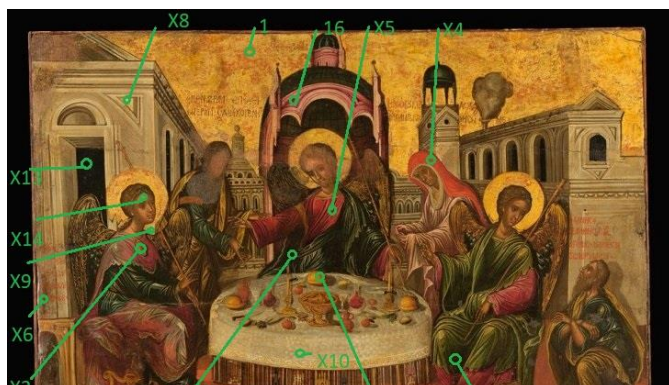


Figure 78: XRF analysis points (digital processing Lida Kyriopoulou).

revealed the composition of inorganic pigments and the ground layer¹⁰⁷. In the analysis of the painting, 16 paint points were studied (Figure 78). It

¹⁰⁷For the interpretation of the XRF and Raman Spectra, the following bibliography was studied: Burgio, Clark, & Theodoraki, 2007; Cartwright, 2020; Daniilia, Andrikopoulos, Sotiropoulos, & Karapanagiotis, 2008; Eastaugh, Walsh, Chaplin, & Siddall, 2004; Ganitis, Pavlidou, Zorba, Paraskevopoulos, & Bikiaris, 2004; Harrison, Ambers, Stacey, Cartwright, & Lymberopoulou, 2011; Karapanagiotis, Mantzouris, & Rosenberg, 2008; Karapanagiotis, Lampakis, Konstanta, & Farmakalidis, 2013; Kenna, 1985; Kesidis, 2020; Kouloumpi, Moutsatsou, & Terlixi, 2012; Mafredas, 2018; Marucci, Beeby, Parker, & Nicholson, 2018; Mastrotheodoros, Beltsios, & Bassiakos, 2021; Mastrotheodoros, Theodosis, & Filippaki,

is important to mention that the icon is placed chronologically by Professor Manolis Chatzidakis at the end of the 16th century¹⁰⁸. Until this time, the pigments used had not changed since antiquity. So, pigments that were discovered later will be excluded.

The portable XRF's elemental analysis of red pigments suggests the presence of red ochre, red lead, and vermilion.

More specifically, at paint 1 (Figure 79), the presence of iron (Fe) and lead (Pb) shows that they are derived from the pigments red ochre (Fe_2O_3)¹⁰⁹ and red lead (Pb_3O_4)¹¹⁰. Also, calcium (Ca) indicates that the pigments were mixed with calcite (CaCO_3)¹¹¹ to lighten the red shade, or that comes from the ground layer's gypsum ($\text{CaSO}_4 \cdot 2\text{H}_2\text{O}$)¹¹². On the other hand, lead white ($2\text{PbCO}_3 \cdot \text{Pb}(\text{OH})_2$) could have been used for lightening. The XRF of paint 4 is similar, so it is hypothesized that it has the same red pigments.

2020 Mastrotheodoros, Theodosios, & Filippaki, 2020 Διονύσιος εκ Φουρνά, 1900 Φαρδί, 2012.

¹⁰⁸ Χατζηδάκη & Κατερίνη, 2005, p. 244.

¹⁰⁹ Eastaugh, Walsh, Chaplin, & Siddall, 2004, pp. 320-321.

¹¹⁰ Eastaugh, Walsh, Chaplin, & Siddall, 2004, pp. 105-106.

¹¹¹ Eastaugh, Walsh, Chaplin, & Siddall, 2004, p. 74.

¹¹² Colombini, Andreotti, Bonaduce, Modugno, & Ribechini, 2010, p. 716.

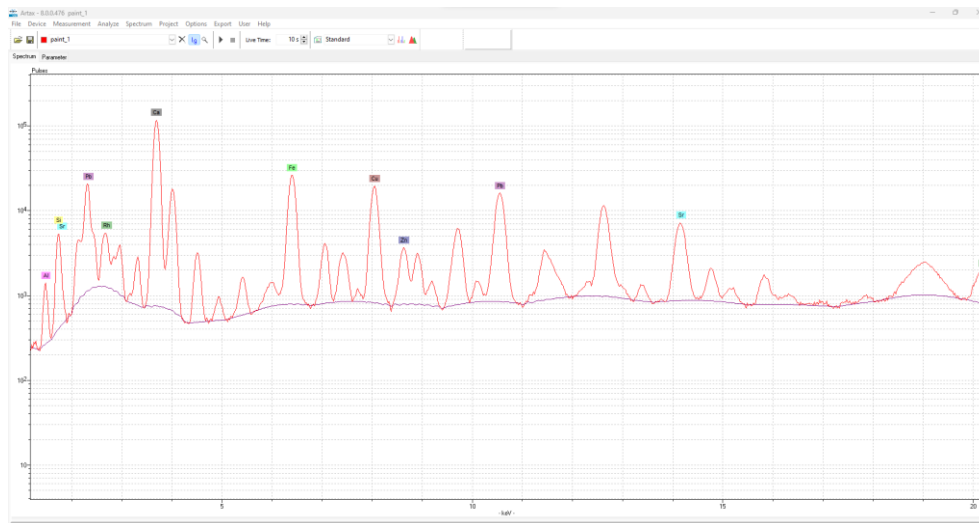


Figure 79: XRF analysis results of paint 1 (derived from: personal archive Lida Kyriopoulou).

At paint 2 (Figure 80), iron (Fe) and lead (Pb) are also present, so it is assumed that the two red pigments used, are red ochre (Fe_2O_3) and red lead (Pb_3O_4). But mercury (Hg) also appears, so it is assumed that there is vermilion (HgS)¹¹³. Also, in this case, calcium is present (Ca), so it is hypothesized that it comes from the ground layer's gypsum ($\text{CaSO}_4 \cdot 2\text{H}_2\text{O}$) or the red pigment was mixed with calcite (CaCO_3) to be lightened.

¹¹³ Eastaugh, Walsh, Chaplin, & Siddall, 2004, 105-106.

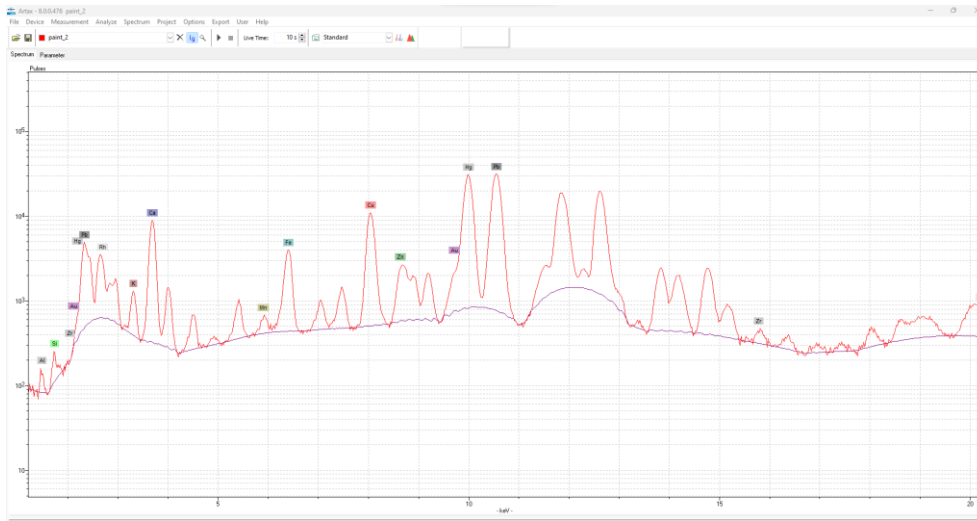


Figure 80: XRF analysis results of paint 2 (derived from: personal archive Lida Kyriopoulou).

The same motive is observed in paints 3 (Figure 81), and 5 (Figure 82). It is most likely in the two paints that the red pigment was mixed with black to make the shade darker. Based on the chemical data of the analyses, magnetite (Fe_3O_4)¹¹⁴ and/or manganese black (MnO_2)¹¹⁵ may have been used. Carbon black (C)¹¹⁶ may also have been used, but XRF cannot track carbon black because C (carbon) is a light element, and XRF cannot trace light elements¹¹⁷.

In paint 6, the portable stereomicroscope picture of the point shows that there are two colors, white and red (Figure 83). Based on the XRF analysis of the point the red pigments used could be red lead (Pb_3O_4), vermilion (HgS), and/or red ochre (Fe_2O_3) and the white pigment could be calcite (CaCO_3), lead white ($2\text{PbCO}_3 \cdot \text{Pb}(\text{OH})_2$), and/or gypsum ($\text{CaSO}_4 \cdot 2\text{H}_2\text{O}$) from the prime layer. As can be observed at the stereomicroscope image, both the red and white pigment must have been mixed with black to make the shade

¹¹⁴ Eastaugh, Walsh, Chaplin, & Siddall, 2004, p. 248.

¹¹⁵ Eastaugh, Walsh, Chaplin, & Siddall, 2004, p. 249.

¹¹⁶ Eastaugh, Walsh, Chaplin, & Siddall, 2004, p. 82.

¹¹⁷ Donais & George, 2018, p. 4.

darker. Based on the chemical data of the analyses, magnetite (Fe_3O_4), manganese black (MnO_2) and/ or carbon black (C) were chosen.

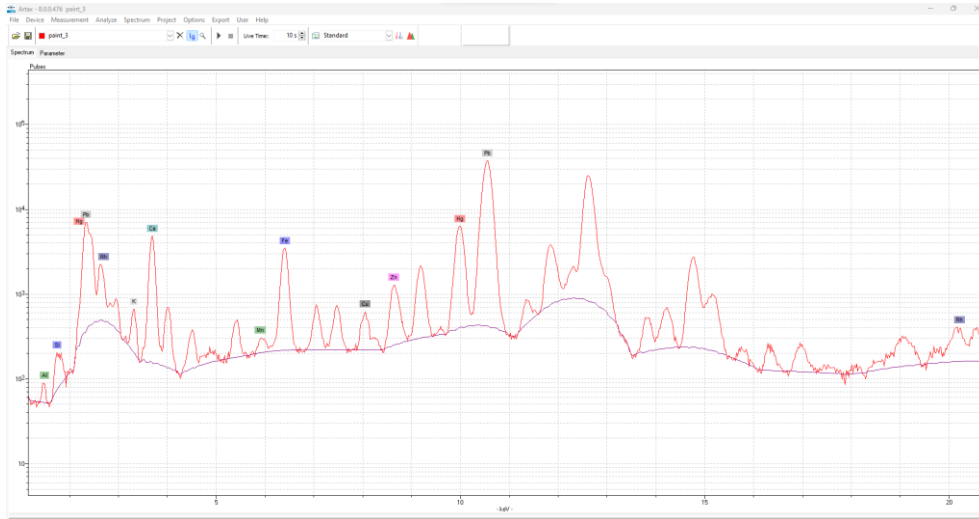


Figure 81: XRF analysis of paint 3 (derived from: personal archive Lida Kyriopoulou)..

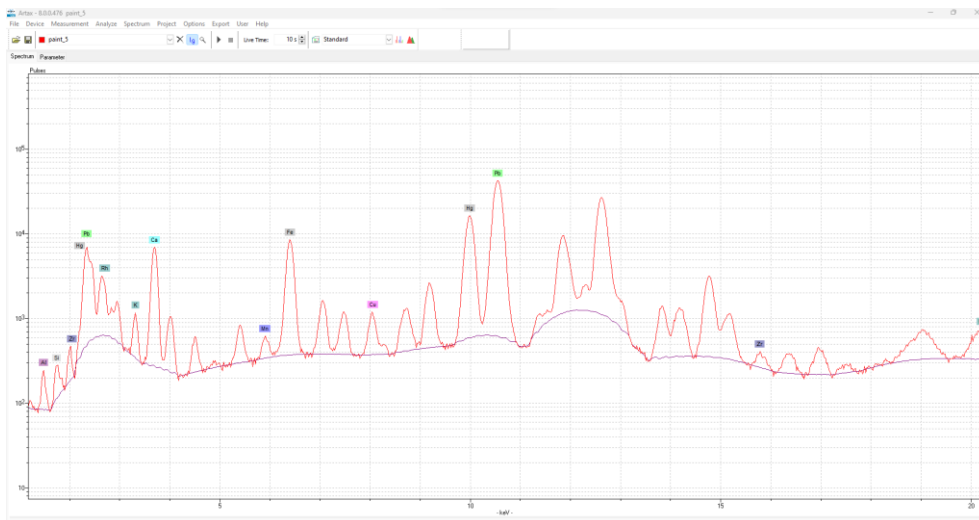


Figure 82: XRF analysis results of paint 5 (derived from: personal archive Lida Kyriopoulou).

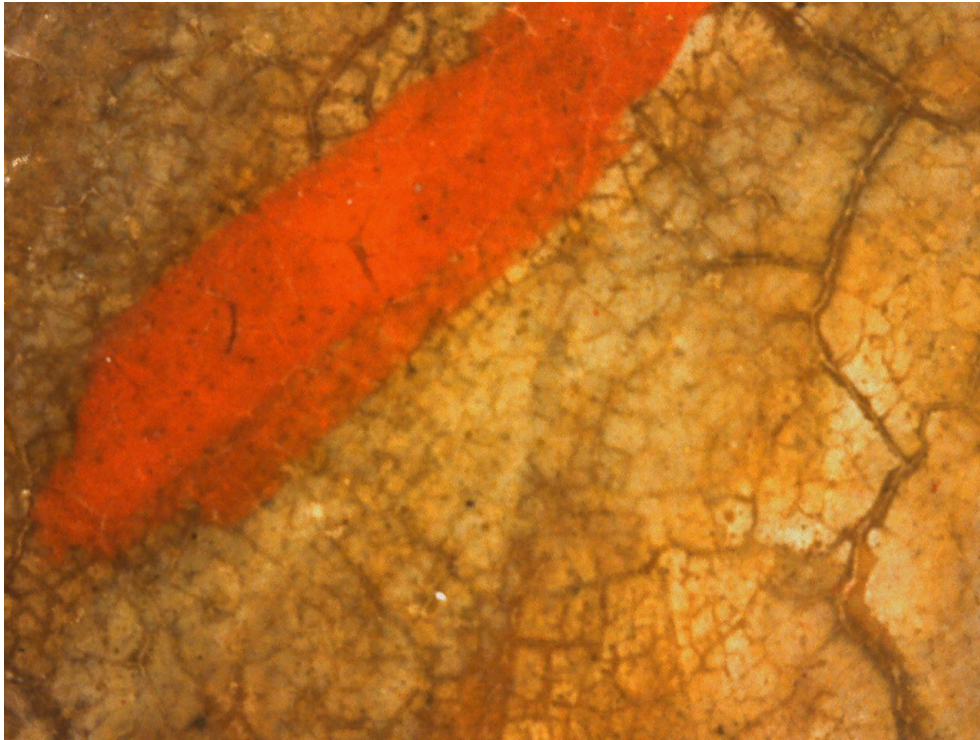


Figure 83: Portable stereomicroscope picture of paint 6 (derived from: personal archive Lida Kyriopoulou).

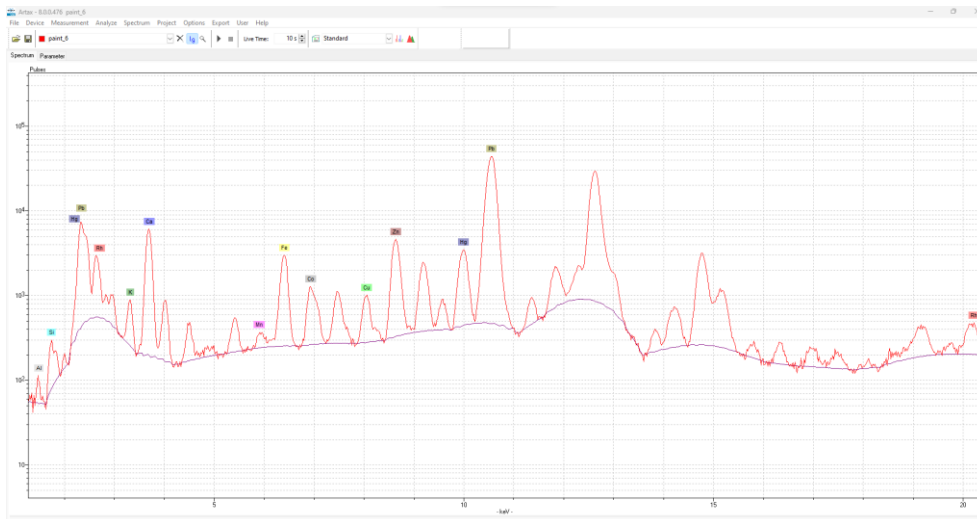


Figure 84: XRF analysis results of paint 6 (derived from: personal archive Lida Kyriopoulou).

For white pigments, analyses with the XRF spectrometer show that most probably lead white ($2\text{PbCO}_3 \cdot \text{Pb}(\text{OH})_2$) and calcite (CaCO_3) were used. In

particular, in paints 7(Figure 85), 8 (Figure 86), 9a (Figure 87), 9b (Figure 88), and 10 (Figure 89), the presence of lead (Pb) indicates the use of lead white ($2\text{PbCO}_3 \cdot \text{Pb}(\text{OH})_2$) and the presence of calcium (Ca), the existence of calcite (CaCO_3). Also, as mentioned before, maybe calcium comes from the gypsum ($\text{CaSO}_4 \cdot 2\text{H}_2\text{O}$). In paint 9, the presence of gold (Au) is apparently due to the gold leaf used to decorate the wreath of the left angel¹¹⁸. However, in paints 7 and 10, the shades are greyish leading to the presumption that the white pigment was mixed with black pigment. The presence of iron (Fe), and manganese (Mn) indicates the use of magnetite (Fe_3O_4) and/or manganese black (MnO_2). In addition, carbon black (C) might have been used.

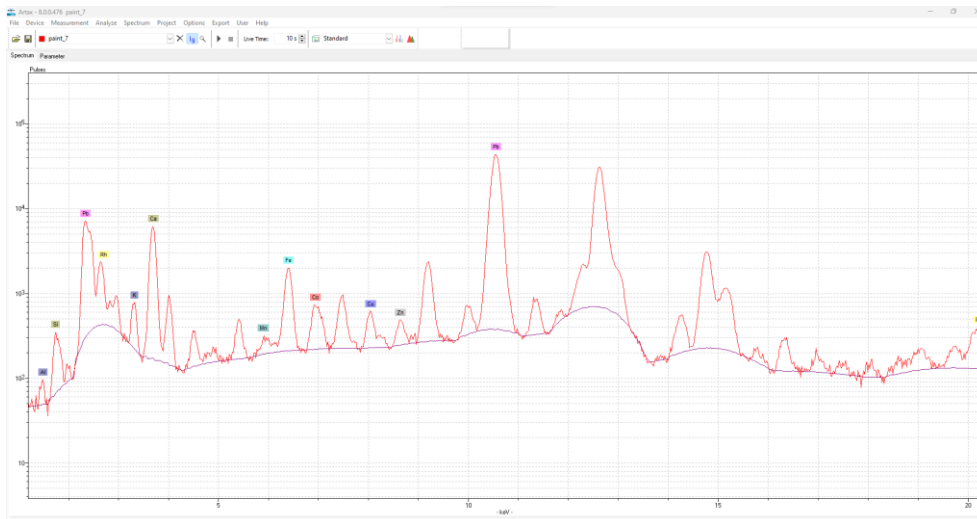


Figure 85: XRF analysis results of paint 7(derived from: personal archive Lida Kyriopoulou).

¹¹⁸ Ζαμβακέλλης, 1985, p. 35.

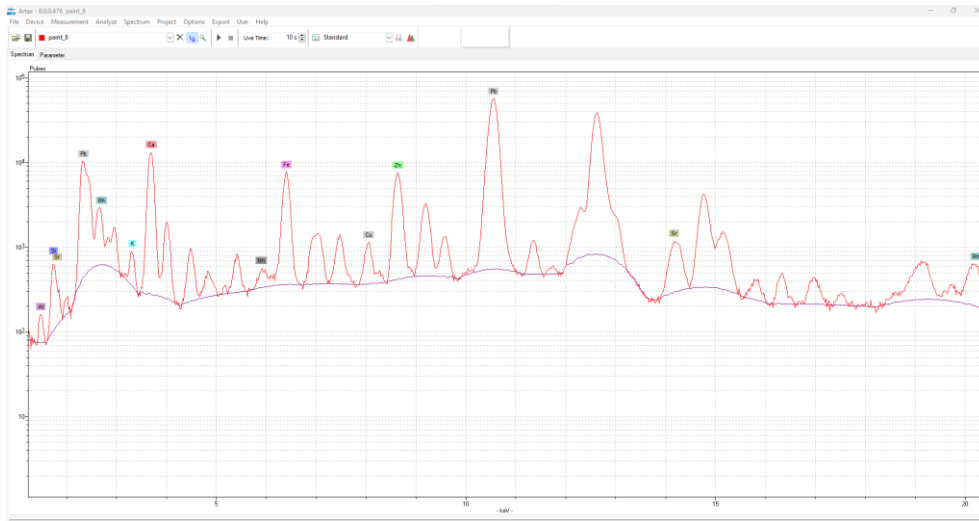


Figure 86: XRF analysis results of paint 8 (derived from: personal archive Lida Kyriopoulou).

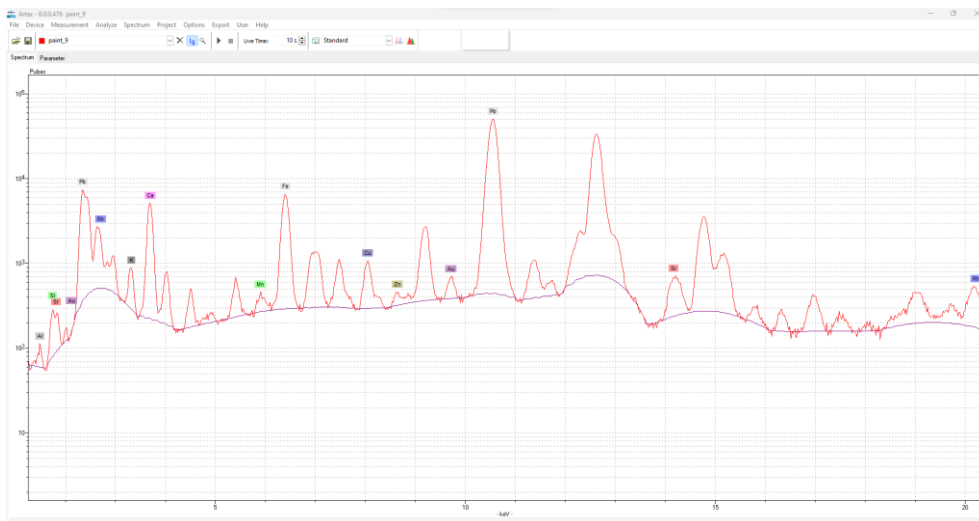


Figure 87: XRF analysis results of paint 9a (derived from: personal archive Lida Kyriopoulou).

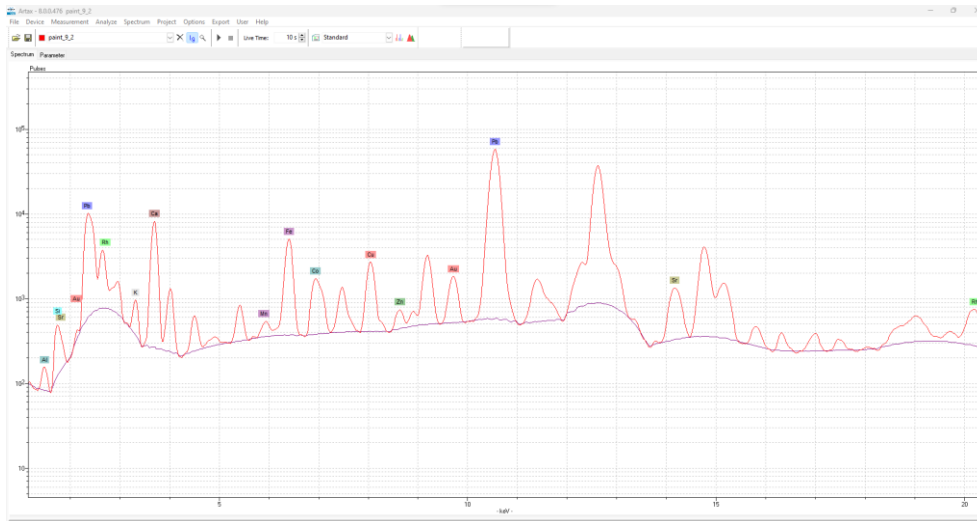


Figure 88: XRF analysis results of paint 9b (derived from: personal archive Lida Kyriopoulou)..

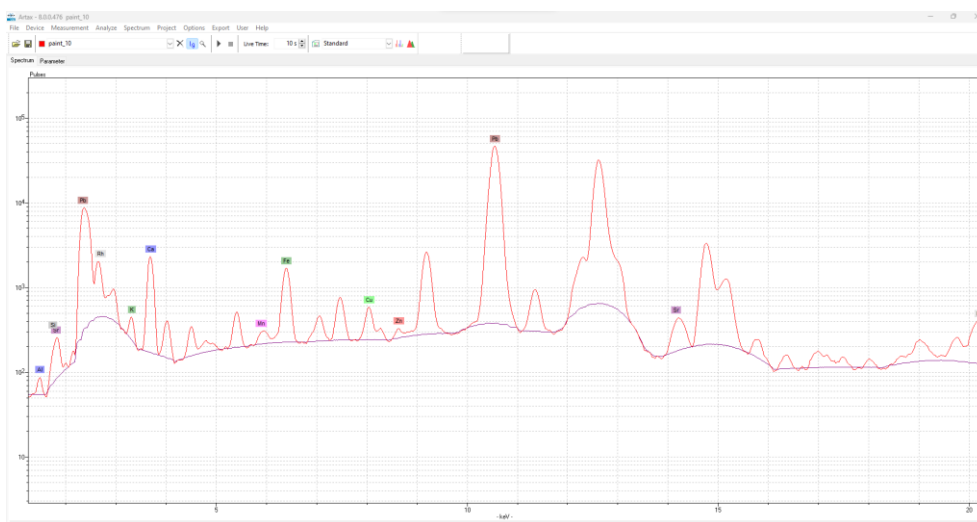


Figure 89: XRF analysis results of paint 10 (derived from: personal archive Lida Kyriopoulou).

Based on the chemical elements provided by the XRF analysis of paint 11 (Figure 90), which renders green color, malachite ($\text{Cu}_2\text{CO}_3(\text{OH})_2$)¹¹⁹, verdigris ($\text{Cu}(\text{CH}_3\text{COO})_2 \cdot \text{H}_2\text{O}$)¹²⁰ and/or green earth ($\text{K}[(\text{Al}, \text{Fe}^{3+}), (\text{Fe}^{2+}, \text{Mg})](\text{AlSi}_3, \text{Si}_4)\text{O}_{10}(\text{OH})_2$)¹²¹ could have been used.

¹¹⁹ Eastaugh, Walsh, Chaplin, & Siddall, 2004, p. 249.

¹²⁰ Eastaugh, Walsh, Chaplin, & Siddall, 2004, pp. 385-386.

¹²¹ Eastaugh, Walsh, Chaplin, & Siddall, 2004, pp. 174-175.

Besides, as can be seen at the stereomicroscope image of paint 11, red pigment is observed at some points (Figure 91). The possible red pigment used based on the XRF analysis, is red lead (Pb_3O_4). On the other hand, the green shade could be a combination of blue and yellow pigment. Based on the chemical elements traced, the blue pigment could be azurite ($\text{Cu}_3(\text{CO}_3)_2(\text{OH})_2$)¹²², indigo ($\text{C}_{16}\text{H}_{10}\text{N}_2\text{O}_2$)¹²³, egyptian blue ($\text{CaCuSi}_4\text{O}_{10}$)¹²⁴, ultramarine ($\text{Na}_7\text{Al}_6\text{Si}_6\text{O}_{24}\text{S}_3$)¹²⁵ and/or smalt ($\text{SiO}_2(\text{vit})\text{Co}_x$)¹²⁶, while the yellow pigment could be yellow ochre ($\alpha\text{-FeOOH}$)¹²⁷ and/or lead oxide yellow (PbO)¹²⁸. Nonetheless, as mentioned above, XRF cannot track down the light elements, so indigo ($\text{C}_{16}\text{H}_{10}\text{N}_2\text{O}_2$) cannot be identified. In addition, because the final shade is dark, calcium (Ca) probably comes from the primer layer's gypsum ($\text{CaSO}_4 \cdot 2\text{H}_2\text{O}$). On the other hand, the darkness of the paint may be due to the mixing of the blue pigment with black pigment magnetite (Fe_3O_4), manganese black (MnO_2), and/or carbon black (C).

¹²² Eastaugh, Walsh, Chaplin, & Siddall, 2004, pp. 33-34.

¹²³ Eastaugh, Walsh, Chaplin, & Siddall, 2004, p. 194.

¹²⁴ Eastaugh, Walsh, Chaplin, & Siddall, 2004, pp. 147-148.

¹²⁵ Eastaugh, Walsh, Chaplin, & Siddall, 2004, pp. 375-376.

¹²⁶ Eastaugh, Walsh, Chaplin, & Siddall, 2004, pp. 345-346.

¹²⁷ Eastaugh, Walsh, Chaplin, & Siddall, 2004, pp. 401-402.

¹²⁸ Eastaugh, Walsh, Chaplin, & Siddall, 2004, p. 228.

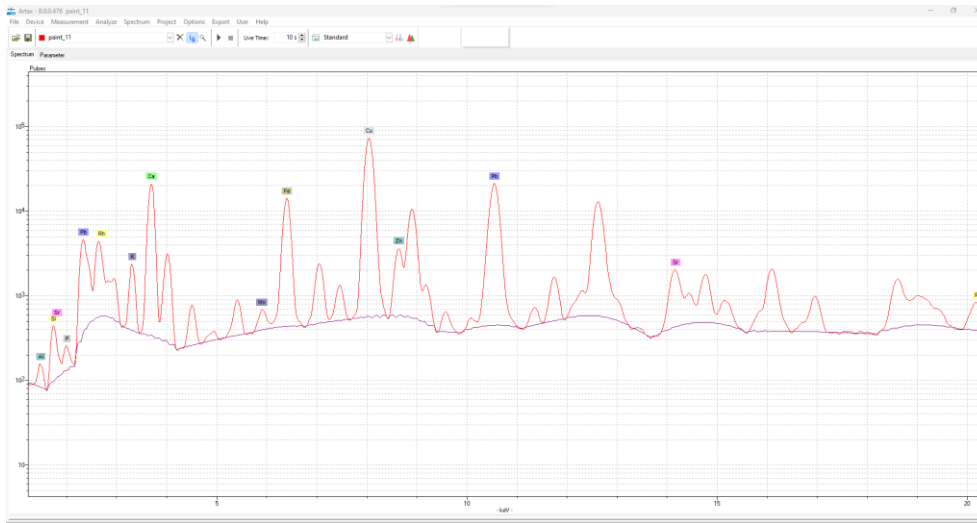


Figure 90: XRF analysis results of paint 11 (derived from: personal archive Lida Kyriopoulou).

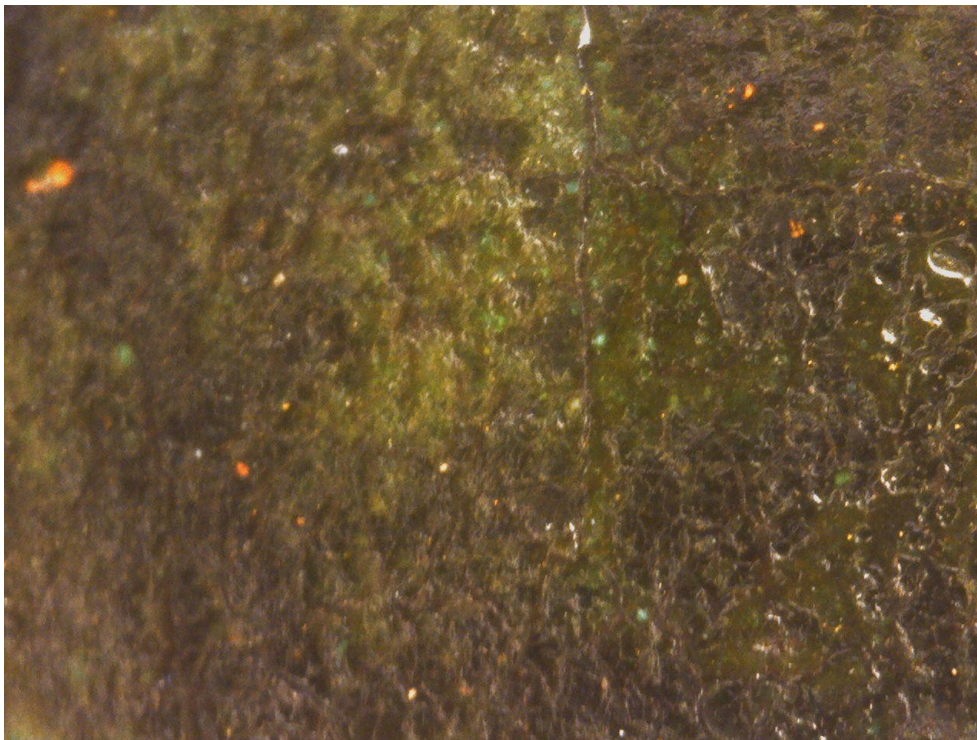


Figure 91: Portable stereomicroscope picture of paint 11 (derived from: personal archive Lida Kyriopoulou).

As can be observed at the stereomicroscope of the paint 12 (Figure 92), which gives a greenish-blue color, is likely a mixture of blue and yellow. Based on the results of the XRF analysis for paint 12 (Figure 93), the possible blue pigments are azurite ($\text{Cu}_3(\text{CO}_3)_2(\text{OH})_2$), indigo ($\text{C}_{16}\text{H}_{10}\text{N}_2\text{O}_2$), egyptian blue ($\text{CaCuSi}_4\text{O}_{10}$), ultramarine ($\text{Na}_7\text{Al}_6\text{Si}_6\text{O}_{24}\text{S}_3$)¹²⁹, and/or smalt ($\text{SiO}_2(\text{vit})\text{Co}_x$), while the possible yellow pigments are yellow ochre ($\alpha\text{-FeOOH}$) and/or lead yellow (PbO). The current shade is dark, which, suggests the presence of black pigment, like magnetite (Fe_3O_4), manganese black (MnO_2), and/or carbon black (C). However, the stereomicroscope image shows that the artist used white pigment at some points. The possible white pigments used are lead white ($2\text{PbCO}_3\cdot\text{Pb}(\text{OH})_2$), calcite (CaCO_3), and/or gypsum ($\text{CaSO}_4\cdot 2\text{H}_2\text{O}$) from the prime layer.

¹²⁹ Eastaugh, Walsh, Chaplin, & Siddall, 2004, pp. 375-376.

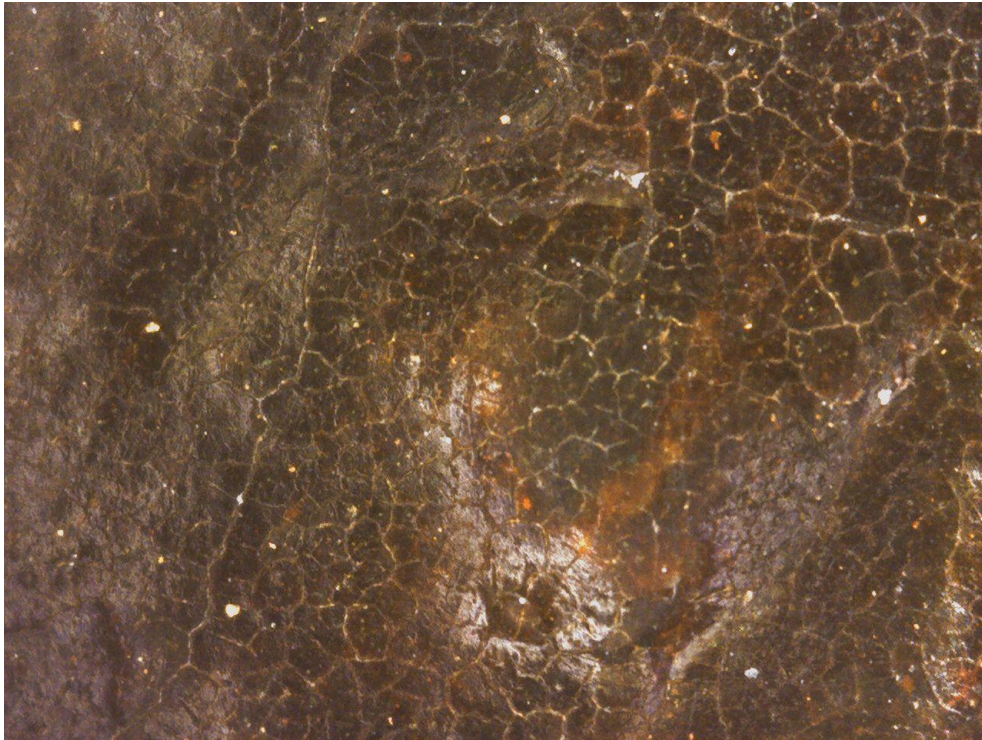


Figure 92: Portable stereomicroscope picture of paint 12 (derived from: personal archive Lida Kyriopoulou).

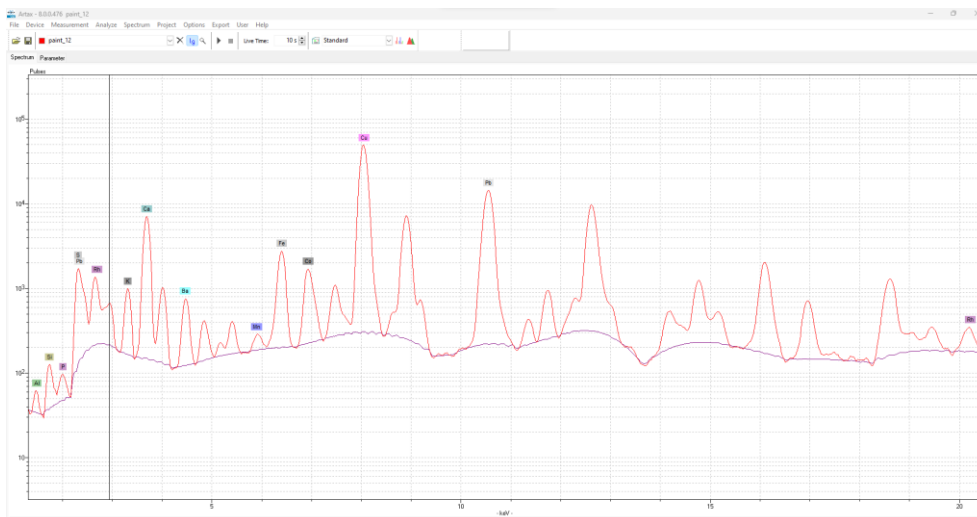


Figure 93: XRF analysis results of paint 12 (derived from: personal archive Lida Kyriopoulou).

In paint 13 (Figure 94), the color is black. Based on the XRF results, the presence of iron (Fe) indicates the use of magnetite (Fe_3O_4), and of

manganese (Mn), the presence of manganese black (MnO_2). Also, carbon black (C) might have been used, but XRF cannot trace light elements. Notably, in this case, calcium derives from the primer layer's gypsum ($\text{CaSO}_4 \cdot 2\text{H}_2\text{O}$).

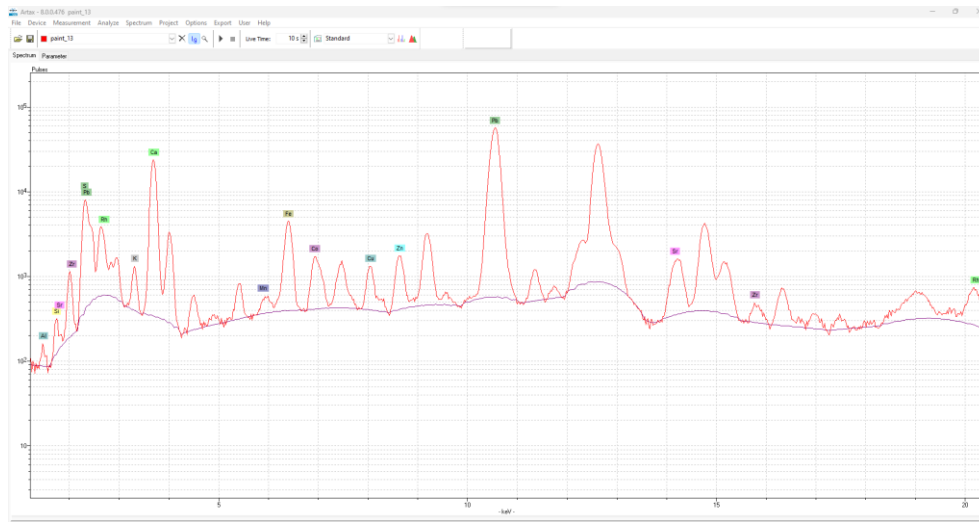


Figure 94: XRF analysis results of paint 13 (derived from: personal archive Lida Kyriopoulou).

Paint 14 (Figure 95) is a brown-ochre shade. The presence of iron (Fe) and manganese (Mn) indicates the use of Fe/Mn brown and brown ochre ($\text{FeO}(\text{OH})$)¹³⁰. On the other hand, the brown shade could result from a mixture of yellow, red, and black pigment. The yellow pigments could be yellow ochre ($\alpha\text{-FeOOH}$) and/ or lead oxide yellow (PbO). The red pigments could be red ochre (Fe_2O_3) and red lead (Pb_3O_4), while the black, magnetite (Fe_3O_4), manganese black (MnO_2), and carbon black (C). It also should be noted that the shade is quite pale, so the artist added white pigment to lighten the brown pigment. The presence of calcium (Ca) indicates the use of calcite, and the presence of lead (Pb) suggests the use of lead white ($2\text{PbCO}_3 \cdot \text{Pb}(\text{OH})_2$). Also calcium could come from the gypsum ($\text{CaSO}_4 \cdot 2\text{H}_2\text{O}$)

¹³⁰ Eastaugh, Walsh, Chaplin, & Siddall, 2004, p. 63.

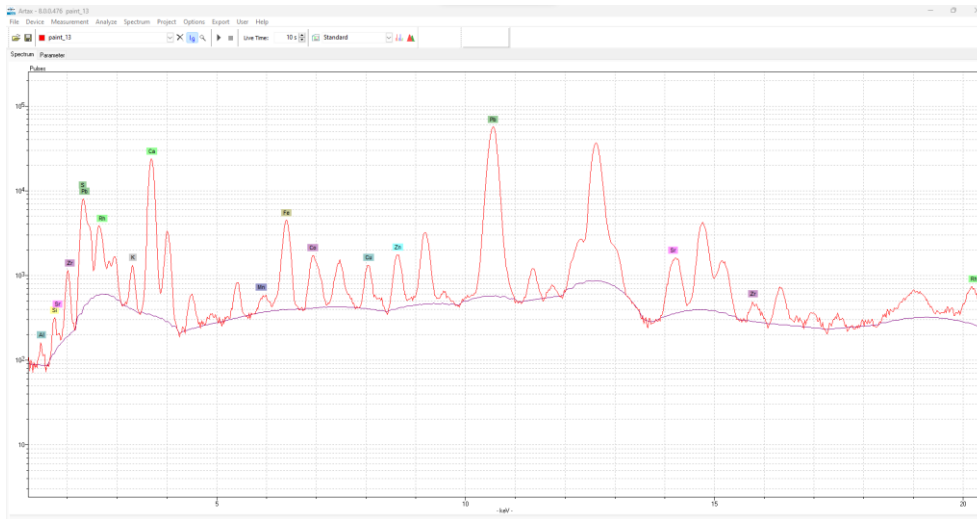


Figure 95: XRF analysis results of paint 14 (derived from: personal archive Lida Kyriopoulou).

In paint 15, which renders yellow, iron (Fe) implies that yellow ochre (α - FeOOH) and lead (Pb) that lead oxide yellow (PbO) were used. The yellow color of the paint is quite light, so the yellow pigment was mixed with calcite (CaO_3) and/or lead white ($2\text{PbCO}_3 \cdot \text{Pb}(\text{OH})_2$), without excluding the origin of calcium from the gypsum ($\text{CaSO}_4 \cdot 2\text{H}_2\text{O}$).

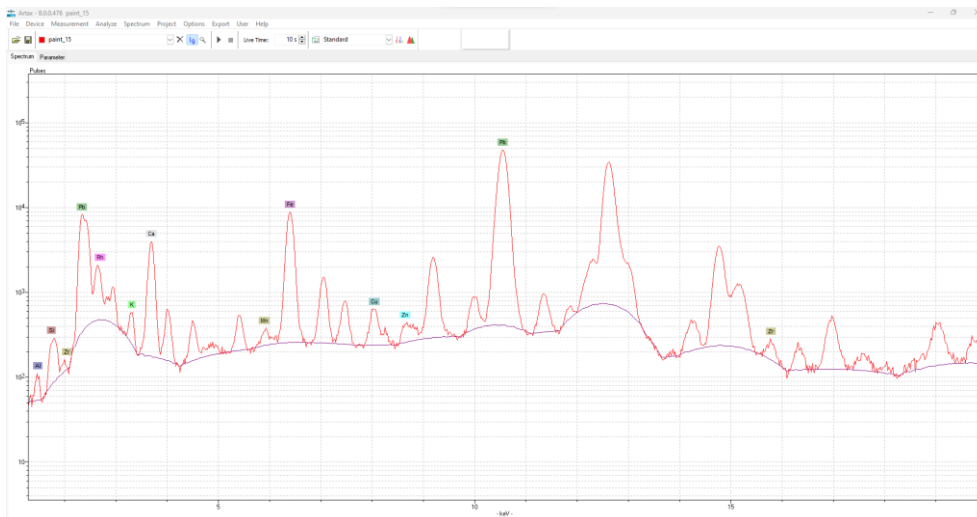


Figure 96: XRF analysis results of paint 15 (derived from: personal archive Lida Kyriopoulou).

Paint 16 (Figure 97) is a purple color. Iron (Fe) indicates the presence of caput mortuum (Fe_3O), a purple-red pigment. On the other hand, the purple color is likely to be the result of a mixture of red and blue pigment. Based on the chemical elements identified by XRF analysis, the red pigments could be red ochre (Fe_2O_3), and/or red lead (Pb_3O_4), while the blue pigments could be azurite ($\text{Cu}_3(\text{CO}_3)_2(\text{OH})_2$), indigo ($\text{C}_{16}\text{H}_{10}\text{N}_2\text{O}_2$), and/or ultramarine ($\text{Na}_7\text{Al}_6\text{Si}_6\text{O}_{24}\text{S}_3$). And in this case, it is worth noting that in paint 16 the purple shade is dark, so black pigment would have been used for darkening. The black pigments are probably black magnetite (Fe_3O_4), manganese black (MnO_2), and/or carbon black (C). The presence of calcium (Ca) probably comes from gypsum ($\text{CaSO}_4 \cdot 2\text{H}_2\text{O}$). It is noteworthy that the stereomicroscope of paint 16 reveals the presence of yellow pigment. Based on XRF analysis, the possible yellow pigments used are yellow ochre ($\alpha\text{-FeOOH}$) and lead oxide yellow (PbO) (Figure 98).

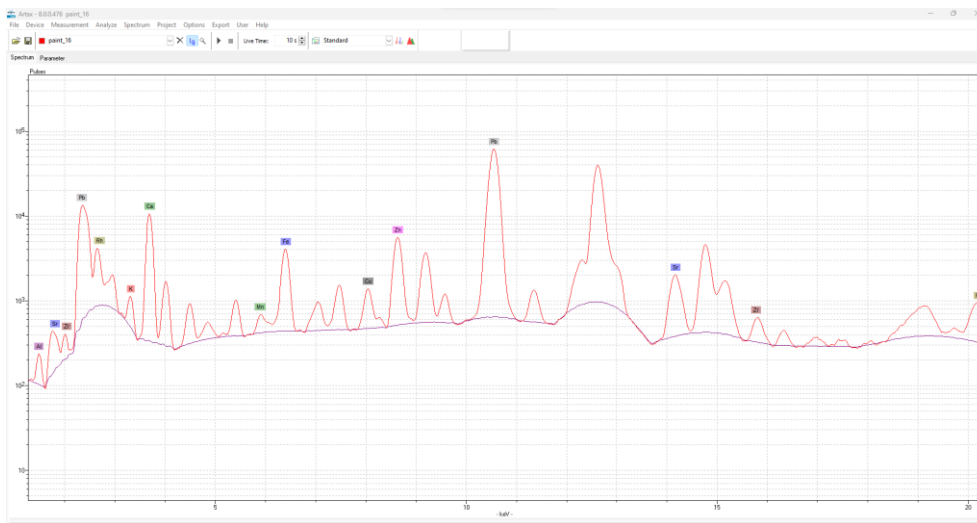


Figure 97: XRF analysis results of paint 16 (derived from: personal archive Lida Kyriopoulou).

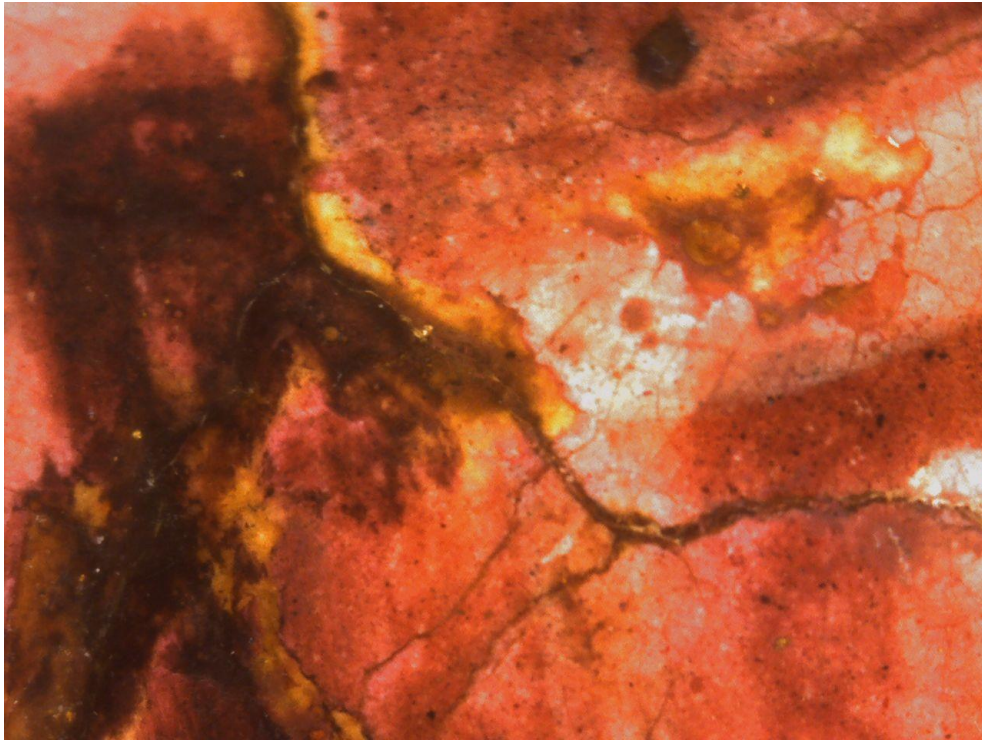


Figure 98: Portable stereomicroscope picture of paint 16 (derived from: personal archive Lida Kyriopoulou).

The table below shows the possible pigments in each XRF paint.

Name of Paint	Color of Sample	Chemical Elements	Possible Pigments
Paint 1	Red Bole (right of the central building)	Al, Si, Sr, Pb, Rh, Ca, Fe, Cu, Zn, Pb, Sr, Rh	Red Ochre (Fe_2O_3), red lead (Pb_3O_4)

			calcite (CaCO_3), lead white ($2\text{PbCO}_3 \cdot \text{Pb}(\text{OH})_2$), gypsum ($\text{CaSO}_4 \cdot 2\text{H}_2\text{O}$)
Paint 2	Red (Gemstone on chest of the left angel)	Al, Si, Zr, Au, Hg, Pb, Rh, K, Ca, Mn, Fe, Cu, Zn, Au, Hg, Pb, Zr, Rh	<p>Red lead (Pb_3O_4), vermilion (HgS), red ochre (Fe_2O_3)</p> <p>calcite (CaCO_3), lead white ($2\text{PbCO}_3 \cdot \text{Pb}(\text{OH})_2$), gypsum ($\text{CaSO}_4 \cdot 2\text{H}_2\text{O}$)</p>
Paint 3	Orange Red (floor, to the left of the table's base)	Al, Si, Hg, Pb, Rh, K, Ca, Mn, Fe, Cu, Zn, Hg, Pb, Rh	<p>Red lead (Pb_3O_4), vermilion (HgS), red ochre (Fe_2O_3)</p> <p>calcite (CaCO_3), lead white ($2\text{PbCO}_3 \cdot \text{Pb}(\text{OH})_2$), gypsum ($\text{CaSO}_4 \cdot 2\text{H}_2\text{O}$)</p> <p>magnetite ($\text{Fe}_3\text{O}_4$), manganese black ($\text{MnO}_2$), carbon black (C)</p>
Paint 4	Red (head drape of the figure between central and right angel)	Al, Si, Pb, Rh, K, Ca, Mn, Fe, Co, Cu, Zn, Pb, Rh	<p>Red ochre (Fe_2O_3), red lead (Pb_3O_4)</p> <p>calcite (CaCO_3), lead white ($2\text{PbCO}_3 \cdot \text{Pb}(\text{OH})_2$), gypsum ($\text{CaSO}_4 \cdot 2\text{H}_2\text{O}$)</p>

Paint 5	Red (chest of the central angel)	Al, Si, Zr, Hg, Pb, Rh, K, Ca, Mn, Fe, Cu, Hg, Pb, Zr, Rh	<p>red lead (Pb_3O_4), vermilion (HgS), red ochre (Fe_2O_3)</p> <p>calcite ($CaCO_3$), lead white ($2PbCO_3 \cdot Pb(OH)_2$), gypsum ($CaSO_4 \cdot 2H_2O$)</p> <p>magnetite (Fe_3O_4), manganese black (MnO_2), carbon black (C)</p>
Paint 6	Red (letters, to the left of the painting, in front of the building)	Al, Si, Hg, Pb, Rh, K, Ca, Mn, Fe, Co, Cu, Zn, Hg, Pb, Rh	<p>red lead (Pb_3O_4), vermilion (HgS), red ochre (Fe_2O_3)</p> <p>calcite ($CaCO_3$), lead white ($2PbCO_3 \cdot Pb(OH)_2$), gypsum ($CaSO_4 \cdot 2H_2O$)</p> <p>magnetite (Fe_3O_4), manganese black (MnO_2), carbon black (C)</p>
Paint 7	White (table's base, left of the horizontal part)	Al, Si, Pb, Rh, K, Ca, Mn, Fe, Co, Cu, Zn, Pb, Rh	<p>lead white ($2PbCO_3 \cdot Pb(OH)_2$), calcite ($CaCO_3$), gypsum ($CaSO_4 \cdot 2H_2O$)</p> <p>magnetite (Fe_3O_4), manganese black (MnO_2), carbon black (C)</p>

Paint 8	White (left building, inside the right triangular alcove)	Al, Si, Sr, Pb, Rh, K, Ca, Mn, Fe, Cu, Zn, Pb, Sr, Rh	lead white ($2\text{PbCO}_3 \cdot \text{Pb}(\text{OH})_2$), calcite (CaCO_3), gypsum ($\text{CaSO}_4 \cdot 2\text{H}_2\text{O}$)
Paint 9	White (left building between the neck of the left angel and the golden robe of the left standing figure)	Al, Si, Sr, Au, Pb, Rh, K, Ca, Mn, Fe, Cu, Zn, Au, Pb, Sr, Rh	lead white ($2\text{PbCO}_3 \cdot \text{Pb}(\text{OH})_2$), calcite (CaCO_3), gypsum ($\text{CaSO}_4 \cdot 2\text{H}_2\text{O}$) gold leaf (Au)
		Al, Si, Sr, Au, Pb, Rh, K, Ca, Mn, Fe, Co, Cu, Zn, Au, Pb, Sr, Rh	lead white ($2\text{PbCO}_3 \cdot \text{Pb}(\text{OH})_2$), calcite (CaCO_3), gypsum ($\text{CaSO}_4 \cdot 2\text{H}_2\text{O}$) gold leaf (Au)
Paint 10	White (tablecloth)	Al, Si, Sr, Pb, Rh, K, Ca, Mn, Fe, Cu, Zn, Pb, Sr, Rh	lead white ($2\text{PbCO}_3 \cdot \text{Pb}(\text{OH})_2$), calcite (CaCO_3), gypsum ($\text{CaSO}_4 \cdot 2\text{H}_2\text{O}$) magnetite (Fe_3O_4), manganese black (MnO_2), carbon black (C)
Paint 11	Green (green robe of the	Al, Si, Sr, P, Pb, Rh, K, Ca, Mn,	malachite ($\text{Cu}_2\text{CO}_3(\text{OH})_2$), verdigris ($\text{Cu}(\text{CH}_3\text{COO})_2 \cdot \text{H}_2\text{O}$),

	right angel, triangular fold between its legs)	Fe, Cu, Zn, Pb, Sr, Rh	<p>green earth $(K[(Al,Fe^{3+}), (Fe^{2+},Mg)](AlSi_3Si_4)O_{10}(OH)_2)$ red lead (Pb_3O_4) azurite ($Cu_3(CO_3)_2(OH)_2$), indigo ($C_{16}H_{10}N_2O_2$), egyptian blue ($CaCuSi_4O_{10}$), ultramarine ($Na_7Al_6Si_6O_{24}S_3$), smalt $(SiO_2(vit)Co_x)$ yellow ochre (α-FeOOH), lead oxide yellow (PbO) gypsum ($CaSO_4 \cdot 2H_2O$) magnetite (Fe_3O_4), manganese black (MnO_2), carbon black (C)</p>
Paint 12	Blue- green (blue- green robe under central angel's left arm)	Al, Si, P,S, Pb, Rh, K, Ca, Ba, Mn, Fe, Co, Cu, Pb, Rh	<p>azurite ($Cu^{2+}_3(CO_3)_2(OH)_2$), egyptian blue ($CaCuSi_4O_{10}$), ultramarine ($Na_7Al_6Si_6O_{24}S_3$) indigo ($C_{16}H_{10}N_2O_2$) smalt ($SiO_2(vit)Co_x$) yellow ochre (α-FeOOH), lead oxide yellow (PbO)</p>

			<p>magnetite (Fe₃O₄), manganese black (MnO₂), carbon black (C)</p> <p>lead white (2PbCO₃·Pb (OH)₂), calcite (CaCO₃), gypsum (CaSO₄·2H₂O)</p>
Paint 13	Black (the black shading in the front window of the left building)	Al, Si, Sr, Zr, S/ Pb, Rh, K, Ca, Mn, Fe, Co, Cu, Zn, Pb, Sr, Zr, Rh	<p>magnetite (Fe₃O₄), manganese black (MnO₂), carbon black (C)</p>
Paint 14	Brown-Ochre (forehead of the left angel)	Al, Si, Sr, Zr, S/ Pb, Rh, K, Ca, Mn, Fe, Co, Cu, Zn, Pb, Sr, Zr, Rh	<p>Fe/Mn brown, brown ochre (FeO(OH)),</p> <p>yellow ochre (α-FeOOH), lead oxide yellow (PbO)</p> <p>red ochre (Fe₂O₃), red lead (Pb₃O₄)</p> <p>magnetite (Fe₃O₄), manganese black (MnO₂), and carbon black (C)</p>

			lead white ($2\text{PbCO}_3 \cdot \text{Pb}(\text{OH})_2$), calcite (CaCO_3), gypsum ($\text{CaSO}_4 \cdot 2\text{H}_2\text{O}$)
Paint 15	Yellow (the bread in front of the central angel	Al, Si, Zr, Pb, Rh, K, Ca, Mn, Fe, Cu, Zn, Pb, Zr	yellow ochre ($\alpha\text{-FeOOH}$), lead oxide yellow (PbO) calcite (CaCO_3), lead white ($2\text{PbCO}_3 \cdot \text{Pb}(\text{OH})_2$), gypsum ($\text{CaSO}_4 \cdot 2\text{H}_2\text{O}$)
Paint 16	Purple (the left triangular alcove of the central domed building)	Al, Sr, Zr, Pb, Rh, K, Ca, Mn, Fe, Cu, Zn, Pb, Sr, Zr, Rh	caput mortuum (Fe_3O), red ochre (Fe_2O_3), red lead (Pb_3O_4), azurite ($\text{Cu}_3(\text{CO}_3)_2(\text{OH})_2$), indigo ($\text{C}_{16}\text{H}_{10}\text{N}_2\text{O}_2$) and ultramarine ($\text{Na}_7\text{Al}_6\text{Si}_6\text{O}_{24}\text{S}_3$) magnetite (Fe_3O_4), manganese black (MnO_2), carbon black (C). gypsum ($\text{CaSO}_4 \cdot 2\text{H}_2\text{O}$) yellow ochre ($\alpha\text{-FeOOH}$), lead oxide yellow (PbO)

Table 1: Summary of the results obtained with the XRF analysis technique.

6.4. Raman Spectroscopy

The application of Raman Spectroscopy on the painting specified the identification of the pigments achieved by the other techniques of the research protocol. In the analysis of the painting with Raman Spectroscopy, 16 paint point analyses were performed. The Raman analysis points are the same as the OM and XRF ones (Figure 99).

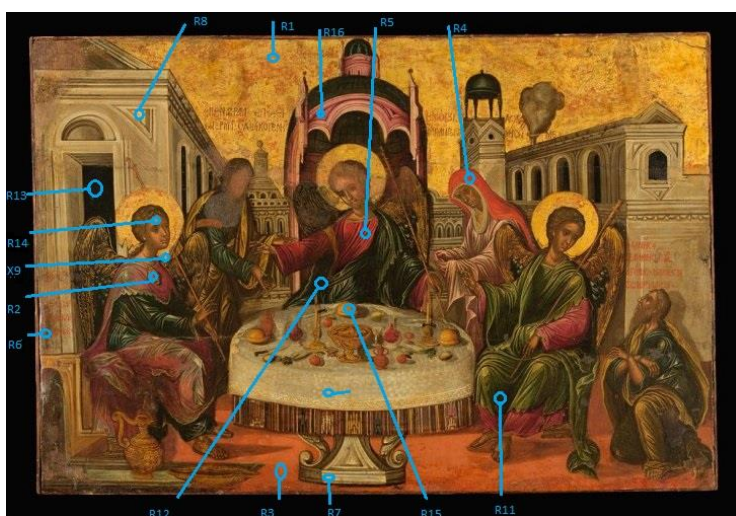


Figure 99: Raman analysis points (digital processing Lida Kyriopoulou).

At point 1 (Figure 100), Raman Analysis traced only gypsum ($\text{CaSO}_4 \cdot 2\text{H}_2\text{O}$) from the primer layer.

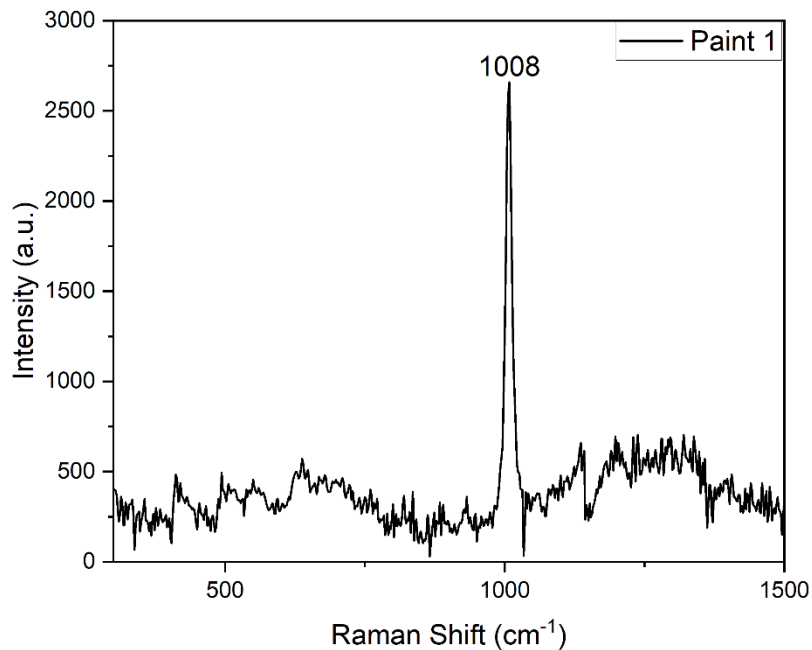


Figure 100: Raman analysis results of paint 1 (derived from: personal archive Lida Kyriopoulou).

At paint 2 (Figure 101), the pigments identified are gypsum ($\text{CaSO}_4 \cdot 2\text{H}_2\text{O}$), white lead ($2\text{PbCO}_3 \cdot \text{Pb}(\text{OH})_2$), verdigris ($\text{Cu}(\text{CH}_3\text{COO})_2 \cdot \text{H}_2\text{O}$), red lead (Pb_3O_4) and raw umber (Fe_2O_3). The presence of gypsum ($\text{CaSO}_4 \cdot 2\text{H}_2\text{O}$), as mentioned above, probably comes from the primer layer, while the lead white ($2\text{PbCO}_3 \cdot \text{Pb}(\text{OH})_2$) was probably used by the artist to lighten the pigment red lead (Pb_3O_4). Brown pigment raw umber (Fe_2O_3) and green pigment verdigris ($\text{Cu}(\text{CH}_3\text{COO})_2 \cdot \text{H}_2\text{O}$) were probably mixed for the rendering of the shadows and *grapsimata*, as can be seen in the image of paint 2, using the portable stereomicroscope (Figure 102).

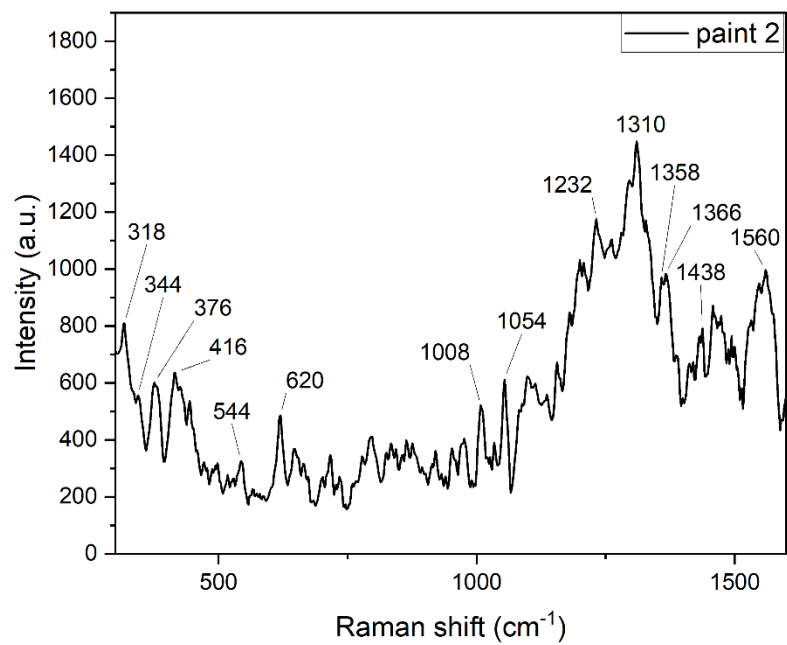


Figure 101: Raman analysis results of paint 2 points (derived from: personal archive Lida Kyriopoulou).

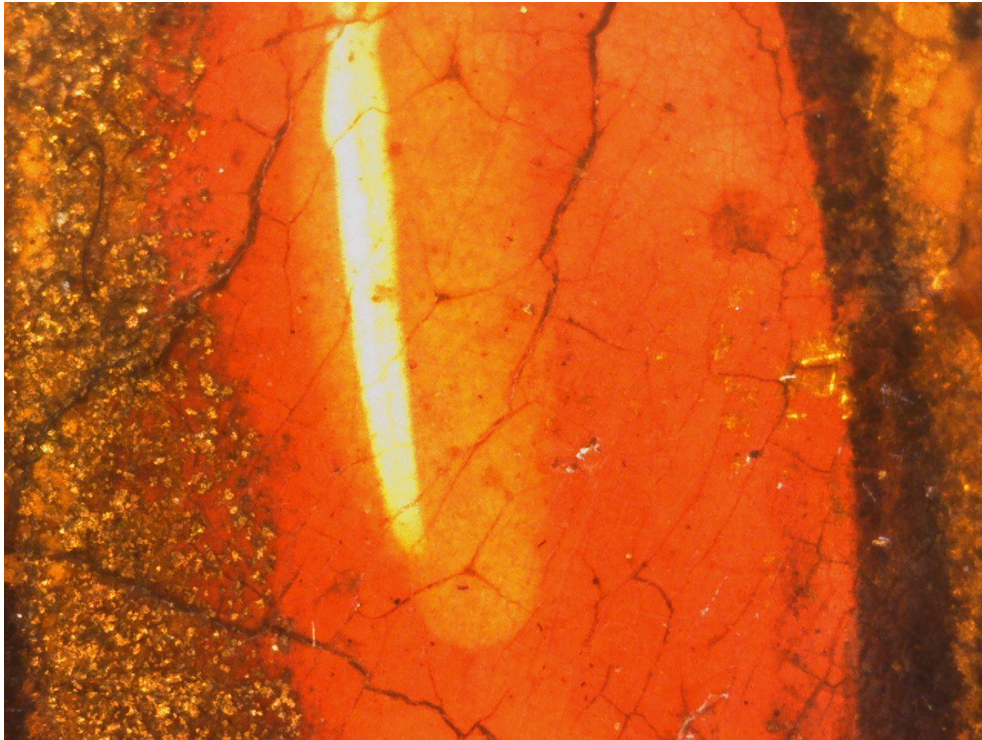


Figure 102: Portable stereomicroscope picture of paint 2 (derived from: personal archive Lida Kyriopoulou).

At paint 3 (Figure 80), vermilion (HgS), gypsum ($\text{CaSO}_4 \cdot 2\text{H}_2\text{O}$), and lead white ($2\text{PbCO}_3 \cdot \text{Pb}(\text{OH})_2$) are tracked. And in this case, gypsum ($\text{CaSO}_4 \cdot 2\text{H}_2\text{O}$) probably comes from the primer layer, and lead white ($2\text{PbCO}_3 \cdot \text{Pb}(\text{OH})_2$) was used to lighten the red pigment vermilion (HgS). In paint 6 (Figure 104) the same pattern is observed, except that instead of vermilion (HgS) as a red pigment, the artist may have used red ochre (Fe_2O_3).

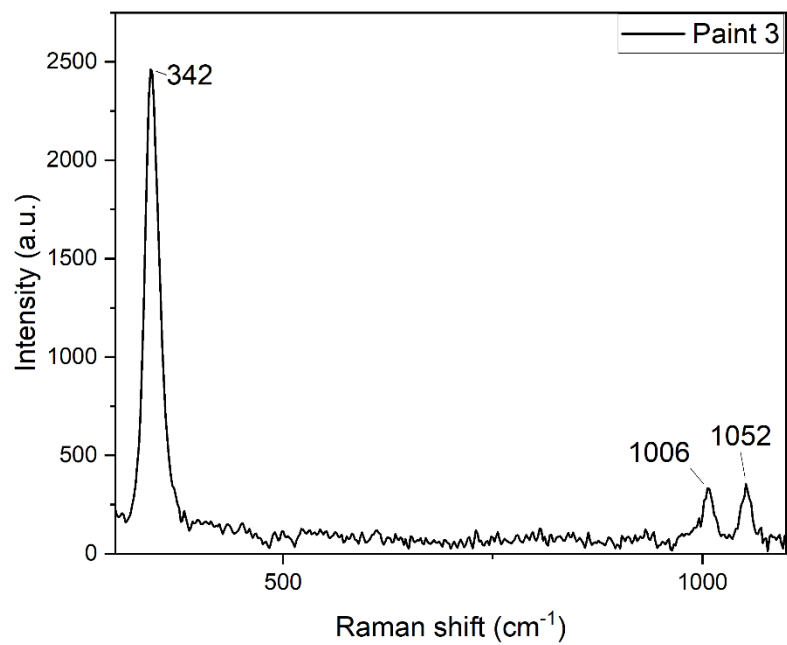


Figure 103: Raman analysis results of paint 3 (derived from: personal archive Lida Kyriopoulou).

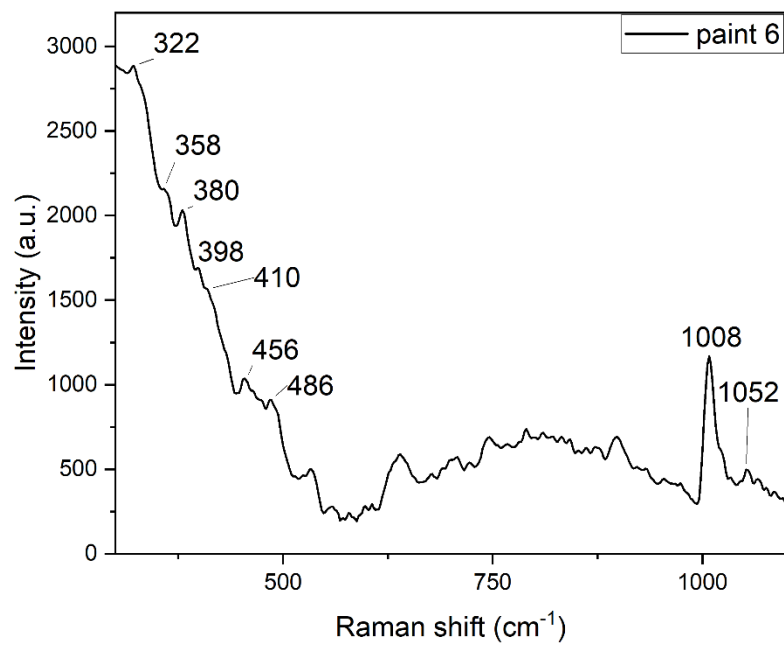


Figure 104: Raman analysis results of paint 6 (derived from: personal archive Lida Kyriopoulou).

At paints 4 and 5 only vermilion (HgS) is detected.

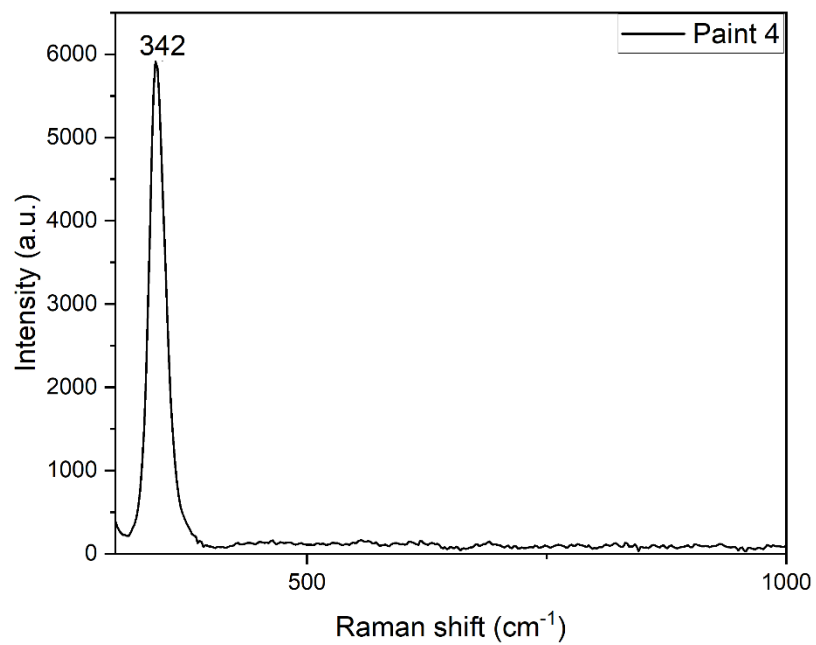


Figure 105: Raman analysis results of paint 4 (derived from: personal archive Lida Kyriopoulou).

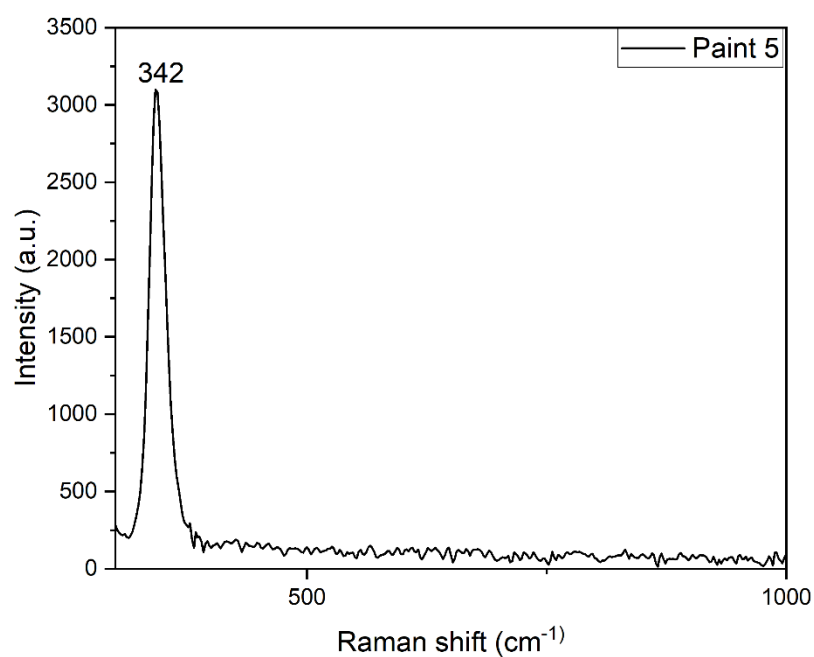


Figure 106: Raman analysis results of paint 5 (derived from: personal archive Lida Kyriopoulou).

Regarding paints 7 (Figure 107), 8 (Figure 108), and 10 (Figure 109) that render white color, lead white ($2\text{PbCO}_3 \cdot \text{Pb}(\text{OH})_2$) is detected, while in paint 10 apart from the lead white, gypsum ($\text{CaSO}_4 \cdot 2\text{H}_2\text{O}$) is also traced. At paint 9, the Raman spectrum is not interpretable due to high fluorescence¹³¹.

¹³¹ Smith & Clark, 2004, p. 1140.

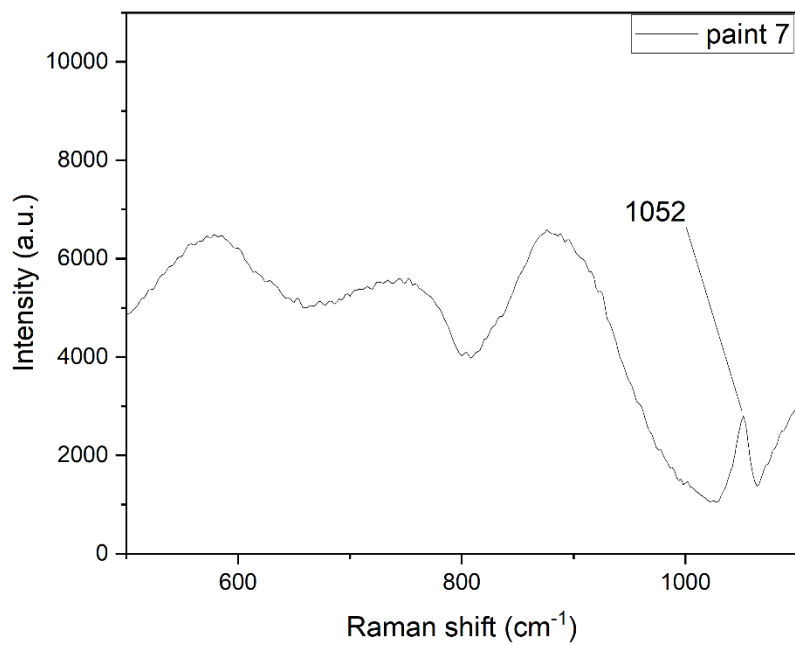


Figure 107: Raman analysis results of paint 7 (derived from: personal archive Lida Kyriopoulou).

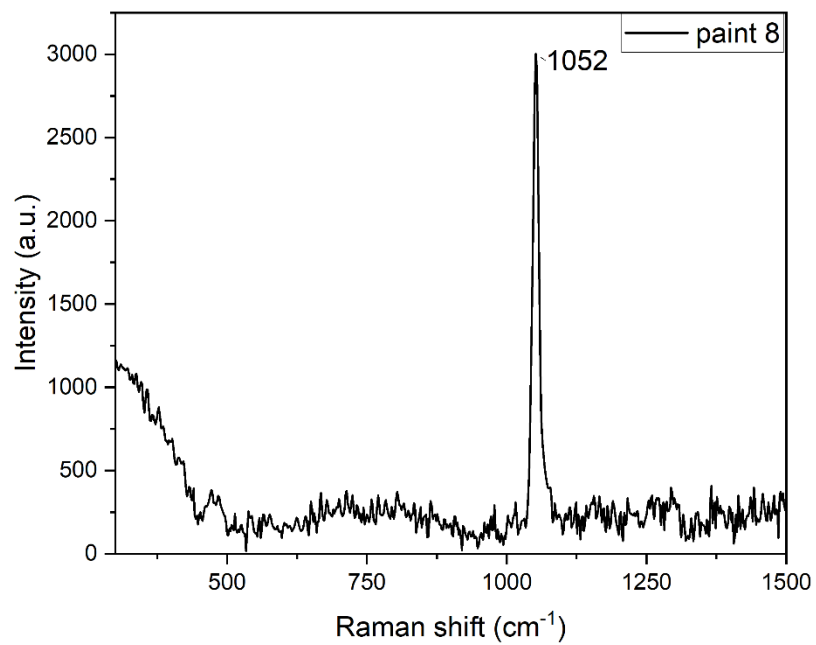


Figure 108: Raman analysis results of paint 8 (derived from: personal archive Lida Kyriopoulou).

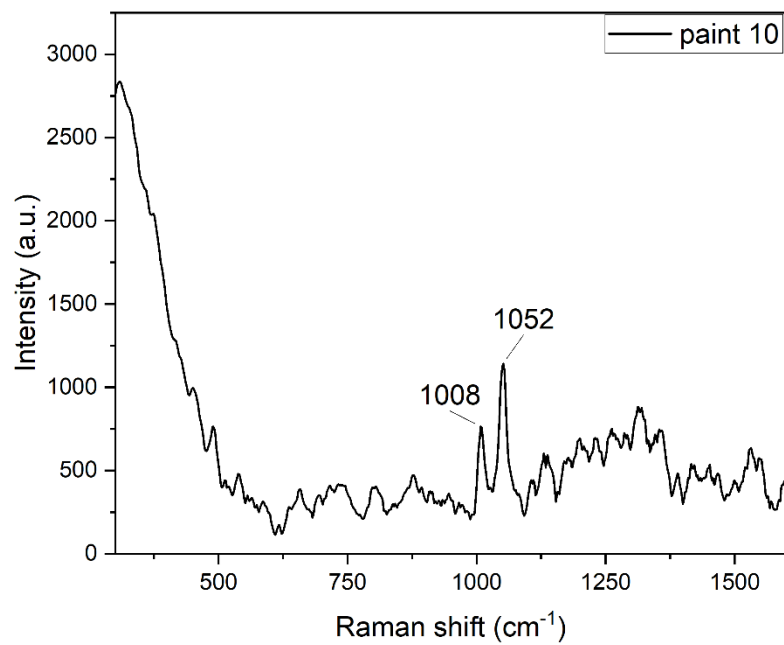


Figure 109: Raman results of paint 10 (derived from: personal archive Lida Kyriopoulou).

At paint 11 (Figure 110) which gives a green color, only gypsum ($\text{CaSO}_4 \cdot 2\text{H}_2\text{O}$) was detected from the prime layer.

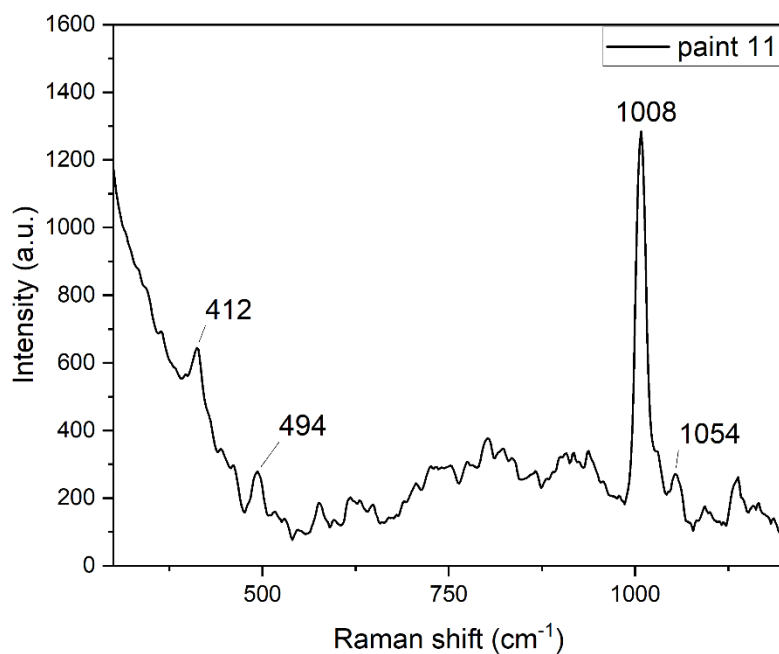


Figure 110: Raman results of paint 11 (derived from: personal archive Lida Kyriopoulou).

At paint 12, the signal was low, so it was impossible to interpret the spectrum.

No pigment was detected in paint 13 either, due to high fluorescence¹³².

In paints 14 (Figure 111) and 15 (Figure 112), vermilion (HgS) and lead white ($2\text{PbCO}_3 \cdot \text{Pb}(\text{OH})_2$) pigments were detected.

¹³² Smith & Clark, 2004, p. 1140.

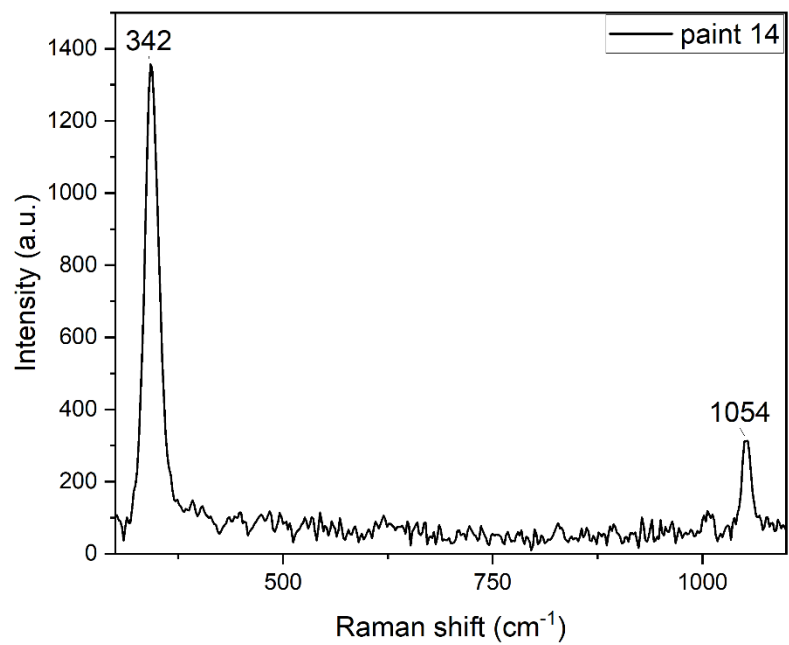


Figure 111: Raman analysis results of paint 14 (derived from: personal archive Lida Kyriopoulou).

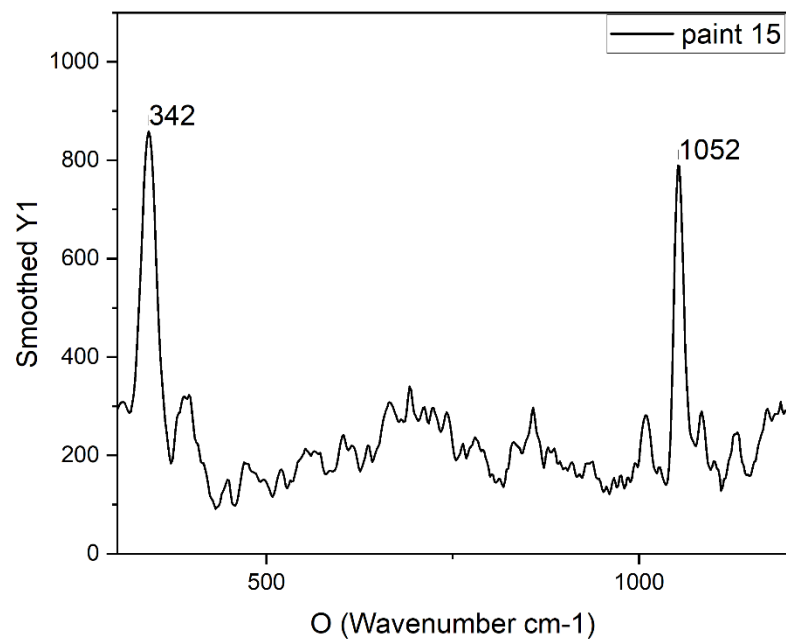


Figure 112: Raman analysis results of paint 15 (derived from: personal archive Lida Kyriopoulou).

At paint 16 (Figure 113), gypsum ($\text{CaSO}_4 \cdot 2\text{H}_2\text{O}$), and red lead (Pb_3O_4) were detected.

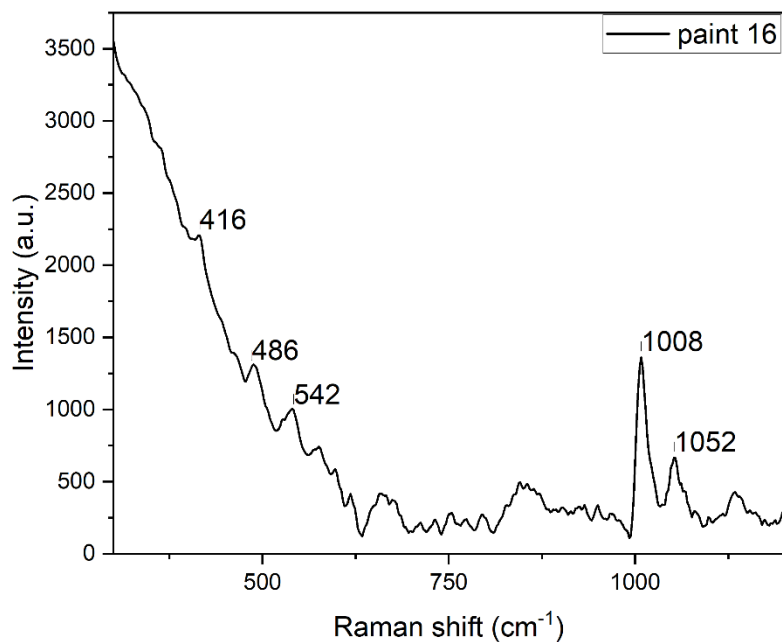


Figure 113: Raman analysis results of paint 16 (derived from: personal archive Lida Kyriopoulou).

The table below shows the pigments detected in the table by Raman Spectroscopy.

Paint of analysis	Color of Sample	Identified pigment/s and detected peaks (cm ⁻¹)
Paint 1	Red Bole (right of the central building)	gypsum (1008)
Paint 2	Red (gemstone on chest of the left angel)	lead white (416, 1054, 1366) gypsum (416, 620, 1008)

		<p>verdigris? (318, 1054, 1358, 1438)</p> <p>red lead (376, 544)</p> <p>raw umber (1232, 1310)</p>
Paint 3	Orange Red (floor, to the left of the table's base)	<p>vermillion (343)</p> <p>gypsum (1006)</p> <p>lead white (1052)</p>
Paint 4	Red (head drape of figure between central and right angel)	vermillion (342)
Paint 5	Red (chest of the central angel)	vermillion (342)
Paint 6	Red (letters, to the left of the painting, in front of the building)	<p>gypsum [diopside?] (323, 358, 380, 1008)</p> <p>lead white (410, 1052)</p> <p>red ochre (398, 486)</p>
Paint 7	White (table base, left of the horizontal part)	high fluorescence, lead white (1052)
Paint 8	White (left building, inside the right triangular alcove)	lead white (1052)
Paint 9	White (left building between the neck of the left angel and the golden robe of the left standing figure)	low signal
Paint 10	White (tablecloth)	lead white (1052)

		gypsum (1008)
Paint 11	Green (green robe of the angel on the right, triangular fold between its legs)	gypsum (412, 494, 1008)
Paint 12	Blue-green (blue-green robe under central angel's left arm)	low signal
Paint 13	Black (the black shading in the front window of the left building)	high fluorescence
Paint 14	Brown-Ochre (the forehead of the left angel)	vermillion (342), lead white (1054)
Paint 15	Yellow (the bread in front of the central angel)	vermillion (342), lead white (1052)
Paint 16	Purple (the left triangular alcove of the central domed building)	gypsum (416, 486, 1008), red lead? (542)

Table 2: Summary of the results obtained with the Raman analysis technique.

7. Discussion/Conclusion

The purpose of the work was the thorough study of the painting *The Hospitality of Abraham* (GE 20547) exhibited in the Benaki Museum of Greek Culture. This painting was chosen to be studied because it is a typical example of the Cretan School, where the Byzantine Tradition is harmoniously connected with the Italian Renaissance and Venetian Mannerism. The questions posed were the influence of Byzantine Tradition and Western Art on the artist's styles, as well as the construction techniques and color palette that chose.

To be answered these questions, initially, the painting was studied iconographically and stylistically. Finally, imaging and spectroscopic techniques were performed on the painting to identify the manufacturing techniques and pigments used.

Current research has shown that the artist painted the work basically according to the Byzantine Art and has created details, mainly in the architectures influenced by the Italian Renaissance and the Venetian Mannerism.

Regarding the study of construction techniques, a multispectral camera MuSIS MS by the Forth Photonics (now DySIS™ medical) Company was used. It was revealed that an on-site draft was used, which varied slightly in the final result, for example, the table was larger in the original draft than the final depiction. In addition, it can be distinguished whether wet or dry medium was used in some points in the drawing. Finally, with the false color technique, it was possible to make some assumptions about the pigments used by the artist.

For the study of the artist's color palette, analyses of the six primary colors were done: red, white, green, blue, black, brown, yellow, purple. The colors

detected by XRF and identified by Raman Spectroscopy are red and white. The red pigments used by the artist are red lead, vermillion, and red ochre. For the rendering of the white color, lead white and gypsum of the primer layer were used. The green pigment verdigris and the brown pigment brown ochre were also identified. In the remaining colors, some indications were made based on XRF results, but were not identified by Raman. It is assumed that the green pigments were used are malachite, verdigris and green earth. The blue pigments are azurite, indigo, egyptian blue, bluestone, and smalt. The yellow pigments are yellow ochre, and lead oxide yellow. The black magnetite, manganese black, and carbon black. The purple pigment is the caput mortuum. Beyond this, however, indications were given regarding possible mixtures of pigments to create colors and shades.

7.1. Future Research

The current research has provided answers to the questions posed, however, there are several features of the painting that need to be investigated.

First of all, the painting is dated to the late 16th century and is assumed that it was created by a Cretan workshop influenced by the Cretan painter Georgios Klotzas, based on typological and iconographic evidence. It is proposed to use physicochemical dating techniques, such as dendrochronology for the dating of the wooden support and radiocarbon dating for the dating of the organic elements of the painting.

Also, only non-invasive and non-destructive techniques were used in this research. However, for the most thorough study of the work, it is proposed to use both invasive and destructive methods. For example, SEM (Scanning Electron Microscope) could be used for the recording of the intermediate layers between varnish and wooden support. In addition, the technique of Gas chromatography is recommended for the detection of media of the pigments.

Finally, Synchrotron Radiation X-ray Absorption Spectroscopy (SR-XAS) could be used for the identification of pigments and their quantitative information.

Bibliography

- Alexopoulou, A., Kaminari, A., & Moutsatsou, A. (2018). Multispectral and Hyperspectral Studies on Greek Monuments, Archaeological Objects and Paintings on Different Substrates. Achievements and Limitations. In A. Moropoulou, M. Korres, C. Georgopoulos, & C. Mouzakis, *Transdisciplinary Multispectral Modeling and Cooperation for the Preservation of Cultural Heritage* (p. Transdisciplinary Multispectral Modeling and Cooperation for the Preservation of Cultural Heritage). Athens: Springer.
- Alfeld, M., & Broekaert, J. (2013). Mobile depth profiling and sub-surface imaging techniques for historical paintings-A review. *Spectrochimica Acta Part B Atomic Spectroscopy*, 88, pp. 211-230.
- Anglos, D., Georgiou, S., & Fotakis, C. (2009). Lasers in the Analysis of Cultural Heritage Materials. *Journal of Nano Research*, 8, pp. 47-60.
- Burgio, L., & Clark, R. J. (2001). Library of FT-Raman spectra of pigments, minerals, pigment media and varnishes, and supplement to existing library of Raman spectra of pigments with visible excitation. *Spectrochimica Acta*, 57, pp. 1491–1521.
- Burgio, L., Clark, R. J., & Theodoraki, K. (2007). Raman microscopy of Greek icons: identification of unusual pigments. *Spectrochimica Acta*, 59, pp. 2371-2389.
- Caggiani, M. C., Cosentino, A., & Mangone, A. (2016). Pigments Checker version 3.0, a handy set for conservation scientists: A free online Raman spectra database. *Microchemical Journal*(129), pp. 123-132.

- Calvo Del Castillo, H., & Strivay, D. (2012). X-Ray Methods. In H. Edwards, & P. Vandenabeele (Eds.), *Analytical Archaeometry Selected Topics* (pp. 59-113). Cambridge: The Royal Society of Chemistry Publishing.
- Cartwright, M. (2020). *Colour & Technique in Renaissance Painting-World History Encyclopedia*. Retrieved from <https://www.worldhistory.org/article/1628/colour--technique-in-renaissance-painting/#references>
- Colombini, M. P., & Modugno, F. (2004). Characterization of proteinaceous binders in artistic paintings by chromatographic techniques. *Journal of Separation Science*, 27, pp. 147-160.
- Colombini, M., Andreotti, A., Bonaduce, I., Modugno, F., & Ribechini, E. (2010). Analytical Strategies for Characterizing Organic Paint Media Using Gas Chromatography/Mass Spectrometry. *ACCOUNTS OF CHEMICAL RESEARCH*, Vol. 43, pp. 715-727.
- Cultural Heritage Open Source/ Raw umber*. (n.d.). Retrieved from <https://chsopensource.org/raw-umber-k-40610/>
- Daniilia, S., Andrikopoulos, K., Sotiropoulos, S., & Karapanagiotis, I. (2008). Analytical study into El Greco's baptism of Christ: clues to the genius of his palette. *Applied Physics A*, 90, pp. 565-575.
- Daniilia, S., Bikiaris, D., Burgio, L., Gavala, P., Clark, R. J., & Chryssoulakis, Y. (2002). An extensive non-destructive and micro-spectroscopic study of two post-Byzantine overpainted icons of the 16th century. *Journal of Raman Spectroscopy*, 33, pp. 807-814.
- Eastaugh, N., Walsh, V., Chaplin, T., & Siddall, R. (2004). *Pigment Compendium: a Dictionary and Optical Microscopy of Historic Pigments*. Amsterdam: Elsevier Butterworth-Heinemann.

European Laboratory for Non-Linear Spectroscopy/ Molecular Spectroscopy. (n.d.). Retrieved from <https://sites.google.com/a/lens.unifi.it/molecularspectroscopy/research/topics/applied-spectroscopy/spectral-data-bank/white-lead>

Fotakis, C., Anglos, D., Zafiroopoulos, V., Georgiou, S., & Tornari, V. (2007). *Lasers in the Preservation of Cultural Heritage Principles and Applications*. Florida: Taylor & Francis Group.

Ganitis, V., Pavlidou, E., Zorba, F., Paraskevopoulos, K. M., & Bikiaris, D. (2004). A post-Byzantine icon of St Nicholas painted on a leather support. Microanalysis and characterisation of technique. *Journal of Cultural Heritage*(5), pp. 349-360.

Genesis. Retrieved from https://www.vatican.va/archive/bible/genesis/documents/bible_genesis_en.html#Chapter%2018

Harris, J. (2000). Theophanes the Crete (c. 1490-1559) monk and painter. In *Encyclopedia of Greece and the Hellenic tradition* (Vol. II). Chicago: Fitzroy Dearborn Publishers.

Harrison, L., Ambers, J., Stacey, R., Cartwright, C., & Lymberopoulou, A. (2011). The Noli me Tangere: study and conservation of a Cretan icon. *The British Museum Technical Research Bulletin*, 5, pp. 25-38.

Janssens, K. (2013). *Modern Methods for Analysing Archaeological and Historical Glass*. Chichester: John Wiley & Sons.

Janssens, K., Dik, J., Cotte, M., & Susini, M. (2010). Photon-based techniques for nondestructive subsurface analysis of painted cultural heritage artifacts. *Accounts of chemical research*, 43(6), pp. 814-825.

- Karapanagiotis, I., Mantzouris, D., & Rosenberg, E. (2008). Analytical investigation of painting techniques used in icons of the Cretan school of iconography. *9th International Conference on NDT of Art*. Jerusalem.
- Karapanagiotis, I., Lampakis, D., Konstanta, A., & Farmakalidis, H. (2013). Identification of colourants in icons of the Cretan School of iconography using Raman spectroscopy and liquid chromatography. *Journal of Archaeological Science*, 40, pp. 1471-1478.
- Karydas, A. G. (2007). Application of a Portable XRF Spectrometer for the Non-Invasive Analysis of Museum Metal Artefacts. *Annali di Chimica*, 97, pp. 419-432.
- Katsibiri, O. (2003). Investigation of the technique and materials used for mordant gilding on byzantine and post-byzantine icons and wall paintings. Doctoral thesis. Northumbria University.
- Kenna, M. E. (1985). Icons in Theory and Practice: An Orthodox Christian Example. *History of Religions*, Vol. 24, pp. 345-368.
- Kesidis, S. (2020). Multi-Analytical Study of Two Western European Canvas Paintings from The Series Stations of The Cross. Kalamata.
- Kouloumpi, E., Moutsatsou, A. M., & Terlix, A.-V. (2012). Canvas and Panel Paintings: Techniques and Analyses. In *Analytical Archaeometry: Selected topics*. Royal Society of Chemistry.
- Kouloumpi, E., Moutsatsou, A., Trompeta, M., & Olafsdottir, J. (2007). Laser-based structural diagnosis: A museum's point of view. *Lasers in the Conservation of Artworks, Lacona VII*. Madrid.

- Kozaris, I. A. (2013). Imagine Techniques. In E. A. Varella, *Conservation Science for the Cultural Heritage Applications of Instrumental Analysis* (pp. 38-47). Heidelberg: Springer.
- Larkin, P. (2011). *Infrared and Raman Spectroscopy Principles and Spectral Interpretation*. Elsevier.
- Mafredas, T. (2018). Characterization of technology from four (4) panel paintings of hieromonk Dionysius from Fourná, author of “Hermeneia of the Painting Art” and comparison with his manuscript. Kalamata.
- Mafredas, T., Kouloumpi, E., & Boyatzis, S. (2021). Did Dionysius of Fourná Follow the Material Recipes Described in His Own Treatise? A First of His Panel Paintings. *Heritage*, 4, pp. 3770-3789.
- Marucci, G., Beeby, A., Parker, A. W., & Nicholson, C. E. (2018). Raman spectroscopic library of medieval pigments collected with five different wavelengths for investigation of illuminated manuscripts. *Analytical Methods*(10), pp. 1219-1236.
- Mastrotheodoros, G. P., Beltsios, K. G., & Bassiakos, Y. (2021). On the Red and Yellow Pigments of Post-Byzantine Greek Icons. *Archaeometry*, 63, pp. 753-778.
- Mastrotheodoros, G., Theodosis, M., & Filippaki, E. (2020). By the Hand of Angelos? Analytical Investigation of a Remarkable 15th Century Cretan Icon. *Heritage*(3), pp. 1360-1372.
- Polland, A. M., & Heron, C. (2008). *Archaeological Chemistry*. Cambridge: The Royal Society of Chemistry.
- Raman Spectroscopic Library of Natural and Synthetic Pigments*. Retrieved from <http://www.chem.ucl.ac.uk/resources/raman/index.html#red>

- Ray, P., & Dubey, S. K. (2018). Raman Spectroscopy: A Potential Characterization Tool for Carbon Materials. In S. K. Sharma, D. Sverma, L. U. Khan, & S. Kumar, *Handbook of Materials Characterization* (pp. 405-434). Springer.
- Salzer, R. (2013). Infrared and Raman Spectroscopy. In *Conservation Science for the Cultural Heritage Applications of Instrumental Analysis* (pp. 65-79). Springer.
- Schlotz, R., & Uhlig, S. (2000). *Introduction to X-ray Fluorescence (XRF)*. Karlsruhe: Bruker AXS GmbH.
- Smith, G. D., & Clark, R. J. (2004). Raman microscopy in archaeological science. *Journal of Archaeological Science*(34), pp. 1137-1160.
- Speake, G. (Ed.). (2000). *Encyclopedia of Greece and the Hellenic tradition* (Vol. 2). London- Chicago: Fitzroy Dearborn Publishers.
- Thompson, D. L. (1982). *Mummy Portraits in The J. Paul Getty Museum*. Malibu: The J . Paul Getty Museum.
- Tranter, G., Holmes, J., & Lindon, J. (Eds.). (2017). *Encyclopedia of Spectroscopy and Spectrometry, Three-Volume Set (Volume 1-3)* (Vol. 2). Amsterdam: Elsevier/AP, Academic Press is an imprint of Elsevier.
- Vandenabeele, P. (2013). *Practical Raman Spectroscopy - An Introduction*. John Wiley & Sons.
- Vandenabeele, P., Edwards, H. G., & Moens, L. (2007). A Decade of Raman Spectroscopy in Art and Archaeology. *Chemical Reviews*, 107, pp. 678-686.
- Vassilaki, M. (2009). *The Painter Angelos and the Icon-Painting in Venetian Crete*. Surrey: Ashgate Publishing Limited.

- Βοκοτόπουλος, Π. (1995). *Ελληνική Τέχνη- Βυζαντινές Εικόνες*. Αθήνα: Εκδοτική Αθηνών.
- Βοκοτόπουλος, Π. Λ. (1998). *Η Κρητική Ζωγραφική το 16ο αιώνα* (2η Έκδοση ed.). Αθήνα: Ίδρυμα Γουλανδρή-Χόρν.
- Βολουδάκη, Ν. (2000). *Βυζαντινή ζωγραφική θεωρία*. Γρηγόρη.
- Δελτίο Μουσείο Μπενάκη (Αρ. Ευρ, 20547).
- Διονύσιος εκ Φουρνά. (1900). *Ερμηνεία της Ζωγραφικής Τέχνης*. (Α. Παπαδοπούλου-Κεραμέως, Ed.) Πετρούπολη: τυπογραφία της Αγιοτάτης Συνόδου.
- Δρακοπούλου, Ε., & Χατζηδάκης, Μ. (1997). *Έλληνες ζωγράφοι μετά την Άλωση (1450-1830)*. Αθήνα: Εθνικό Ίδρυμα Ερευνών (Ε.Ι.Ε.). Ινστιτούτο Νεοελληνικών Ερευνών.
- Ζαμβακέλλης, Π. Α. (1985). *Εισαγωγή στη Βυζαντινή ζωγραφική : εικονογραφία, τοιχογραφία, μωσαϊκό, μικρογραφία*. Αθήνα.
- Καλογερόπουλος, Κ. (2007). Οι φορητές εικόνες στη βυζαντινή και μεταβυζαντινή Καλλιτεχνική παραγωγή. *Archive*, 3, pp. 6-13.
- Καπετανίδης, Ν. Τεχνικές Μέθοδοι Βυζαντινής και Μεταβυζαντινής Αγιογραφίας Μέρος Πρώτο: χρωστικές.
- Κουλουμπή, Ε., Μουτσάτσου, Α. Π., Τερλιζή, Α.-Β., Κατσιμπήρη, Ο., & Δουλγερίδης, Μ. "Η ΑΝΑΤΡΟΦΗ ΤΟΥ ΕΡΩΤΑ" ΤΟΥ CORREGGIO: ΦΥΣΙΚΟΧΗΜΙΚΗ ΤΕΚΜΗΡΙΩΣΗ ΤΗΣ ΤΕΧΝΙΚΗΣ ΚΑΙ ΤΩΝ ΥΛΙΚΩΝ ΚΑΤΑΣΚΕΥΗΣ ΤΟΥ ΕΡΓΟΥ.
- Κριτσωτάκης, Ι. Μ. (1934). Οι Κρήτες Ζωγράφοι. *Μύσων, Γ*.
- Κωσταντουδάκη-Κιτρομηλίδου, Μ. (1999). *Η ζωγραφική στην Κρήτη τον 15ο και 16ο αιώνα: ο μακρύς δρόμος προς το Δομήνικο Θεοτοκόπουλο και*

η πρώτη παραγωγή του. Retrieved from <http://archive.eclass.uth.gr/eclass/modules/document/file.php/SEAD216/%CE%9C.%20%CE%9A%CF%89%CE%BD%CF%83%CF%84%CE%B1%CE%BD%CF%84%CE%BF%CF%85%CE%B4%CE%AC%CE%BA%CE%B7-%CE%9A%CE%B9%CF%84%CF%81%CE%BF%CE%BC%CE%B7%CE%BB%CE%AF%CE%B4%CE%BF%CF%85%2C%20%CE%97%20%CE>

Μαστροθεόδωρος, Γ. Μ. (2016). Χρωστικές κονίες και άλλα υλικά μεταβυζαντινής ζωγραφικής. Ιωάννινα.

Πανσελήνου, Ν. (2000). *Βυζαντινή Ζωγραφική: Η βυζαντινή κοινωνία και οι εικόνες της*. Αθήνα: Καστανιώτη Α.Ε.

Παπαμαστοράκης, Τ. (1995, Ιούλιος- Σεπτεμβριος). Η Βυζαντινή Ζωγραφική. *Αρχαιολογία & Τέχνες*. Retrieved from <https://www.archaiologia.gr/wp-content/uploads/2011/07/56-2.pdf>

Πλάτζος, Δ. (2013). *Ελληνική Τέχνη και Αρχαιολογία (1100-30 π.Χ.)*. Αθήνα: Κάπον.

Φαρδή, Θ. (2012). Στρωματογραφική Μελέτη Βυζαντινών Εικόνων: υλικά, τεχνικές και ζητήματα διαλυτότητας. Θεσσαλονίκη.

Χαραλαμπίδης, Α. (2014). *Η Ιταλική Αναγέννηση: Αρχιτεκτονική Γλυπτική Ζωγραφική*. Θεσσαλονίκη: University Studio Press.

Χαραλάμπους-Μουρίκη, Ν. (1964). Η παράσταση της Φιλοξενίας του Αβραάμ σε μια εικόνα του Βυζαντινού Μουσείου (πίν. 33-39). *Δελτίον της Χριστιανικής Αρχαιολογικής Εταιρείας, Γ*, pp. 87-114.

Χατζηδάκη, Ν., & Κατερίνη, Έ. (2005). Η εικόνα του αρχαγγέλου Μιχαήλ με δώδεκα σκηνές του κύκλου του στην Καλαμάτα. Ένα άγνωστο

έργο του Γεωργίου Κλόντζα. *Δελτίον της Χριστιανικής Αρχαιολογικής Εταιρείας, ΚΣΤ*, pp. 241-262.

Χατζηδάκης, Μ. (1950). Ο Δομήνικος Θεοτοκόπουλος και η κρητική ζωγραφική. *Κρητικά Χρονικά*, 4, pp. 371-440.

Χατζηδάκης, Μ. (1987). *Έλληνες Ζωγράφοι μετά την Άλωση (1453-1830)* (Vol. I). Αθήνα: Κέντρο Νεοελληνικών Ερευνών Ε.Ι.Ε.